



ELSEVIER

Nuclear Physics B 552 [FS] (1999) 529–598

NUCLEAR
PHYSICS B

www.elsevier.nl/locate/npe

Polymers and manifolds in static random flows: a renormalization group study

Kay Jörg Wiese^{a,1}, Pierre Le Doussal^{b,2}^a *Fachbereich Physik, Universität GH Essen, 45117 Essen, Germany*^b *CNRS-Laboratoire de Physique Théorique de l'Ecole Normale Supérieure, 24 rue Lhomond,
75231 Paris Cedex, France³*

Received 29 August 1998; revised 25 February 1999; accepted 16 March 1999

Abstract

We study the dynamics of a polymer or a D -dimensional elastic manifold diffusing and connected in a non-potential static random flow (the “randomly driven polymer model”). We find that short-range (SR) disorder is relevant for $d \leq 4$ for directed polymers (each monomer sees a different flow) and for $d \leq 6$ for isotropic polymers (each monomer sees the same flow) and more generally for $d < d_c(D)$ in the case of a manifold. This leads to new large scale behavior, which we analyze using field theoretical methods. We show that all divergences can be absorbed in multilocal counter-terms which we compute to one loop order. We obtain the non-trivial roughness ζ , dynamical z and transport exponents ϕ in a dimensional expansion. For directed polymers we find $\zeta \approx 0.63$ ($d = 3$), $\zeta \approx 0.8$ ($d = 2$) and for isotropic polymers $\zeta \approx 0.8$ ($d = 3$). In all cases $z > 2$ and the velocity versus applied force characteristics is sublinear, i.e. at small forces $v(f) \sim f^\phi$ with $\phi > 1$. It indicates that this new state is glassy, with dynamically generated barriers leading to trapping, even by a divergenceless (transversal) flow. For random flows with long-range (LR) correlations, we find continuously varying exponents with the ratio g_L/g_T of potential to transversal disorder, and interesting crossover phenomena between LR and SR behavior. For isotropic polymers new effects (e.g. a sign change of $\zeta - \zeta_0$) result from the competition between localization and stretching by the flow. In contrast to purely potential disorder, where the dynamics gets frozen, here the dynamical exponent z is not much larger than 2, making it easily accessible by simulations. The phenomenon of pinning by transversal disorder is further demonstrated using a two monomer “dumbbell” toy model. © 1999 Elsevier Science B.V. All rights reserved.

PACS: 74.60.Ge; 05.20.-y

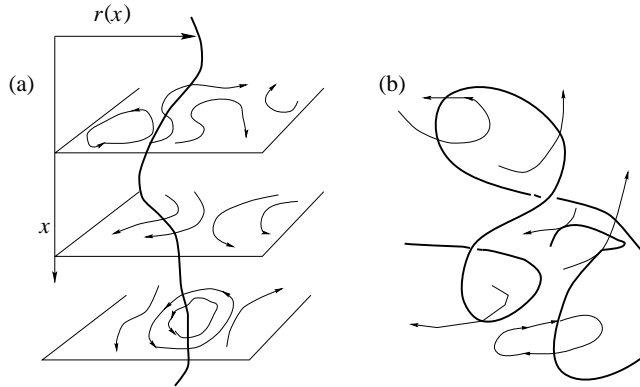


Fig. 1. Elastic manifolds (polymers $D = 1$) in random flows: (a) directed polymer (b) isotropic chain.

1. Introduction

In this paper, we study the model of a polymer diffusing in a static random flow and its extension to an elastic manifold of arbitrary internal dimension D . The velocity pattern of the flow $v(r)$ is constant in time and leads to convection of the polymer in addition to diffusion. We are interested in the general case of a *non-potential* flow: the extreme example is the hydrodynamic divergenceless flow, with $\nabla \cdot v(r) = 0$, but mixtures of potential and divergenceless flows are also considered. See Figs. 2, 3 and 4 for a visualization. The physical motivations to study this model, which we call a “randomly driven polymer”, are the following.

First, it is a prototype of an out of equilibrium system in the presence of quenched disorder which generalizes the much studied problem of an elastic manifold in a *random potential* [1–11], i.e. for the present model the case of a purely *potential* flow. This problem has been very popular in the last decade due to its numerous physical realizations such as vortex lines in superconductors, interfaces in random magnets and charge density waves [12–15]. Equally fascinating, albeit more formal, relations exist to growth processes and potential fluid dynamics, via the Cole–Hopf transformation onto the Burgers and Kardar–Parisi–Zhang equations [16]. In addition, it is one of the simplest models which exhibits glassy properties, typically ultra slow dynamics, anomalously small response to external perturbations and pinning [2,12,17], which are also present in more complex systems, such as spin glasses [18–20] or random field systems [21,22]. However, little is known about what of the glassy properties remains in the presence of *non-potential* disorder. This question is important for numerous physical systems such as driven systems in the presence of quenched disorder [23–26] or domain growth in the presence of shear [27]. The model studied in this paper is simple enough to allow for some answers to this question.

¹ E-mail: wiese@theo-phys.uni-essen.de

² E-mail: ledou@physique.ens.fr

³ LPTENS is a Unité Propre du C.N.R.S. associée à l’Ecole Normale Supérieure et à l’Université Paris Sud.

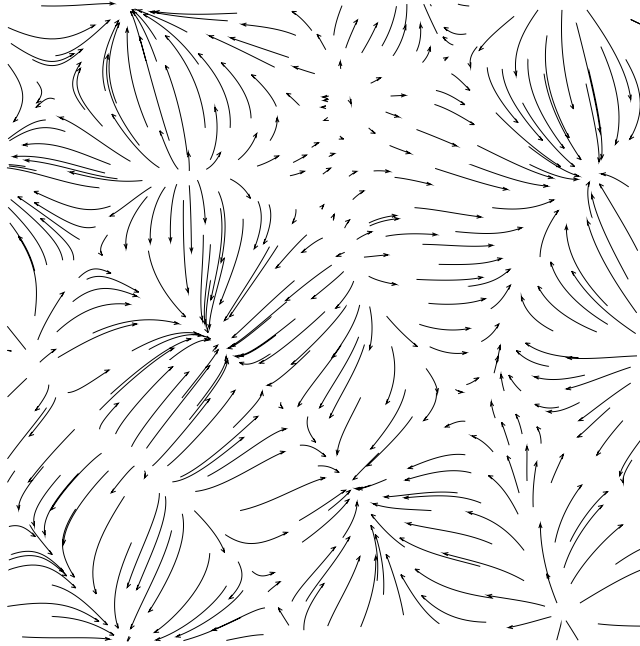


Fig. 2. Longitudinal (potential) disorder, obtained from the disorder of Figure 4 through application of the longitudinal projector.

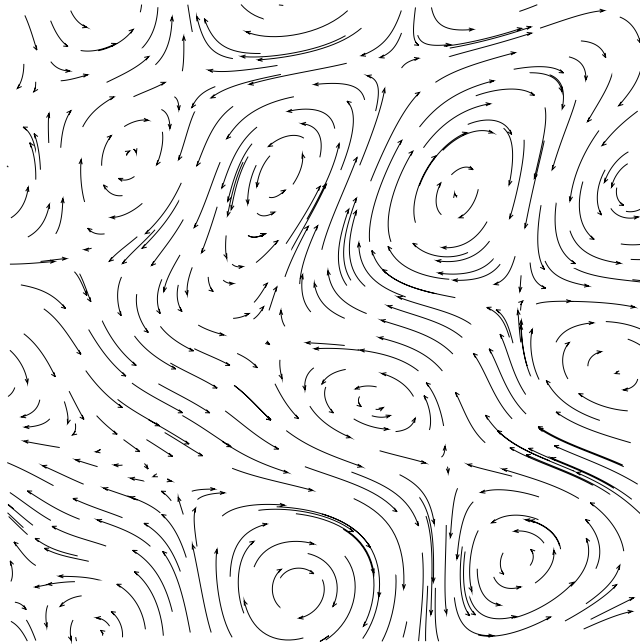


Fig. 3. Transversal disorder, obtained from the disorder of Figure 4 through application of the transversal projector.

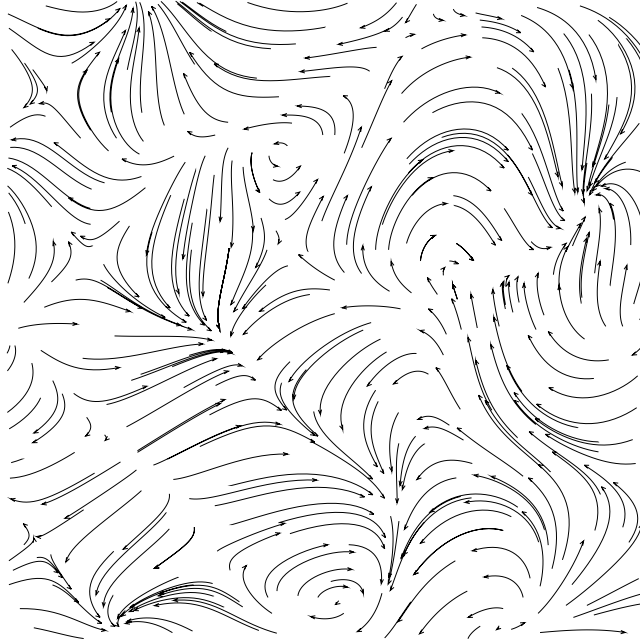


Fig. 4. Isotropic disorder, obtained through superposition of 7×7 Fourier modes. One observes purely transversal (“turbulent”) regions and potential wells.

The second motivation concerns real systems of elastic objects convected by hydrodynamic flows. Recently, experiments on polymers in spatially varying stationary flows, such as elongational flows have been performed [28–31] and these experiments can be extended to longer objects and more complex flows. Of course the model studied here is a toy model in the sense that it disregards hydrodynamic forces (the back reaction of the polymer on the flow) and additional time dependent components of the flow. The main interest is to illustrate in a simple way some of the fascinating properties arising from the competition between the convecting flow and the elasticity of the structure. We believe that some of these properties, for instance the existence of preferred regions in the flow, will be present in more realistic situations. Experimentally, inhomogeneities in the polymer distribution and non-linearities in the response of the drift velocity $v(f)$ to an uniform applied external force f are worth being investigated [32].

In the case of non-potential disorder new effects arise from the competition between on one hand disorder and elasticity – which tend to create pinned or frozen states – and on the other hand the energy which is constantly pumped into the system and which tends to destroy the glassy properties. Very few systematic studies of these effects exist at present. One extensive work was performed in the context of driven lattices [25,33]: it was shown that some glassy features, such as pinning in the displacement transverse to the motion, barriers and strongly non-linear transverse velocity force-characteristics, survive in the moving state. Some glassy features were also found to survive in infinite range random spin systems with non-relaxational dynamics [34]. Another example,

studied long ago [35–43] and recently solved analytically in the limit of $d \rightarrow \infty$ for long-range (LR) disorder [44], is the problem of a single-particle diffusing in a quenched random flow, the $D = 0$ limit of the present model. This problem was found to exhibit some glassy features, also seen in recent simulations of a related spin model [34]. In the present paper we generalize the single-particle study to an elastic manifold, which is expected to lead to new physics due to the crucial role of internal elasticity in generating barriers. It also generalizes the studies of the dynamics of self-avoiding manifolds [45,46] to a quenched disorder situation, though self-avoidance is found to be perturbatively less relevant in most of the regimes studied here.

In this paper we work directly in finite dimension using dynamical renormalization group techniques, and establish the existence of new universal fixed points for short-range disorder. We also treat the case of long-range disorder, which leads to a line of fixed points. In all cases we compute explicitly the non-trivial roughness exponent, the dynamical exponent and the velocity force characteristics at small applied force f . We study two cases: either the polymer is directed (each monomer sees a different flow) or it is isotropic (all monomers are in the same flow) as depicted in Fig. 1. A short account of our results has already appeared in [48], which was presented using a Wilson RG technique as in related studies [33,49]. The aim of the present paper is to give a detailed account of our results using a field theoretical derivation. This derivation, based on the powerful multilocal operator product expansion (MOPE) techniques developed in the context of self-avoiding manifolds [50–54,45,46], deserves a detailed presentation, as it is generally useful to treat problems involving manifolds. In addition, we give here a detailed treatment of the crossover between long-range and short-range disorder, as well as an in depth discussion of the results.

This article is organized as follows. In Section 2 we define the model, the physical observables and present a simple analysis based on dimensional and Flory arguments. Section 3 is devoted to the field theoretic treatment of the model. We start by defining the generating functional (Section 3.1), and then show that divergences are short-range (Section 3.2). This allows to identify local (Section 3.3) and bilocal (Section 3.4) counter-terms, summarized in Section 3.6. Their divergent parts are calculated in Sections 3.7 and 3.8, followed by a discussion of the particle limit in Section 3.9. This yields the RG equations in Sections 3.10 and 3.11.

The section which contains a presentation and a discussion of the results, and can be read independently is Section 4. There we analyze the RG equations, report the results of our calculation and specify them to the four cases of interest (directed and isotropic disorder, short-range and long-range correlations). The crossover from long-range to short-range correlated disorder is discussed in Section 4.6. We compare with previous results for Hartree limit ($d = \infty$) and particle case ($D = 0$) and discuss the crossover from short-range to long-range correlated disorder. This is followed by an analysis of the effect of self-avoidance in Section 4.7. The section terminates with the study of a toy model, involving two particles in a (directed) random flow which illustrates how barriers are generated dynamically. Conclusions and perspectives are presented in Section 5. Some technicalities are relegated to Appendices A, B and C.

2. Model and physical observables

2.1. The model

We consider a manifold of internal dimension D parameterized by a d -component field $r_\alpha(x)$. The polymer corresponds to $D = 1$ (x labels the monomers), and a single-particle to $D = 0$. Membranes have $D = 2$. We study the Langevin dynamics (for the dimensional analysis see Section 2.3)

$$\dot{r}_\alpha(x, t) = \lambda (\Delta r_\alpha(x, t) + \eta_\alpha(x, t) + F_\alpha[r(x, t), x]), \quad (2.1)$$

where the term proportional to $\Delta r_\alpha(x, t)$ is the derivative of the internal (entropic) elasticity (“stiffness”). The Gaussian thermal noise $\eta_\alpha(x, t)$ satisfies

$$\langle \eta_\alpha(x, t) \eta_\beta(x', t') \rangle = \frac{2}{\lambda} \delta_{\alpha\beta} \delta(t - t') \delta^D(x - x'). \quad (2.2)$$

Angular brackets denote thermal averages and overbars disorder averages.

$F_\alpha[r, x]$ is a Gaussian quenched random force field of correlations:

$$\overline{F_\alpha[r, x] F_\beta[r', x']} = \Delta_{\alpha\beta}(r - r') h(x - x'). \quad (2.3)$$

We study two main cases of interest illustrated in Fig. 1. If the manifold is *directed* (e.g. a polymer oriented by an external field), then

$$h(x - x') = \delta^D(x - x'). \quad (2.4)$$

If the manifold is *isotropic*, (e.g. a Gaussian chain in a static flow), the force field does not depend on the internal coordinate,

$$F_\alpha[r, x] = F_\alpha[r] \quad (2.5)$$

and

$$h(x - x') = 1. \quad (2.6)$$

Note that the isotropic polymer (or more generally the manifold) in a static flow can also be seen as a directed polymer in a flow completely correlated (i.e. constant) along its internal dimension.

We consider a statistically rotationally invariant force field with both a potential (L) (“electric”) and a divergence-free (T) part (“magnetic”) which depends only on the distance $|r - r'|$. Both parts contribute separately to the correlator:

$$\Delta_{\alpha\beta}(r) = -\partial_{r_\alpha} \partial_{r_\beta} \Delta_L(|r|) - \left(\delta_{\alpha\beta} \sum_\gamma \partial_{r_\gamma}^2 - \partial_{r_\alpha} \partial_{r_\beta} \right) \Delta_T(|r|). \quad (2.7)$$

In Fourier space we use

$$\Delta_{\alpha\beta}(r) = \int_k \Delta_{\alpha\beta}(k) e^{ik \cdot r}, \quad (2.8)$$

where we specify the normalization of the k -integral below. There are several cases of interest for the correlation of the random force.

Model SRF: force with short-range correlations.

The *force* correlator scales like a δ -distribution $\Delta_{\alpha\beta}(r-r') \sim \delta^d(r-r')$, with however a non-trivial index structure. In Fourier space the correlator reads at small k

$$\Delta_{\alpha\beta}(k) = g_L P_{\alpha\beta}^L(k) + g_T P_{\alpha\beta}^T(k), \quad (2.9)$$

where $P_{\alpha\beta}^L(k) = k_\alpha k_\beta / k^2$ is the longitudinal and $P_{\alpha\beta}^T(k) = \delta_{\alpha\beta} - P_{\alpha\beta}^L(k)$ the transverse projector. As we shall show below, this is the generic situation, since it is relevant for all short-ranged correlations, even those, for which one starts with a force correlator which is formally shorter ranged than the δ -distribution (e.g. decaying faster than $1/r^d$).

Model SRP: potentials with short-range correlations.

In this case, the *potential* correlator scales like a δ -distribution $\Delta_{L,T}(r-r') \sim \delta^d(r-r')$. The corresponding force-correlator reads in Fourier space at small k

$$\Delta_{\alpha\beta}(k) = \tilde{g}_L k_\alpha k_\beta + \tilde{g}_T (\delta_{\alpha\beta} k^2 - k_\alpha k_\beta) \equiv k^2 [\tilde{g}_L P_{\alpha\beta}^L(k) + \tilde{g}_T P_{\alpha\beta}^T(k)]. \quad (2.10)$$

Except for $\tilde{g}_T = 0$, which is preserved by a fluctuation dissipation theorem [12,5,55], this model is unstable and will renormalize to model SRF discussed above (except in the transversal case $g_L = 0$ for the particle $D = 0$).

Model LR: forces with long-range correlations.

In this model, correlations at large scale obey a power law $\Delta_{\alpha\beta}(r-r') \sim |r-r'|^{-a}$, with $a < d$. The Fourier transforms of the correlators with respect to r behave, for small values of their argument k , as

$$\Delta_{\alpha\beta}(k) \sim |k|^{a-d} (g_L P_{\alpha\beta}^L(k) + g_T P_{\alpha\beta}^T(k)). \quad (2.11)$$

Let us also note that in order to simplify calculations, we normalize the integral over k such that

$$\int_k |k|^{a-d} e^{-Ck^2} = C^{-a/2}. \quad (2.12)$$

2.2. Physical observables

We study the time translational invariant steady state. It can be constructed by taking a finite size sample L and considering the large time limit first, before taking the system size to ∞ . We will not address here the subtle issue of whether, or in which case, these limits commute (for a partial discussion in the case $g_T > 0$ see e.g. Ref. [44]). The radius of gyration (or roughness) exponent ζ is then defined by

$$\overline{\langle (r(x, t) - r(x', t))^2 \rangle} \sim |x - x'|^{2\zeta}, \quad (2.13)$$

and the single monomer diffusion exponent ν by

$$\overline{\langle (r(x, t) - r(x, t'))^2 \rangle} \sim |t - t'|^{2\nu}. \quad (2.14)$$

We assume scaling behavior

$$\overline{\langle (r(x, t) - r(0, 0))^2 \rangle} \sim |x|^{2\zeta} \overline{B}(t/x^z) \quad (2.15)$$

with $\zeta = z\nu$.

We also consider the anomalous dimension of the elasticity of the membrane, β (for the precise definition see Eq. (3.108)), which evaluates to 0 in the directed case.

The drift velocity under a small additional applied force f in Eq. (2.1) is

$$v \sim \overline{\langle r(x, t) \rangle} / t. \quad (2.16)$$

We find

$$v \sim f^\phi \quad (2.17)$$

at small f , with

$$\phi = \frac{z - \zeta}{2 - \zeta + \beta} > 1, \quad (2.18)$$

indicating trapping of the polymer by the flow.

2.3. Dimensional analysis

Power counting at the Gaussian fixed point without disorder yields (denoting for example by $[r]_x$ the dimension of r in units of x)

$$\begin{aligned} [r]_x = \zeta_0 = \frac{2-D}{2}, \quad [r]_t = \nu_0 = \frac{2-D}{4}, \\ \tilde{\zeta}_0 = [\eta]_x = [\tilde{r}]_x = -\frac{2+D}{2}, \quad \beta = 0 \end{aligned} \quad (2.19)$$

for $D < 2$. The dimensions of the couplings are

$$\varepsilon^{\text{dir}}(D, d) = -[g_L]_x^{\text{dir}} = -[g_T]_x^{\text{dir}} = 2 - \zeta_0 a \quad (2.20)$$

$$\varepsilon^{\text{iso}}(D, d) = -[g_L]_x^{\text{iso}} = -[g_T]_x^{\text{iso}} = 2 + D - \zeta_0 a \quad (2.21)$$

in the directed and isotropic case respectively. Thus short-range disorder (formally $a := d$) is relevant for positive ε , i.e. when (see Fig. 5) $d < d_c^{\text{dir}}(D)$ for directed manifolds and $d < d_c^{\text{iso}}(D)$ for isotropic manifolds, with

$$d_c^{\text{dir}}(D) = \frac{4}{2-D}, \quad d_c^{\text{iso}}(D) = \frac{4+2D}{2-D}. \quad (2.22)$$

Thus we find that short-range disorder is relevant for directed polymers when $d < 4$ and for isotropic polymers for $d < 6$. This is interesting because it means that in physical dimensions ($d = 2$, $d = 3$) polymers should be affected by quenched random flows while for particles short-range disorder is irrelevant for $d = 3$ and only marginal in $d = 2$. Disorder can also be relevant if the interaction is long enough ranged: disorder is relevant for $a < a_c(D) = d_c(D)$ for LR disorder.

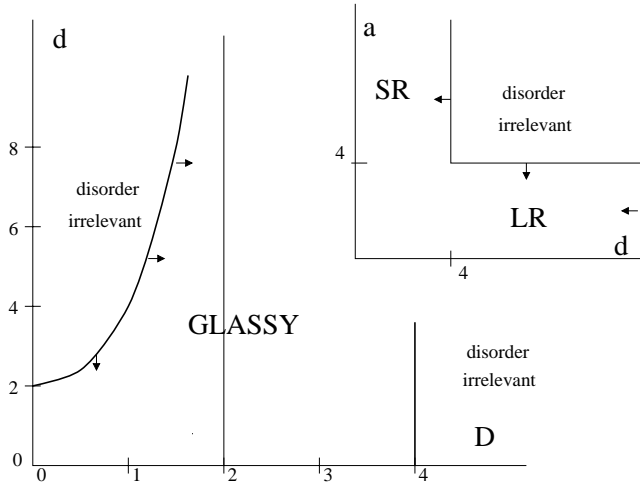


Fig. 5. Regions in the (d, D) plane where SR disorder is relevant for a directed manifold. Inset: Regions in the (a, d) plane where SR or LR disorder is relevant for the directed polymer $D = 1$.

A qualitative idea of the effect of disorder is obtained by using Flory-like estimates. Balancing in Eq. (2.1) friction or elasticity with disorder⁴ yields

$$\zeta_F^{\text{dir}} = 2\nu_F^{\text{dir}} = \frac{4 - D}{2 + d}, \quad \zeta_F^{\text{iso}} = 2\nu_F^{\text{iso}} = \frac{4}{2 + d} \tag{2.23}$$

for directed and isotropic manifolds, respectively. Results for LR disorder are obtained upon replacing $d \rightarrow a$. Note that this argument is too rough to distinguish between the potential or divergenceless nature of the flow. It suggests however that the manifold will be stretched by disorder. As we will see below, the precise calculation will indeed confirm that the manifolds are stretched in most (but not all!) of the cases, and will yield the deviations away from Flory.

The expected “phase diagram” in the d, D plane is illustrated in Fig. 5 for directed manifolds. The new glassy regime extends from the line $d = d_c(D)$ to the upper critical (internal) dimension $D = D_c = 4$ beyond which disorder is perturbatively irrelevant. For isotropic manifolds the diagram has the same topology except that the upper critical internal dimension is pushed to $D_c = +\infty$. We know of three ways to investigate perturbatively the nature of the glassy regime in Fig. 5. First one can start from large d (any D), which was done in [44]. The second approach is to start from $D = 4$ using a functional RG method [73]. The last approach is to start from the line $d = d_c(D)$ which is the aim of this paper.

⁴The idea of the Flory-estimate is to suppose that all terms in the equation of motion scale in the same way, and by this to obtain the critical exponents. For directed manifolds in short-range correlated forces, one sets $\partial_t r \sim \Delta r \sim F(r, x)$, replaces ∂_t by $1/t$, Δ by $1/x^2$ and from Eq. (2.3) $F(r, x)$ by $r^{-d/2}x^{-D/2}$ to obtain $r/t \sim r/x^2 \sim r^{-d/2}x^{-D/2}$, and the exponents stated in the main text. For isotropic manifolds in short-range correlated forces, the same argument reads $r/t \sim r/x^2 \sim r^{-d/2}$.

3. Field theoretic treatment of the renormalization group equations

3.1. Definition of the field-theoretic model

We start from the equation of motion (2.1) and convert it into an effective field theory following Ref. [56]. The effective dynamical action in prepoint (Itô) discretization reads

$$J[r, \tilde{r}] = \int_{x,t} \tilde{r}_\alpha(x, t) (\dot{r}_\alpha(x, t) + \lambda(-\Delta r_\alpha(x, t) + \eta_\alpha(x, t) + F_\alpha[r(x, t), x])) . \quad (3.1)$$

The noise $\eta(x, t)$ as well as the disorder force $F(r)$ are Gaussian, see Eqs. (2.2) and (2.3), and can thus be integrated over. This gives the dynamic functional

$$J[r, \tilde{r}] = \int_{x,t} \tilde{r}(x, t) (\dot{r}(x, t) - \lambda \Delta r(x, t)) - \lambda \tilde{r}(x, t)^2 - \frac{1}{2} \lambda^2 \int_{x,y,t,t'} \tilde{r}_\alpha(x, t) \Delta_{\alpha\beta}(r(x, t) - r(y, t')) h(x-y) \tilde{r}_\beta(y, t') . \quad (3.2)$$

Here and in the following, contraction over indices is implied, where ever confusion is impossible. In order to simplify notations, we will in the following suppress the factor of λ , i.e. set

$$\lambda t \rightarrow t. \quad (3.3)$$

This is not problematic, as λ always appears with time. At the end of the calculations one has to replace t by λt which is necessary in order to get the renormalization factors correct. Note also that the factor $\frac{1}{2}$ disappears, if we use the time-ordered vertex.

The disorder correlator is

$$\Delta_{\alpha\beta}(r(x, t) - r(y, t)) = \int_k e^{ik(r(x,t)-r(y,t))} (g_L P_{\alpha\beta}^L(k) + g_T P_{\alpha\beta}^T(k)) |k|^{a-d} h(x-y). \quad (3.4)$$

The function $h(x)$ may be specified to the directed case with

$$h(x-x') = \delta^D(x-x') \quad (3.5)$$

or to the isotropic case

$$h(x-x') = 1. \quad (3.6)$$

Eventually, one may also want to study an interpolating case, where

$$h(x-x') = \delta(x_\perp - x'_\perp). \quad (3.7)$$

In order to simplify notations, we introduce the following graphical symbols:

$$\begin{aligned}
 \text{wavy line with dot} &= \tilde{r}(x, t) (-\Delta_x) r(x, t) \\
 \text{wavy line with dot and arrow} &= \tilde{r}(x, t) \dot{r}(x, t) \\
 \text{two wavy lines} &= \tilde{r}(x, t)^2 \\
 \alpha \text{ wavy line} \text{---} \text{wavy line} \beta &= \int_k \tilde{r}_\alpha(x, t) e^{ik(r(x,t)-r(y,t'))} \tilde{r}_\beta(y, t') |k|^{a-d} h(x-y) \\
 \text{wavy line} \text{---} \text{wavy line} &= \int_k \tilde{r}(x, t) e^{ik(r(x,t)-r(y,t'))} \tilde{r}(y, t') |k|^{a-d} h(x-y) \\
 \text{wavy line} \text{---}^L \text{---} \text{wavy line} &= \int_k P_{\alpha\beta}^L(k) \tilde{r}_\alpha(x, t) e^{ik(r(x,t)-r(y,t'))} \tilde{r}_\beta(y, t') |k|^{a-d} h(x-y) \\
 \text{wavy line} \text{---}^T \text{---} \text{wavy line} &= \int_k P_{\alpha\beta}^T(k) \tilde{r}_\alpha(x, t) e^{ik(r(x,t)-r(y,t'))} \tilde{r}_\beta(y, t') |k|^{a-d} h(x-y).
 \end{aligned} \tag{3.8}$$

The action takes the symbolic form

$$\begin{aligned}
 J[r, \tilde{r}] &= \int_{x,t} \text{wavy line with dot} + \text{wavy line with dot and arrow} - \text{two wavy lines} \\
 &\quad - \frac{1}{2} \int_{x,y,t,t'} \left(\text{wavy line} \text{---}^L \text{---} \text{wavy line} g_L + \text{wavy line} \text{---}^T \text{---} \text{wavy line} g_T \right).
 \end{aligned} \tag{3.9}$$

The free theory ($g_L = g_T = 0$) is easily investigated to obtain the free response $R(x, t)$ and correlation function $C(x, t)$:

$$R(x, t) = \frac{1}{d} \langle r(x, t) \tilde{r}(0, 0) \rangle_0, \tag{3.10}$$

$$C(x, t) = \frac{1}{d} \left\langle \frac{1}{2} (r(x, t) - r(0, 0))^2 \right\rangle_0, \tag{3.11}$$

where $\langle \dots \rangle_0$ denotes averages in the free theory. Explicit analytical expressions are given in appendix A. Here it is only important to note that for $0 < D < 2$ both functions are well defined in the continuum. $C(x, t)$ vanishes for $x = t = 0$, and is monotonically increasing in both arguments. They are non-trivially related by the fluctuation–dissipation theorem

$$\Theta(t) \frac{\partial}{\partial t} C(x, t) = R(x, t). \tag{3.12}$$

3.2. General considerations about renormalization

Before embarking upon calculations, let us follow [51,45] to show that divergences are always short range. This is necessary for the renormalization program to work. To this aim write down the perturbation expansion, the interaction vertex being

$$\text{---}\bullet\text{---}\bullet\text{---} := \int_k \tilde{r}(x, t) e^{ik(r(x,t)-r(y,t'))} \tilde{r}(y, t'), \tag{3.13}$$

where for the sake of transparency, we have neglected the index structure. The reader will easily be able to generalize the analysis given below to the model defined in Eq. (3.2).

The perturbative expansion of an observable \mathcal{O} can then be written as

$$\langle \mathcal{O} \text{---}\bullet\text{---}\bullet\text{---}^n \rangle_0 = \text{Norm} \sum_n \frac{g^n}{n!} \int_{\{x_i, t_i\}} \langle \mathcal{O} \text{---}\bullet\text{---}\bullet\text{---}^n \rangle_0, \tag{3.14}$$

where $\langle \dots \rangle$ denotes the expectation value with respect to the free, non-interacting theory, and the normalization Norm has to be chosen so that $\langle 1 \rangle = 1$. The integral is taken over all arguments of the interaction vertex. We claim that divergences only occur at short distances and short times. To prove this look at a typical expectation value with fixed x_i and t_i

$$\langle \mathcal{O} \text{---}\bullet\text{---}\bullet\text{---}^n \rangle_0 = \sum_{\alpha} \int_{\{k_i\}} f_{\alpha}(x_l - x_m, t_l - t_m, k_l, k_m) e^{-\sum_{i,j} Q_{ij} k_i k_j}, \tag{3.15}$$

where each contribution consists of a function f_{α} , which is a polynomial product of correlation and response functions and k 's and an exponential factor, with

$$Q_{ij} = -C(x_i - x_j, t_i - t_j). \tag{3.16}$$

As f_{α} is a regular function of the distances, divergences in the k -integral in Eq. (3.15) can only occur if Q_{ij} is not a positive form. We will show that Q_{ij} is a positive form for all k_i which satisfy the constraint

$$\sum_i k_i = 0. \tag{3.17}$$

This constraint always holds, see Eq. (3.13). For equal times it is just the statement that the Coulomb energy of a globally neutral assembly of charges is positive by identifying C with the Coulomb-propagator and k_i with the charges. In the dynamic case, write

$$Q_{ij} = \int \frac{d^D p}{(2\pi)^D} \int \frac{d\omega}{2\pi} \frac{2}{\omega^2 + (p^2)^2} (e^{ip(x_i-x_j)+i\omega(t_i-t_j)} - 1). \tag{3.18}$$

The exponential in Eq. (3.15) then reads

$$\begin{aligned} \sum_{i,j} k_i k_j Q_{ij} &= \int \frac{d^D p}{(2\pi)^D} \int \frac{d\omega}{2\pi} \frac{2}{\omega^2 + (p^2)^2} \sum_{ij} k_i k_j (e^{ip(x_i-x_j)+i\omega(t_i-t_j)} - 1) \\ &= \int \frac{d^D p}{(2\pi)^D} \int \frac{d\omega}{2\pi} \frac{2}{\omega^2 + (p^2)^2} \left| \sum_i k_i e^{ipx_i + \omega t_i} \right|^2. \end{aligned} \tag{3.19}$$

To get the second line, Eq. (3.17) has been used. Note that again due to Eq. (3.17), the integral is ultraviolet convergent and thus positive. It vanishes if and only if the

charge-density, regarded as a function of space *and* time, vanishes. This is possible if and only if endpoints of the dipoles (which form the interaction) are at the same point in space *and* time.

Thus when integrating in Eq. (3.14) over x_i and t_i , no divergence can occur at finite distances. To renormalize the theory, only short distance divergences have to be removed by adding appropriate counter-terms. They are analyzed via a multilocal operator product expansion (MOPE) [50,51]. For a detailed discussion of the MOPE and examples see Refs. [50–52,54,47]. The main result of this analysis is, like in scalar field theory, that *in any order of perturbation theory, only a finite number of counter-terms is necessary and that these are exactly those terms, which are already present in the original theory.* The theory is thus multiplicatively renormalizable. To actually evaluate the counter-terms, a multilocal operator product expansion is used, which is described in the next sections. The general idea is always to study the behavior of n disorder-vertices on approaching their end-points. The resulting term is expanded into a product of a (multi-local) operator, times a MOPE coefficient, which is a homogeneous function of the distances involved. Power-counting then indicates that as long as the operator is relevant or marginal in the RG sense, the integral over the distances possesses an UV-divergence, and thus requires a counter-term in the Hamiltonian. On the other hand, when the operator is irrelevant in the RG sense, then the integral over the MOPE coefficient is globally UV-convergent, and no counter-term is needed. This procedure is constructed such, that possible sub-divergences are taken care of recursively as in the BPHZ scheme. A formal proof of this statement is given in the context of a simpler model in [51], see also Ref. [47].

3.3. Divergences associated with local operators

We now analyze our specific model, using the techniques of the multilocal operator product expansion (MOPE) [50,51]. The first class of divergences stems from configurations where the two end-points of the interaction vertex are approached. The interaction vertex is

$$\begin{aligned}
 \text{---} \bullet \xrightarrow{\text{L}} \text{---} \bullet \text{---} g_{\text{L}} + \text{---} \bullet \xrightarrow{\text{T}} \text{---} \bullet \text{---} g_{\text{T}} &= \int_k \tilde{r}_{\alpha}(x, t) e^{ik[r(x,t) - r(y,t')]} \tilde{r}_{\beta}(y, t') \\
 &\times (P_{\alpha\beta}^{\text{L}}(k) g_{\text{L}} + P_{\alpha\beta}^{\text{T}}(k) g_{\text{T}}) |k|^{a-d} h(x - y).
 \end{aligned}
 \tag{3.20}$$

For short-range forces set $a = d$.

In order to extract the divergences for small $x - y$ and $t - t'$, the first possibility is not to contract any response-field. We then start by normal-ordering the r.h.s. of Eq. (3.20). As usual in statistical field theory, we define the normal-ordered operator $: \mathcal{O} :$ starting from the operator \mathcal{O} by

$$: \mathcal{O} := \mathcal{O} - \text{all self-contractions},
 \tag{3.21}$$

where the self-contractions are taken with respect to the free theory. The idea is that in order to calculate the insertion of $:\mathcal{O}:$ into some expectation value only contractions of $:\mathcal{O}:$ with the other operators in this expectation value have to be taken. This implies that the operator $:\mathcal{O}_1(x, t)\mathcal{O}_2(0, 0):$ is always free of divergences for $(x, t) \rightarrow (0, 0)$.

Using the identity

$$e^{ikr(x,t)} e^{-ikr(y,t')} =: e^{ikr(x,t)} e^{-ikr(y,t')} : e^{-k^2 C(x-y, t-t')}, \tag{3.22}$$

one can expand the normal-ordered vertex-operators on the r.h.s. for small $x - y$ and $t - t'$. The leading contribution is

$$\mathbf{1} e^{-k^2 C(x-y, t-t')}, \tag{3.23}$$

yielding the first term in the short-distance expansion of Eq. (3.20) (for the normalization of the k -integral cf. Eq. (2.12)):

$$\begin{aligned} & \int_k e^{-k^2 C(x-y, t-t')} : \tilde{r}_\alpha(x, t) \tilde{r}_\beta(y, t') : (P_{\alpha\beta}^L(k) g_L + P_{\alpha\beta}^T(k) g_T) |k|^{a-d} h(x-y) \\ &= \tilde{r} \left(\frac{x+y}{2}, \frac{t+t'}{2} \right)^2 \left(g_T \left(1 - \frac{1}{d} \right) + g_L \frac{1}{d} \right) C(x-y, t-t')^{-a/2} h(x-y) \\ & \quad + \text{subleading terms} \\ &= \text{---} \left(g_T \left(1 - \frac{1}{d} \right) + g_L \frac{1}{d} \right) C(x-y, t-t')^{-a/2} h(x-y) \\ & \quad + \text{subleading terms.} \end{aligned} \tag{3.24}$$

By going from the first to the second line, two things have been used: First, since the integral over k is rotationally invariant, only terms with $\alpha = \beta$ survive, with a geometric factor of $1/d$ for the transversal and $(1 - 1/d)$ for the longitudinal projector. Second, since $:\tilde{r}(x, t)\tilde{r}(y, t'):$ is *normal-ordered*, i.e. all contractions between the two fields \tilde{r} have been eliminated and no short-distance singularities remain, it can be written as

$$\begin{aligned} : \tilde{r}(x, t) \tilde{r}(y, t') : &= : \tilde{r} \left(\frac{x+y}{2}, \frac{t+t'}{2} \right)^2 : \\ &+ : \tilde{r} \left(\frac{x+y}{2}, \frac{t+t'}{2} \right) [2(x-y)\nabla] \tilde{r} \left(\frac{x+y}{2}, \frac{t+t'}{2} \right) : \\ &+ : \tilde{r} \left(\frac{x+y}{2}, \frac{t+t'}{2} \right) \left[2(t-t') \frac{2\partial}{\partial t} \right] \tilde{r} \left(\frac{x+y}{2}, \frac{t+t'}{2} \right) : \\ &+ \mathcal{O}((x-y)^2) + \mathcal{O}((t-t')^2) + \mathcal{O}(x-y) \mathcal{O}(t-t'). \end{aligned} \tag{3.25}$$

From this expansion, only the first term has to be retained and will give a correction to the marginal operator $\text{---} = \tilde{r}^2$ in the action. The following terms are *irrelevant* (in the RG sense) with respect to this dominant term and can therefore be neglected.

Dropping the explicit normal ordering of \tilde{r}^2 which is a pure number, and zero by analytic continuation, leads to Eq. (3.24).

Note that when expanding the product of two operators as sum of normal ordered ones, this sum runs over all possible contractions. The second contribution to the normal-ordered product of Eq. (3.20) is therefore obtained upon contracting one response field. Due to causality, this must be the field with the smaller time-argument. For simplicity, let us take $t > 0$ and put $y = t' = 0$. By the same procedure as above, we obtain the following contribution:

$$\int_k : \tilde{r}_\alpha(x, t) e^{ik(r(x,t)-r(0,0))} : R(x, t) (ik)_\beta e^{-k^2 C(x,t)} \times (P_{\alpha\beta}^L(k) g_L + P_{\alpha\beta}^T(k) g_T) |k|^{a-d} h(x-y). \tag{3.26}$$

The next step is to expand : $e^{ik(r(x,t)-r(0,0))}$: about (x, t) . (It is important to expand about (x, t) as otherwise $\tilde{r}(x, t)$ had to be expanded, too.) This expansion is

$$: e^{ik(r(x,t)-r(0,0))} : = \mathbf{1} + (ik)_\gamma \left(t \dot{r}_\gamma(x, t) + (x \nabla)_\gamma r_\gamma(x, t) - \frac{1}{2} (x \nabla)^2 r_\gamma(x, t) \right) + \text{subleading terms.} \tag{3.27}$$

Upon inserting Eq. (3.27) into Eq. (3.26) and integration over k , only terms even in k survive. We can also neglect the term linear in x , which is odd under space reflection. The remaining terms are

$$\int_k : \tilde{r}_\alpha(x, t) \left(t \dot{r}_\gamma(x, t) - \frac{1}{2} (x \nabla)^2 r_\gamma(x, t) \right) : (ik)_\gamma (ik)_\beta R(x, t) e^{-k^2 C(x,t)} \times (P_{\alpha\beta}^L(k) g_L + P_{\alpha\beta}^T(k) g_T) |k|^{a-d} h(x) = -R(x, t) \frac{a}{2d} C(x, t)^{-a/2-1} h(x) \left(t \text{ } \rightsquigarrow \bullet + \frac{x^2}{2D} \text{ } \rightsquigarrow \blacklozenge \right) g_L. \tag{3.28}$$

For the contribution proportional to $\rightsquigarrow \blacklozenge$, we have retained from the tensor operator $\tilde{r}(x, t) (x \nabla)^2 r(x, t)$ only the diagonal contribution $\frac{1}{D} \tilde{r}(x, t) x^2 (\Delta) r(x, t)$, which is sufficient at 1-loop order. For the subtleties associated with the insertion of this operator at the 2-loop level cf. Ref. [52]. Using the FDT, Eq. (3.12), this can still be simplified to

$$\frac{\partial}{\partial t} C(x, t)^{-a/2} \left(\frac{t}{d} \text{ } \rightsquigarrow \bullet + \frac{x^2}{2dD} \text{ } \rightsquigarrow \blacklozenge \right) g_L. \tag{3.29}$$

Eqs. (3.24) and (3.29) contain all possible divergent terms in the short-distance expansion of Eq. (3.20) and all terms which have to be taken into account in 1-loop order. Notably, due to causality, no term independent of \tilde{r} appears.

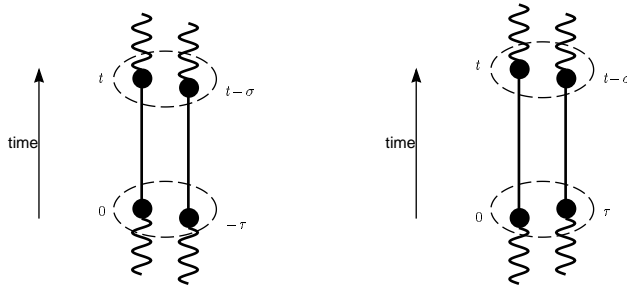


Fig. 6. The diagrams D_1 (left) and D_2 (right).

3.4. The renormalization of the disorder (divergences associated with bilocal operators)

There are also UV-divergent configurations associated to bilocal operators, which renormalize the disorder, and which are depicted in Fig. 6. A dashed line indicates that the end-points of the interaction vertices are approached in space and time. Up to permutations of the two interaction vertices, there are two possibilities to order their end-points in time, namely D_1 and D_2 in Fig. 6. We first calculate D_1 , starting from

$$\begin{aligned}
 \tilde{r}_\alpha(y, t) &\int_k (g_T P_{\alpha\beta}^T(k) + g_L P_{\alpha\beta}^L(k)) |k|^{a-d} h(x - y) e^{ik(r(y,t) - r(x,0))} \tilde{r}_\beta(x, 0) \\
 &\times \tilde{r}_\gamma(y', t - \sigma) \int_p (g_T P_{\gamma\delta}^T(p) + g_L P_{\gamma\delta}^L(p)) |p|^{a-d} h(x' - y') \\
 &\times e^{ik(r(y', t - \sigma) - r(x', -\tau))} \tilde{r}_\delta(x', -\tau).
 \end{aligned}
 \tag{3.30}$$

For small $x - x'$, $y - y'$, τ and σ , with $\tau, \sigma > 0$, there is one contribution for the renormalization of the interaction vertex. First, due to causality, $\tilde{r}_\gamma(y', t - \sigma)$ and $\tilde{r}_\delta(x', -\tau)$ have to be contracted with a correlator field in order to obtain two response fields at the end. Then the short-distance expansion for nearby vertex-operators reads

$$\begin{aligned}
 e^{ikr(y,t)} e^{ipr(y', t - \sigma)} &\approx e^{i(k+p)r(y,t)} e^{kpC(y - y', \sigma)}, \\
 e^{-ikr(x,0)} e^{-ipr(x', -\tau)} &\approx e^{-i(k+p)r(x,0)} e^{kpC(x - x', \tau)}.
 \end{aligned}
 \tag{3.31}$$

This yields up to subleading terms

$$\begin{aligned}
 &\int_k \int_p \tilde{r}_\alpha(y, t) \tilde{r}_\beta(x, 0) e^{i(k+p)(r(y,t) - r(x,0))} \\
 &\times (g_T P_{\alpha\beta}^T(k) + g_L P_{\alpha\beta}^L(k)) (g_T P_{\gamma\delta}^T(p) + g_L P_{\gamma\delta}^L(p)) \\
 &\times (ik)_\gamma (-ik)_\delta R(y - y', \sigma) R(x - x', \tau) e^{kp(C(y - y', \sigma) + C(x - x', \tau))} \\
 &\times |k|^{a-d} |p|^{a-d} h(x - y) h(x' - y').
 \end{aligned}
 \tag{3.32}$$

In the next step, first k and second p are shifted:

$$k \rightarrow k - p, \quad p \rightarrow p + \frac{k}{2}. \tag{3.33}$$

The result is

$$\int_k \tilde{r}_\alpha(y, t) \tilde{r}_\beta(x, 0) e^{ik(r(y,t) - r(x,0))} \left[\int_p (g_T P_{\alpha\beta}^T(p - k/2) + g_L P_{\alpha\beta}^L(p - k/2)) \right. \\ \times (g_T P_{\gamma\delta}^T(p + k/2) + g_L P_{\gamma\delta}^L(p + k/2)) \\ \times (k/2 - p)_\gamma (k/2 - p)_\delta |p + k/2|^{a-d} |p - k/2|^{a-d} \\ \left. \times R(y - y', \sigma) R(x - x', \tau) e^{(k^2/4 - p^2)(C(y - y', \sigma) + C(x - x', \tau))} h(x - y) h(x' - y') \right]. \tag{3.34}$$

To compute the correction proportional to the disorder vertex, the expression in the rectangular brackets is expanded for small k . As the integral has a well-defined limit for $k \rightarrow 0$, convergent for $d > 2$, neither a term of the form $k_\alpha k_\beta / k^2$, nor a term of the form $|k|^{a-d}$ with $a < d$ can be generated. We conclude that in the LR-case only SR disorder is generated. In the remainder of this sections, we therefore focus on short-range correlated forces setting $a = d$. The leading term of the above expansion is then (the p -integral being defined in Eq. (2.12))

$$\alpha \text{---} \text{---} \text{---} \beta \int_p (g_T (\delta_{\alpha\beta} - p^{-2} p_\alpha p_\beta) + g_L p^{-2} p_\alpha p_\beta) g_L p^2 e^{-p^2(C(y - y', \sigma) + C(x - x', \tau))} \\ \times R(y - y', \sigma) R(x - x', \tau) h(x' - y') \\ = \text{---} \text{---} \text{---} \left(g_T \left(1 - \frac{1}{d} \right) + g_L \frac{1}{d} \right) g_L \frac{d}{2} (C(y - y', \sigma) + C(x - x', \tau))^{-d/2-1} \\ \times \dot{C}(y - y', \sigma) \dot{C}(x - x', \tau) h(x' - y') \\ = \text{---} \text{---} \text{---} \left(g_T \left(1 - \frac{1}{d} \right) + g_L \frac{1}{d} \right) g_L \\ \times \frac{2}{d-2} \frac{\partial}{\partial \tau} \frac{\partial}{\partial \sigma} (C(y - y', \sigma) + C(x - x', \tau))^{-d/2+1} \\ \times h((x - y) - (x' - y')). \tag{3.35}$$

In the last formula we have rearranged the product of h -functions, using the fact that they are always δ -distributions for the cases of interest. Note also that we have used the (perturbative) FDT, Eq. (3.12), for the first transformation.

The second possible way to do the contraction, see D_2 in Fig. 6, is performed similarly. The leading term is

$$\text{---} \text{---} \text{---} \frac{-1}{d} g_L^2 \frac{2}{d-2} \frac{\partial}{\partial \tau} \frac{\partial}{\partial \sigma} (C(y - y', \sigma) + C(x - x', \tau))^{-d/2+1} \\ \times h((x - y) - (x' - y')). \tag{3.36}$$

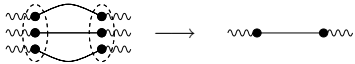
Note that there are two other possible contractions, which can be obtained from D_1 and D_2 by replacing τ and σ with $-\tau$ and $-\sigma$ respectively. Together they add up to

$$\begin{aligned}
 \text{---}\bullet\text{---}\bullet\text{---} & g_L g_T \frac{4}{d-2} \left(1 - \frac{1}{d}\right) \frac{\partial}{\partial \tau} \frac{\partial}{\partial \sigma} \left(C(y-y', \sigma) + C(x-x', \tau)\right)^{-d/2+1} \\
 & \times h((x-y) - (x'-y')). \tag{3.37}
 \end{aligned}$$

This result is remarkable in several respects: First, the contribution to the renormalization of disorder from the disorder-disorder contraction is *isotropic*. We will see that this stabilizes the isotropic fixed point. Second, there is no divergent contribution in the purely transversal or purely longitudinal case at 1-loop order. (Note however that there are finite contributions in the transversal case, see appendix C, such that isotropic disorder will be generated at 2-loop order.)

3.5. Beyond the leading order

The MOPE coefficients evaluated in the last two subsections are sufficient to derive the RG equations at leading order. Subleading orders are analyzed similarly, with the result that the only diverging contributions, and thus those which have to be renormalized, are proportional to the terms already present in the action. An explicit example is the second order term from the contraction of three disorder-vertices towards a single one as



$$\text{---}\bullet\text{---}\bullet\text{---}\bullet\text{---} \longrightarrow \text{---}\bullet\text{---} \tag{3.38}$$

Another question is, whether the fixed point as given in leading order, is stable towards perturbations with respect to subleading terms, i.e. those which are irrelevant at the trivial (Gaussian) fixed point. This is a difficult question, and cannot be studied in its generality here. However, we shall show later in Section 4.7 that the physically important perturbation by self-avoidance is indeed irrelevant at the 1-loop fixed point to be described below.

3.6. List of the MOPE coefficients

We have identified the 1-loop divergences, and shall now compute explicitly the counter-terms needed to render the action finite to 1-loop order. To summarize, we first give a list of the corrections to each term in the original action in the form of the MOPE coefficients for the diagonal case ($g_L = g_T$). Then the MOPE coefficients for the transversal and longitudinal disorder are expressed with its help. To simplify notations, the fluctuation-dissipation theorem (3.12) has been used. Concerning the notation: $(A|B)$ means the contribution from the contraction A proportional to B , and is expressed in terms of the relative distances. From Eq. (3.24) we obtain

$$\left(\text{---}\bullet\text{---}\bullet\text{---} \left| \text{---}\bullet\text{---} \right. \right) = C(x, t)^{-a/2} h(x) \tag{3.39}$$

$$\left(\begin{array}{c} \text{L} \\ \text{---} \end{array} \left| \begin{array}{c} \text{---} \\ \text{---} \end{array} \right. \right) = \frac{1}{d} \left(\begin{array}{c} \text{---} \\ \text{---} \end{array} \left| \begin{array}{c} \text{---} \\ \text{---} \end{array} \right. \right) \quad (3.40)$$

$$\left(\begin{array}{c} \text{T} \\ \text{---} \end{array} \left| \begin{array}{c} \text{---} \\ \text{---} \end{array} \right. \right) = \left(1 - \frac{1}{d} \right) \left(\begin{array}{c} \text{---} \\ \text{---} \end{array} \left| \begin{array}{c} \text{---} \\ \text{---} \end{array} \right. \right). \quad (3.41)$$

The other local divergences are determined from Eq. (3.29):

$$\left(\begin{array}{c} \text{---} \\ \text{---} \end{array} \left| \begin{array}{c} \text{---} \\ \text{---} \end{array} \right. \right) = \frac{1}{d} t \frac{\partial}{\partial t} C(x, t)^{-a/2} h(x) \quad (3.42)$$

$$\left(\begin{array}{c} \text{L} \\ \text{---} \end{array} \left| \begin{array}{c} \text{---} \\ \text{---} \end{array} \right. \right) = \left(\begin{array}{c} \text{---} \\ \text{---} \end{array} \left| \begin{array}{c} \text{---} \\ \text{---} \end{array} \right. \right) \quad (3.43)$$

$$\left(\begin{array}{c} \text{T} \\ \text{---} \end{array} \left| \begin{array}{c} \text{---} \\ \text{---} \end{array} \right. \right) = 0 \quad (3.44)$$

and

$$\left(\begin{array}{c} \text{---} \\ \text{---} \end{array} \left| \begin{array}{c} \text{---} \\ \text{---} \end{array} \right. \right) = \frac{1}{2dD} x^2 \frac{\partial}{\partial t} C(x, t)^{-a/2} h(x) \quad (3.45)$$

$$\left(\begin{array}{c} \text{L} \\ \text{---} \end{array} \left| \begin{array}{c} \text{---} \\ \text{---} \end{array} \right. \right) = \left(\begin{array}{c} \text{---} \\ \text{---} \end{array} \left| \begin{array}{c} \text{---} \\ \text{---} \end{array} \right. \right) \quad (3.46)$$

$$\left(\begin{array}{c} \text{T} \\ \text{---} \end{array} \left| \begin{array}{c} \text{---} \\ \text{---} \end{array} \right. \right) = 0. \quad (3.47)$$

Diagrams proportional to $\text{---} \text{---}$, renormalizing the stiffness, will of course vanish in the directed case.

The bilocal divergences, proportional to the disorder vertex, are

$$\left(\begin{array}{c} \text{---} \\ \text{---} \end{array} \left| \begin{array}{c} \text{---} \\ \text{---} \end{array} \right. \right) = \frac{4}{d-2} \left(1 - \frac{1}{d} \right) \times \frac{\partial}{\partial \tau} \frac{\partial}{\partial \sigma} (C(x, \tau) + C(y, \sigma))^{-d/2+1} h(x-y) \quad (3.48)$$

$$\left(\begin{array}{c} \text{L} \\ \text{---} \\ \text{T} \\ \text{---} \end{array} \left| \begin{array}{c} \text{---} \\ \text{---} \end{array} \right. \right) = \frac{1}{2} \left(\begin{array}{c} \text{---} \\ \text{---} \end{array} \left| \begin{array}{c} \text{---} \\ \text{---} \end{array} \right. \right) \quad (3.49)$$

$$\left(\begin{array}{c} \text{L} \\ \text{---} \\ \text{L} \\ \text{---} \end{array} \left| \begin{array}{c} \text{---} \\ \text{---} \end{array} \right. \right) = 0 \quad (3.50)$$

$$\left(\begin{array}{c} \text{T} \\ \text{---} \\ \text{T} \\ \text{---} \end{array} \left| \begin{array}{c} \text{---} \\ \text{---} \end{array} \right. \right) = 0. \quad (3.51)$$

Remember that in the LR-case, this class of diagrams vanishes.

3.7. The residues in the directed case

Let us start by analyzing the directed case, i.e. $h(x) = \delta^D(x)$. Using the MOPE coefficients given in the last subsection, we can calculate the diverging part of the

diagrams as pole in

$$\varepsilon = 2 - \zeta_0 a, \tag{3.52}$$

where

$$\zeta_0 = \frac{2 - D}{2}, \tag{3.53}$$

and setting $a = d$ for SR. For $\varepsilon > 0$, the integrals are UV-convergent and we put an IR-cutoff L in position space and L^2 in time. Note that reintroducing λ this would yield a “physical” time cut-off λL^2 . The precise procedure is irrelevant at 1-loop order, cf. Ref. [53]. Note that

$$h(x) = \delta^D(x) \tag{3.54}$$

always eliminates one space integration.

Start with an explicit example. Let us define a Feynman diagram as the integral of the MOPE coefficient over all distances in space and time, bounded by L and L^2 respectively (for details, see Ref. [52]). For the MOPE coefficient $\left(\text{loop diagram} \mid \text{external line} \right)$ this reads

$$\begin{aligned} \left\langle \text{loop diagram} \mid \text{external line} \right\rangle_L &:= \int_{t < L^2} \left(\text{loop diagram} \mid \text{external line} \right) \\ &= \int_0^{L^2} dt C(0, t)^{-a/2} \\ &= P \int_0^{L^2} dt t^{-\zeta_0 a/2} \\ &= P \frac{2}{\varepsilon} L^\varepsilon, \end{aligned} \tag{3.55}$$

where

$$P = C(0, t = 1)^{-a/2} = \left(\frac{(2 - D)(4\pi)^{D/2}}{2} \right)^{a/2}. \tag{3.56}$$

We introduce the following abbreviation for the pole term, which has to be subtracted in the minimal subtraction scheme:

$$\mathcal{A}^{\text{dir}} := \left\langle \text{loop diagram} \mid \text{external line} \right\rangle_\varepsilon = 2P. \tag{3.57}$$

The divergent contribution to the friction coefficient is obtained from

$$\left\langle \text{loop diagram} \mid \text{external line} \right\rangle_L = \int_{t < L^2} \left(\text{loop diagram} \mid \text{external line} \right)$$

$$\begin{aligned}
 &= \int_0^{L^2} dt \frac{t}{d} \frac{\partial}{\partial t} C(0, t)^{-a/2} \\
 &= - \int_0^{L^2} dt \frac{1}{d} C(0, t)^{-a/2} + \mathcal{O}(\varepsilon^0) \\
 &= -\frac{1}{d} P \int_0^{L^2} dt t^{-\zeta_0 a/2} + \mathcal{O}(\varepsilon^0) \\
 &= -\frac{1}{d} P \frac{2}{\varepsilon} L^\varepsilon + \mathcal{O}(\varepsilon^0), \tag{3.58}
 \end{aligned}$$

with P introduced in Eq. (3.56). The pole term, which has to be subtracted in the minimal subtraction scheme, is

$$\left\langle \left(\text{diagram} \right) \middle| \text{diagram} \right\rangle_\varepsilon = -\frac{2}{d} P. \tag{3.59}$$

Remarkably

$$\left\langle \left(\text{diagram} \right) \middle| \text{diagram} \right\rangle_\varepsilon = -d \left\langle \left(\text{diagram} \right) \middle| \text{diagram} \right\rangle_\varepsilon. \tag{3.60}$$

This relation can be viewed as a consequence of the (perturbative) FDT, and is responsible for the non-renormalization of the temperature in the longitudinal case, where a FDT holds in the full theory.

Since the disorder vertex is local in x -space (“statistical tilt invariance”), there is no contribution proportional to $\tilde{r}(-\Delta)r$:

$$\left\langle \left(\text{diagram} \right) \middle| \text{diagram} \right\rangle_\varepsilon = 0. \tag{3.61}$$

The renormalization of the disorder interaction is (for $a = d$ only) obtained from

$$\begin{aligned}
 &\left\langle \left(\text{diagram} \right) \middle| \text{diagram} \right\rangle_L \\
 &= \int_0^L d^D x \int_0^{L^2} d\tau \int_0^{L^2} d\sigma \frac{4}{d-2} \left(1 - \frac{1}{d}\right) \frac{\partial}{\partial \tau} \frac{\partial}{\partial \sigma} (C(x, \tau) + C(x, \sigma))^{-d/2+1} \\
 &= \frac{4}{d-2} \left(1 - \frac{1}{d}\right) S_D \int_0^L \frac{dx}{x} x^D (2C(x, 0))^{-d/2+1} + \text{finite terms}, \tag{3.62}
 \end{aligned}$$

resulting in

$$\mathcal{B}^{\text{dir}} := \left\langle \left(\text{diagram} \right) \middle| \text{diagram} \right\rangle_\varepsilon = \frac{4}{d-2} \left(1 - \frac{1}{d}\right) Q, \tag{3.63}$$

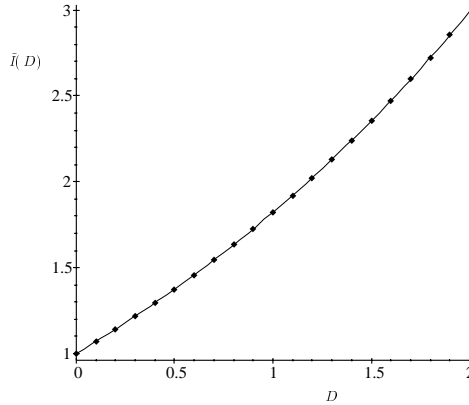


Fig. 7. The function $\tilde{I}(D)$. The dots have been obtained numerically, the interpolating line is a polynomial fit of fifth degree, later used in the extrapolations.

where

$$Q = \left(\frac{2}{(2 - D)S_D} \right)^{1-d/2} S_D. \tag{3.64}$$

with $S_D = 2\pi^{D/2}/\Gamma[D/2]$. This terminates the evaluation of the Feynman diagrams in the directed case.

3.8. The residues in the isotropic (non-directed) case

In the isotropic, i.e. non-directed case with

$$h(x) = 1, \tag{3.65}$$

the dimensional regularization parameter is

$$\varepsilon = 2 + D - \zeta_0 a. \tag{3.66}$$

We now parallel the calculation of diagrams from the last subsection. The term proportional to $\text{---}\bullet\text{---}$ (see Eq. (3.39)) is

$$\begin{aligned} \left\langle \text{---}\bullet\text{---} \left| \text{---}\bullet\text{---} \right\rangle_L &= \int_0^L d^D x \int_0^{L^2} dt \left(\text{---}\bullet\text{---} \left| \text{---}\bullet\text{---} \right\rangle \right) \\ &= S_D \int_0^L \frac{dx}{x} x^D \int_0^{L^2} dt C(x, t)^{-a/2} \\ &= S_D \frac{L^\varepsilon}{\varepsilon} \int_0^\infty dt C(1, t)^{-a/2} + \text{finite}, \end{aligned} \tag{3.67}$$

where in addition a has to be set to $a_c(D)$, defined by $\varepsilon(D, a_c) = 0$. Here $a_c = 2(2 + D)/(2 - D)$. The residue is

$$\mathcal{A}^{\text{iso}} := \left\langle \left[\text{diagram: a loop with two vertices and a wavy line} \right] \left| \left[\text{diagram: a wavy line with a vertex} \right] \right\rangle_\varepsilon = S_D \int_0^\infty dt C(1, t)^{-a_c(D)/2} =: I(D). \tag{3.68}$$

where the expression for the free correlator (obtained e.g. via time integration of the free response function) reads

$$\begin{aligned} C(1, t) &= \frac{\Gamma\left(\frac{D}{2}\right)}{2(2 - D)\pi^{\frac{D}{2}}} + \frac{1}{4\pi^{\frac{D}{2}}} \Gamma\left(-1 + \frac{D}{2}, \frac{1}{4t}\right) \\ &= \frac{1}{2(2 - D)\pi^{\frac{D}{2}}} \left[\Gamma\left(\frac{D}{2}\right) + (4t)^{\frac{2-D}{2}} e^{-\frac{1}{4t}} - \Gamma\left(\frac{D}{2}, \frac{1}{4t}\right) \right], \end{aligned} \tag{3.69}$$

where we have abbreviated the incomplete Γ -function as

$$\Gamma(a, b) = \int_b^\infty dt t^{a-1} e^{-t}. \tag{3.70}$$

We could not find a closed analytical form for the integral $I(D)$. Using the approximation for the correlator

$$C(1, t) \approx \frac{2}{(2 - D)(4\pi)^{D/2}} \left(|t| + \frac{2}{D} \right)^{\zeta_0}, \tag{3.71}$$

which works astonishingly well numerically, we obtain for the integral $I(D)$

$$\begin{aligned} I(D) &= S_D \left(\frac{(2 - D)(4\pi)^{D/2}}{2} \right)^{a/2} \left(\frac{2}{D} \right)^{1-D/2} \tilde{I}(D) \\ &= S_D (S_D(2 - D))^{a/2} \left[2^{D-2} \Gamma\left(\frac{D}{2}\right) \right]^{a/2} \left(\frac{2}{D} \right)^{1-D/2} \tilde{I}(D). \end{aligned} \tag{3.72}$$

where a must be set to $a = a_c(D)$. If the approximation in Eq. (3.71) was exact, $\tilde{I}(D)$ would equal 1. This is not the case, and the value for $\tilde{I}(D)$ obtained from numerical integration is plotted in Fig. 7. It is a slowly varying function though, well behaved at $D = 0$ and $D = 2$. Note also that in Eq. (3.72) a factor of $S_D (S_D(2 - D))^{a/2}$ is factorized which is common to all other diagrams and will therefore cancel at the end.

Proceeding equivalently, the diagram correcting the friction coefficient is calculated as

$$\left\langle \left[\text{diagram: a loop with two vertices and a wavy line} \right] \left| \left[\text{diagram: a wavy line with a vertex} \right] \right\rangle_\varepsilon = -\frac{S_D}{d} \int_0^\infty dt C(1, t)^{-a/2} = -\frac{1}{d} I(D). \tag{3.73}$$

Like in the directed case, we have

$$\left\langle \left[\text{diagram: a loop with two vertices and a wavy line} \right] \left| \left[\text{diagram: a wavy line with a vertex} \right] \right\rangle_\varepsilon = -d \left\langle \left[\text{diagram: a loop with two vertices and a wavy line} \right] \left| \left[\text{diagram: a wavy line with a vertex} \right] \right\rangle_\varepsilon. \tag{3.74}$$

This relation can be used to simplify the RG-calculations. As in the directed case, it is a reflection of the FDT, valid in perturbation theory, and in the longitudinal case in the full theory.

In contrast to the directed case, the stiffness of the membrane is renormalized through

$$\begin{aligned}
 \left\langle \text{Diagram} \middle| \text{Diagram} \right\rangle_L &= \int_0^L d^D x \int_0^{L^2} dt \left(\text{Diagram} \middle| \text{Diagram} \right) \\
 &= \frac{1}{2dD} \int_0^L d^D x \int_0^{L^2} dt x^2 \frac{\partial}{\partial t} C(x, t)^{-a/2} \\
 &= -\frac{1}{2dD} S_D \int_0^L \frac{dx}{x} x^{D+2} C(x, 0)^{-a/2} + \text{finite} \\
 &= -\frac{1}{2dD} S_D ((2 - D) S_D)^{a/2} \frac{L^\varepsilon}{\varepsilon} + \text{finite}. \tag{3.75}
 \end{aligned}$$

The residue is therefore given by

$$-\frac{C^{\text{iso}}}{d} := \left\langle \text{Diagram} \middle| \text{Diagram} \right\rangle_\varepsilon = -\frac{1}{2dD} \times S_D ((2 - D) S_D)^{a/2}. \tag{3.76}$$

Finally, the diagram correcting the disorder vertex is (for $a = d$ only) evaluated as follows:

$$\begin{aligned}
 &\left\langle \text{Diagram} \middle| \text{Diagram} \right\rangle_L \\
 &= \int_0^L d^D x \int_0^L d^D y \int_0^{L^2} d\tau \int_0^{L^2} d\sigma \frac{4}{d-2} \left(1 - \frac{1}{d}\right) \frac{\partial}{\partial \tau} \frac{\partial}{\partial \sigma} (C(x, \tau) + C(y, \sigma))^{-d/2+1} \\
 &= \frac{4}{d-2} \left(1 - \frac{1}{d}\right) S_D^2 \int_0^L \frac{dx}{x} x^D \int_0^L \frac{dy}{y} y^D (C(x, 0) + C(y, 0))^{-d/2+1} + \text{finite terms} \\
 &= \frac{4}{d-2} \left(1 - \frac{1}{d}\right) S_D^2 \int_0^\infty \frac{dx}{x} x^D (C(x, 0) + C(1, 0))^{-d/2+1} \frac{L^\varepsilon}{\varepsilon} + \text{finite terms} \\
 &= \frac{4}{d-2} \left(1 - \frac{1}{d}\right) S_D^2 ((2 - D) S_D)^{d/2-1} \int_0^\infty \frac{dx}{x} x^D (x^{2-D} + 1)^{-d/2+1} \frac{L^\varepsilon}{\varepsilon} \\
 &\quad + \text{finite terms} \\
 &= \frac{4}{d-2} \left(1 - \frac{1}{d}\right) S_D^2 ((2 - D) S_D)^{d/2-1} \frac{1}{2-D} \frac{\Gamma^2\left(\frac{D}{2-D}\right)}{\Gamma\left(\frac{2D}{2-D}\right)} \frac{L^\varepsilon}{\varepsilon} + \text{finite terms}. \tag{3.77}
 \end{aligned}$$

The residue is given by the expression

$$\begin{aligned}
 \mathcal{B}^{\text{iso}} &:= \left\langle \begin{array}{c} \text{Diagram: A bubble with four vertices and two external wavy lines} \end{array} \middle| \begin{array}{c} \text{Diagram: A propagator with two external wavy lines} \end{array} \right\rangle_{\varepsilon} \\
 &= \frac{4}{d-2} \left(1 - \frac{1}{d}\right) \frac{1}{(2-D)^2} \frac{\Gamma^2\left(\frac{D}{2-D}\right)}{\Gamma\left(\frac{2D}{2-D}\right)} \times S_D ((2-D)S_D)^{d/2}. \quad (3.78)
 \end{aligned}$$

The factor involving the Γ -functions is familiar from the renormalization of the interaction vertex for self-avoiding membranes.

3.9. The particle limit

In this section, we demonstrate that our model reproduces, both in the directed and in the isotropic case, the known results for the particle upon taking the limit $D \rightarrow 0$. Some subtleties have to be taken into account. Study first the directed case. Then unambiguously

$$\lim_{D \rightarrow 0} \left\langle \begin{array}{c} \text{Diagram: A bubble with four vertices and two external wavy lines} \end{array} \middle| \begin{array}{c} \text{Diagram: A propagator with two external wavy lines} \end{array} \right\rangle_{\varepsilon}^{\text{dir}} = 2. \quad (3.79)$$

The other independent and non-vanishing digram is in the limit of small D and ε

$$\left\langle \begin{array}{c} \text{Diagram: A bubble with four vertices and two external wavy lines} \end{array} \middle| \begin{array}{c} \text{Diagram: A propagator with two external wavy lines} \end{array} \right\rangle_{\varepsilon}^{\text{dir}} \approx \frac{2D}{d-2}. \quad (3.80)$$

Note that it was calculated under the tacit assumption that $\varepsilon \rightarrow 0$ is taken *first*. In order to perform the limit $D \rightarrow 0$, we insert $d-2 = 2\frac{D-\varepsilon}{2-D}$ into Eq. (3.80) and then perform the limit $\varepsilon \rightarrow 0$. We obtain

$$\left\langle \begin{array}{c} \text{Diagram: A bubble with four vertices and two external wavy lines} \end{array} \middle| \begin{array}{c} \text{Diagram: A propagator with two external wavy lines} \end{array} \right\rangle_{\varepsilon} \approx \frac{D(2-D)}{D-\varepsilon} \xrightarrow{\varepsilon \rightarrow 0} 2-D \xrightarrow{D \rightarrow 0} 2. \quad (3.81)$$

One easily verifies that these results coincide with a direct calculation for the particle, obtained by using the single-particle propagator and response functions and by omitting the space integration from the very beginning. The isotropic case reduces to the particle case along the same lines. First

$$\begin{aligned}
 \lim_{D \rightarrow 0} \left\langle \begin{array}{c} \text{Diagram: A bubble with four vertices and two external wavy lines} \end{array} \middle| \begin{array}{c} \text{Diagram: A propagator with two external wavy lines} \end{array} \right\rangle_{\varepsilon}^{\text{iso}} &= 2, \\
 \lim_{D \rightarrow 0} \left\langle \begin{array}{c} \text{Diagram: A bubble with four vertices and two external wavy lines} \end{array} \middle| \begin{array}{c} \text{Diagram: A propagator with two external wavy lines} \end{array} \right\rangle_{\varepsilon}^{\text{iso}} &= 0. \quad (3.82)
 \end{aligned}$$

The last diagram is

$$\left\langle \begin{array}{c} \text{Diagram: A bubble with four vertices and two external wavy lines} \end{array} \middle| \begin{array}{c} \text{Diagram: A propagator with two external wavy lines} \end{array} \right\rangle_{\varepsilon}^{\text{iso}} \approx \frac{4D}{d-2}. \quad (3.83)$$

Note the apparent difference in factor of 2 to Eq. (3.80). Inserting now $d - 2 = 2\frac{2D-\varepsilon}{2-D}$ yields

$$\left\langle \left(\text{diagram with two vertices and wavy lines} \right) \middle| \text{diagram with two vertices and straight lines} \right\rangle_{\varepsilon}^{\text{iso}} \approx -\frac{2D(2-D)}{2D-\varepsilon} \xrightarrow{\varepsilon \rightarrow 0} 2-D \xrightarrow{D \rightarrow 0} 2 \quad (3.84)$$

and thus the same final result, cf. Eq. (3.81).

Our calculations, at least at this order, thus always include the particle case.

3.10. The flow equations

We now introduce renormalized quantities. Going back to the original model, (3.2), we take care to reinsert the factors of λ , which were dropped in intermediate expressions. Define

$$\begin{aligned} r_0 &= \sqrt{Z} r, \\ \tilde{r}_0 &= \sqrt{\tilde{Z}} \tilde{r}, \\ \lambda_0 &= Z_\lambda \lambda. \end{aligned} \quad (3.85)$$

Explicitly, the counter-terms are as follows. First, introducing a counter-term for $\text{diagram with two vertices and wavy lines}$ yields

$$\begin{aligned} \sqrt{Z\tilde{Z}} &= 1 + \left\langle \left(\text{diagram with two vertices and wavy lines} \right) \middle| \text{diagram with two vertices and wavy lines} \right\rangle_{\varepsilon} \frac{g_T}{\varepsilon} + \left\langle \left(\text{diagram with two vertices and wavy lines} \right) \middle| \text{diagram with two vertices and wavy lines} \right\rangle_{\varepsilon} \frac{g_L}{\varepsilon} \\ &= 1 + \left\langle \left(\text{diagram with two vertices and wavy lines} \right) \middle| \text{diagram with two vertices and wavy lines} \right\rangle_{\varepsilon} \frac{g_L}{\varepsilon}. \end{aligned} \quad (3.86)$$

The counter-term for $\lambda \text{diagram with two vertices and wavy lines}$ is given by

$$\begin{aligned} \tilde{Z}Z_\lambda &= 1 - \left\langle \left(\text{diagram with two vertices and wavy lines} \right) \middle| \text{diagram with two vertices and wavy lines} \right\rangle_{\varepsilon} \frac{g_T}{\varepsilon} - \left\langle \left(\text{diagram with two vertices and wavy lines} \right) \middle| \text{diagram with two vertices and wavy lines} \right\rangle_{\varepsilon} \frac{g_L}{\varepsilon} \\ &= 1 - \left\langle \left(\text{diagram with two vertices and wavy lines} \right) \middle| \text{diagram with two vertices and wavy lines} \right\rangle_{\varepsilon} \left(\frac{1}{d} \frac{g_L}{\varepsilon} + \left(1 - \frac{1}{d} \right) \frac{g_T}{\varepsilon} \right). \end{aligned} \quad (3.87)$$

In the isotropic (non-directed) case, there is also a counter-term for $\lambda \text{diagram with two vertices and wavy lines}$ namely

$$\begin{aligned} \sqrt{Z\tilde{Z}}Z_\lambda &= 1 + \left\langle \left(\text{diagram with two vertices and wavy lines} \right) \middle| \text{diagram with two vertices and wavy lines} \right\rangle_{\varepsilon} \frac{g_T}{\varepsilon} + \left\langle \left(\text{diagram with two vertices and wavy lines} \right) \middle| \text{diagram with two vertices and wavy lines} \right\rangle_{\varepsilon} \frac{g_L}{\varepsilon} \\ &= 1 + \left\langle \left(\text{diagram with two vertices and wavy lines} \right) \middle| \text{diagram with two vertices and wavy lines} \right\rangle_{\varepsilon} \frac{g_L}{\varepsilon}. \end{aligned} \quad (3.88)$$

These equations are solved for Z , \tilde{Z} and Z_λ :

$$Z_\lambda = 1 + \left(\left\langle \left(\text{diagram with two vertices and wavy lines} \right) \middle| \text{diagram with two vertices and wavy lines} \right\rangle_{\varepsilon} - \left\langle \left(\text{diagram with two vertices and wavy lines} \right) \middle| \text{diagram with two vertices and wavy lines} \right\rangle_{\varepsilon} \right) \frac{g_L}{\varepsilon}, \quad (3.89)$$

$$\tilde{Z} = 1 + \left(\left\langle \left\langle \text{diagram} \right| \text{diagram} \right\rangle_{\varepsilon} - \left\langle \left\langle \text{diagram} \right| \text{diagram} \right\rangle_{\varepsilon} \right) \frac{g_L}{\varepsilon} - \left\langle \left\langle \text{diagram} \right| \text{diagram} \right\rangle_{\varepsilon} \left(\frac{1}{d} \frac{g_L}{\varepsilon} + \left(1 - \frac{1}{d} \right) \frac{g_T}{\varepsilon} \right), \tag{3.90}$$

$$Z = 1 + \left(\left\langle \left\langle \text{diagram} \right| \text{diagram} \right\rangle_{\varepsilon} + \left\langle \left\langle \text{diagram} \right| \text{diagram} \right\rangle_{\varepsilon} \right) \frac{g_L}{\varepsilon} + \left\langle \left\langle \text{diagram} \right| \text{diagram} \right\rangle_{\varepsilon} \left(\frac{1}{d} \frac{g_L}{\varepsilon} + \left(1 - \frac{1}{d} \right) \frac{g_T}{\varepsilon} \right). \tag{3.91}$$

It is more complicated to introduce renormalized couplings g_L and g_T . Set

$$\alpha \text{diagram} \beta (P_{\alpha\beta}^L g_L + P_{\alpha\beta}^T g_T) \lambda^2 \mu^\varepsilon = \alpha \text{diagram} \beta^0 (P_{\alpha\beta}^L g_L^0 + P_{\alpha\beta}^T g_T^0) \lambda_0^2. \tag{3.92}$$

This equation is to be understood such that quantities on the l.h.s. are renormalized, and those on the r.h.s. are bare. Solving the system of equations yields

$$g_L^0 = \mu^\varepsilon Z_\lambda^{-2} Z^{a/2} \tilde{Z}^{-1} \left(g_L - \frac{1}{2} \left\langle \left\langle \text{diagram} \right| \text{diagram} \right\rangle_{\varepsilon} \frac{g_L g_T}{\varepsilon} \right) + \mathcal{O}(g^3) \tag{3.93}$$

$$g_T^0 = \mu^\varepsilon Z_\lambda^{-2} Z^{a/2} \tilde{Z}^{-1} \left(g_T - \frac{1}{2} \left\langle \left\langle \text{diagram} \right| \text{diagram} \right\rangle_{\varepsilon} \frac{g_L g_T}{\varepsilon} \right) + \mathcal{O}(g^3). \tag{3.94}$$

We are now in a position, to define the so-called β -functions, quantifying the flow of the renormalized theory upon a variation of the renormalization scale, through

$$\beta_L(g_L, g_T) := \mu \frac{\partial}{\partial \mu} \Big|_0 g_L, \tag{3.95}$$

$$\beta_T(g_L, g_T) := \mu \frac{\partial}{\partial \mu} \Big|_0 g_T. \tag{3.96}$$

The β -function for the longitudinal disorder coupling is

$$\begin{aligned} \beta_L(g_L, g_T) &= \mu \frac{\partial}{\partial \mu} \Big|_0 g_L \tag{3.97} \\ &= \mu \frac{\partial}{\partial \mu} \left(g_L \mu^{-\varepsilon} Z_\lambda^2 Z^{-a/2} \tilde{Z} + \frac{1}{2} \left\langle \left\langle \text{diagram} \right| \text{diagram} \right\rangle_{\varepsilon} \frac{g_L g_T}{\varepsilon} \mu^{-2\varepsilon} \right) \\ &\quad + \mathcal{O}(g^3) \\ &= -\varepsilon g_L + \left(\frac{a+2}{2} \left\langle \left\langle \text{diagram} \right| \text{diagram} \right\rangle_{\varepsilon} \right) \\ &\quad + \frac{a+2}{2d} \left\langle \left\langle \text{diagram} \right| \text{diagram} \right\rangle_{\varepsilon} + \frac{a-2}{2} \left\langle \left\langle \text{diagram} \right| \text{diagram} \right\rangle_{\varepsilon} \right) g_L^2 \end{aligned}$$

$$\begin{aligned}
 & + \left(\left(1 - \frac{1}{d} \right) \frac{a+2}{2} \left\langle \begin{array}{c} \text{loop with two dots} \\ \text{wavy line} \end{array} \middle| \begin{array}{c} \text{wavy line} \\ \text{dot} \end{array} \right\rangle_{\varepsilon} \right. \\
 & \left. - \frac{1}{2} \left\langle \begin{array}{c} \text{two loops with two dots} \\ \text{wavy line} \end{array} \middle| \begin{array}{c} \text{wavy line} \\ \text{dot} \end{array} \right\rangle_{\varepsilon} \right) g_L g_T + \mathcal{O}(g^3). \tag{3.98}
 \end{aligned}$$

Using the relation

$$\left\langle \begin{array}{c} \text{loop with two dots} \\ \text{wavy line} \end{array} \middle| \begin{array}{c} \text{wavy line} \\ \text{dot} \end{array} \right\rangle_{\varepsilon} = -d \left\langle \begin{array}{c} \text{loop with two dots} \\ \text{wavy line} \end{array} \middle| \begin{array}{c} \text{dot} \end{array} \right\rangle_{\varepsilon}, \tag{3.99}$$

valid both in the directed, see Eq. (3.60), and isotropic, see Eq. (3.74), case, Eq. (3.97), results in the simplification

$$\begin{aligned}
 \beta_L(g_L, g_T) & = -\varepsilon g_L + \frac{a-2}{2} \left\langle \begin{array}{c} \text{loop with two dots} \\ \text{wavy line} \end{array} \middle| \begin{array}{c} \text{wavy line} \\ \text{dot} \end{array} \right\rangle_{\varepsilon} g_L^2 \\
 & + \left(\left(1 - \frac{1}{d} \right) \frac{a+2}{2} \left\langle \begin{array}{c} \text{loop with two dots} \\ \text{wavy line} \end{array} \middle| \begin{array}{c} \text{wavy line} \\ \text{dot} \end{array} \right\rangle_{\varepsilon} \right. \\
 & \left. - \frac{1}{2} \left\langle \begin{array}{c} \text{two loops with two dots} \\ \text{wavy line} \end{array} \middle| \begin{array}{c} \text{wavy line} \\ \text{dot} \end{array} \right\rangle_{\varepsilon} \right) g_L g_T + \mathcal{O}(g^3). \tag{3.100}
 \end{aligned}$$

By an analogous calculation, we obtain for the β -function of the transversal disorder

$$\beta_T(g_L, g_T) = \mu \frac{\partial}{\partial \mu} \Big|_0 g_T \tag{3.101}$$

$$\begin{aligned}
 & = \mu \frac{\partial}{\partial \mu} \left(g_T^0 \mu^{-\varepsilon} Z_{\lambda}^2 Z^{-a/2} \tilde{Z} + \frac{1}{2} \left\langle \begin{array}{c} \text{two loops with two dots} \\ \text{wavy line} \end{array} \middle| \begin{array}{c} \text{wavy line} \\ \text{dot} \end{array} \right\rangle_{\varepsilon} \frac{g_L^0 g_T^0}{\varepsilon} \mu^{-2\varepsilon} \right) \\
 & + \mathcal{O}(g^3) \\
 & = -\varepsilon g_T + \left(\frac{a+2}{2} \left\langle \begin{array}{c} \text{loop with two dots} \\ \text{wavy line} \end{array} \middle| \begin{array}{c} \text{dot} \end{array} \right\rangle_{\varepsilon} + \frac{a+2}{2d} \left\langle \begin{array}{c} \text{loop with two dots} \\ \text{wavy line} \end{array} \middle| \begin{array}{c} \text{wavy line} \\ \text{dot} \end{array} \right\rangle_{\varepsilon} \right. \\
 & + \frac{a-2}{2} \left\langle \begin{array}{c} \text{loop with two dots} \\ \text{wavy line} \end{array} \middle| \begin{array}{c} \text{wavy line} \\ \text{dot} \end{array} \right\rangle_{\varepsilon} - \frac{1}{2} \left\langle \begin{array}{c} \text{two loops with two dots} \\ \text{wavy line} \end{array} \middle| \begin{array}{c} \text{wavy line} \\ \text{dot} \end{array} \right\rangle_{\varepsilon} \Big) g_L g_T \\
 & + \left(\left(1 - \frac{1}{d} \right) \frac{a+2}{2} \left\langle \begin{array}{c} \text{loop with two dots} \\ \text{wavy line} \end{array} \middle| \begin{array}{c} \text{wavy line} \\ \text{dot} \end{array} \right\rangle_{\varepsilon} \right) g_T^2 + \mathcal{O}(g^3). \tag{3.102}
 \end{aligned}$$

With the simplification given by Eq. (3.99) the final result is

$$\begin{aligned}
 \beta_T(g_L, g_T) & = -\varepsilon g_T + \left(\frac{a-2}{2} \left\langle \begin{array}{c} \text{loop with two dots} \\ \text{wavy line} \end{array} \middle| \begin{array}{c} \text{wavy line} \\ \text{dot} \end{array} \right\rangle_{\varepsilon} \right. \\
 & \left. - \frac{1}{2} \left\langle \begin{array}{c} \text{two loops with two dots} \\ \text{wavy line} \end{array} \middle| \begin{array}{c} \text{wavy line} \\ \text{dot} \end{array} \right\rangle_{\varepsilon} \right) g_L g_T \\
 & + \left(1 - \frac{1}{d} \right) \frac{a+2}{2} \left\langle \begin{array}{c} \text{loop with two dots} \\ \text{wavy line} \end{array} \middle| \begin{array}{c} \text{wavy line} \\ \text{dot} \end{array} \right\rangle_{\varepsilon} g_T^2 + \mathcal{O}(g^3). \tag{3.103}
 \end{aligned}$$

In view of a possible stable fixed point for $g_L = g_T$, it is interesting also to study the flow equation for the difference of both couplings $g_L - g_T$:

$$\begin{aligned}
 (\beta_L - \beta_T)(g_L, g_T) &= -\varepsilon(g_L - g_T) + \frac{a-2}{2} \left\langle \begin{array}{c} \text{loop} \\ \left| \begin{array}{c} \text{wavy line} \\ \text{wavy line} \end{array} \right|_{\varepsilon} \end{array} \right\rangle g_L(g_L - g_T) \\
 &+ \left(1 - \frac{1}{d}\right) \frac{a+2}{2} \left\langle \begin{array}{c} \text{loop} \\ \left| \begin{array}{c} \text{wavy line} \\ \text{wavy line} \end{array} \right|_{\varepsilon} \end{array} \right\rangle g_T(g_L - g_T) + \mathcal{O}(g^3). \tag{3.104}
 \end{aligned}$$

3.11. Other RG functions and critical exponents

Several critical exponents can be identified. Taking into account scaling relations among them, there are three independent exponents in the directed case, and four in the isotropic case. The first is the full scaling-dimension of the membrane, given by the fixed point value ζ^* of

$$\begin{aligned}
 \zeta(g_L, g_T) &= \frac{2-D}{2} - \frac{1}{2} \mu \frac{\partial}{\partial \mu} \Big|_0 \ln Z \\
 &= \frac{2-D}{2} - \frac{1}{2} \left(\beta_L(g_L, g_T) \frac{\partial}{\partial g_L} \ln Z + \beta_T(g_L, g_T) \frac{\partial}{\partial g_T} \ln Z \right) \\
 &= \frac{2-D}{2} + \frac{g_L}{2} \left\langle \begin{array}{c} \text{loop} \\ \left| \begin{array}{c} \text{wavy line} \\ \text{wavy line} \end{array} \right|_{\varepsilon} \end{array} \right\rangle \\
 &+ \frac{g_T}{2} \left(1 - \frac{1}{d}\right) \left\langle \begin{array}{c} \text{loop} \\ \left| \begin{array}{c} \text{wavy line} \\ \text{wavy line} \end{array} \right|_{\varepsilon} \end{array} \right\rangle + \mathcal{O}(g^2). \tag{3.105}
 \end{aligned}$$

We again used Eq. (3.99) to simplify the result. The dynamical exponent z is

$$\begin{aligned}
 z(g_L, g_T) &= 2 - \mu \frac{\partial}{\partial \mu} \Big|_0 \ln Z_\lambda \\
 &= 2 - \left(\beta_L(g_L, g_T) \frac{\partial}{\partial g_L} \ln Z_\lambda + \beta_T(g_L, g_T) \frac{\partial}{\partial g_T} \ln Z_\lambda \right) \\
 &= 2 + g_L \left(\left\langle \begin{array}{c} \text{loop} \\ \left| \begin{array}{c} \text{wavy line} \\ \text{wavy line} \end{array} \right|_{\varepsilon} \end{array} \right\rangle - \left\langle \begin{array}{c} \text{loop} \\ \left| \begin{array}{c} \text{wavy line} \\ \text{wavy line} \end{array} \right|_{\varepsilon} \end{array} \right\rangle \right) + \mathcal{O}(g^2). \tag{3.106}
 \end{aligned}$$

The (full) scaling dimension of the response field is

$$\begin{aligned}
 \tilde{\zeta}(g_L, g_T) &= -\frac{2+D}{2} - \frac{1}{2} \mu \frac{\partial}{\partial \mu} \Big|_0 \ln \tilde{Z} \\
 &= -\frac{2+D}{2} - \frac{1}{2} \left(\beta_L(g_L, g_T) \frac{\partial}{\partial g_L} \ln \tilde{Z} + \beta_T(g_L, g_T) \frac{\partial}{\partial g_T} \ln \tilde{Z} \right) \\
 &= -\frac{2+D}{2} - \frac{g_L}{2} \left(\left\langle \begin{array}{c} \text{loop} \\ \left| \begin{array}{c} \text{wavy line} \\ \text{wavy line} \end{array} \right|_{\varepsilon} \end{array} \right\rangle + \frac{2}{d} \left\langle \begin{array}{c} \text{loop} \\ \left| \begin{array}{c} \text{wavy line} \\ \text{wavy line} \end{array} \right|_{\varepsilon} \end{array} \right\rangle \right) \\
 &- \frac{g_T}{2} \left(1 - \frac{1}{d}\right) \left\langle \begin{array}{c} \text{loop} \\ \left| \begin{array}{c} \text{wavy line} \\ \text{wavy line} \end{array} \right|_{\varepsilon} \end{array} \right\rangle + \mathcal{O}(g^2). \tag{3.107}
 \end{aligned}$$

We used Eq. (3.99) to simplify the result.

In the isotropic (non-directed) case, there is still another independent exponent, which is called β (not to be confounded with the β -functions describing the flow of the coupling constants) and which measures the anomalous dimension of the stiffness of the membrane,

$$\begin{aligned} \beta(g_L, g_T) &= -\mu \frac{\partial}{\partial \mu} \ln \left(\sqrt{Z \tilde{Z} Z_\lambda} \right) \\ &= g_L \left\langle \text{Diagram} \right\rangle_\varepsilon + \mathcal{O}(g^2). \end{aligned} \tag{3.108}$$

With the help of the above introduced exponents, we can quantify the non-linearity in the response of the drift velocity to a uniform applied force. Adding a small constant term f to the random force in Eq. (2.1) results into a change in the dynamical functional of the form

$$\lambda \int_{x,t} \tilde{r}(x, t) f. \tag{3.109}$$

Since this term does not require a renormalization, we deduce the exact exponent identity for the full scaling dimension $[f]$ of f

$$[f] + \tilde{\zeta} + z + D = 0. \tag{3.110}$$

From the definition of β in Eq. (3.108), we have a second identity, namely

$$\beta = \zeta + \tilde{\zeta} + z + D - 2. \tag{3.111}$$

Combining these two relations, we obtain

$$[f] = \zeta - \beta - 2. \tag{3.112}$$

Since the drift velocity has dimension

$$[v] = \left[\frac{r}{t} \right], \tag{3.113}$$

we deduce the scaling relation

$$v \sim f^\phi \quad \text{with} \quad \phi = \frac{z - \zeta}{2 + \beta - \zeta}. \tag{3.114}$$

Since, as we will see, always $z > 2$ and $\beta \leq 0$, ϕ is larger than 1 indicating trapping of the membrane by the random flow.

Let us also mention another possible parameterization of our model, where one does not introduce λ and renormalization factors for λ and the field r , but associates a friction coefficient η with \dot{r} , entering into the dynamical functional as

$$\eta \int_{x,t} \tilde{r}(x, t) \dot{r}(x, t) \tag{3.115}$$

and a temperature T associated to disorder, entering into the dynamical functional as

$$\eta T \int_{x,t} \tilde{r}^2(x,t). \tag{3.116}$$

The corresponding renormalization factors then read

$$Z_\eta \equiv \sqrt{Z \tilde{Z}}, \tag{3.117}$$

$$Z_T \equiv Z_\lambda \sqrt{\frac{\tilde{Z}}{Z}}. \tag{3.118}$$

It is especially enlightening to consider the renormalization of temperature, which in conserved systems (i.e. those with longitudinal disorder) is preserved by the fluctuation–dissipation theorem. Stated differently, temperature appears as a parameter in its static partition function, and dynamics is constructed such that via detailed balance the static partition function is reproduced. Only non-conserved forces can give rise to a change in temperature. This is read off from the explicit form of Z_T at 1-loop order:

$$Z_T = 1 - \left(\frac{1}{d} \left\langle \text{diagram 1} \middle| \text{diagram 2} \right\rangle_\varepsilon + \left\langle \text{diagram 3} \middle| \text{diagram 4} \right\rangle_\varepsilon \right) \frac{g_L}{\varepsilon} - \left(1 - \frac{1}{d} \right) \left\langle \text{diagram 5} \middle| \text{diagram 6} \right\rangle_\varepsilon \frac{g_T}{\varepsilon}. \tag{3.119}$$

Since the term proportional to g_L vanishes as found in Eqs. (3.60) and (3.74), anomalous corrections to the temperature are proportional to g_T and present whenever $g_T \neq 0$. Stated differently: In the presence of non-potential forces, the fluctuation–dissipation theorem (FDT) is violated.

4. Results and discussion

In this section we analyze the general renormalization group flow given by the two β -functions in Eqs. (3.100) and (3.103) where the coefficients have been computed in Section 3.7. We identify the fixed points and compute the critical exponents at these fixed points. Before doing so it is useful to recapitulate the results obtained so far in the previous sections.

4.1. Preliminaries

To present conveniently the analysis below we introduce the following notation for the three independent coefficients (two in the directed case) as

$$\mathcal{A} := \left\langle \text{diagram 7} \middle| \text{diagram 8} \right\rangle_\varepsilon, \tag{4.1}$$

$$\mathcal{B} := \left\langle \begin{array}{c} \text{Diagram 1} \\ \text{Diagram 2} \end{array} \middle| \begin{array}{c} \text{Diagram 3} \\ \text{Diagram 4} \end{array} \right\rangle_{\varepsilon}, \tag{4.2}$$

$$\mathcal{C} := -d \left\langle \begin{array}{c} \text{Diagram 5} \\ \text{Diagram 6} \end{array} \middle| \begin{array}{c} \text{Diagram 7} \\ \text{Diagram 8} \end{array} \right\rangle_{\varepsilon}. \tag{4.3}$$

The explicit expressions for these coefficients are given above: for \mathcal{A} see Eqs. (3.57) and (3.68), for \mathcal{B} see Eqs. (3.63) and (3.78) and for \mathcal{C} (only non-zero for isotropic manifolds), see Eq. (3.76). They are non-negative. In terms of these three coefficients, the β -functions of the two coupling constants read

$$\beta_L^g(g_L, g_T) = -\varepsilon g_L + \frac{1}{2} \left(\left(1 - \frac{1}{d}\right) (a + 2)\mathcal{A} - \mathcal{B} \right) g_L g_T - \frac{a - 2}{2d} \mathcal{C} g_L^2, \tag{4.4}$$

$$\beta_T^g(g_L, g_T) = -\varepsilon g_T - \frac{1}{2} \left(\mathcal{B} + \frac{a - 2}{d} \mathcal{C} \right) g_T g_L + \left(1 - \frac{1}{d}\right) \frac{a + 2}{2} \mathcal{A} g_T^2, \tag{4.5}$$

where a must be replaced by d for short-range disorder (the crossover between SR and LR disorder is also studied below). Similarly, the expressions of the exponents are to lowest order (from Section 3.11 above)

$$\zeta(g_L, g_T) = \frac{2 - D}{2} + \frac{g_T}{2} \left(1 - \frac{1}{d}\right) \mathcal{A} - \frac{g_L}{2d} \mathcal{C}, \tag{4.6}$$

$$z(g_L, g_T) = 2 + \frac{1}{d} (\mathcal{A} - \mathcal{C}) g_L, \tag{4.7}$$

$$\beta(g_L, g_T) = -g_L \frac{1}{d} \mathcal{C}, \tag{4.8}$$

where we have used (3.74). Note that in the end the exponents will depend on the amplitudes only through their ratios \mathcal{B}/\mathcal{A} and \mathcal{C}/\mathcal{A} which are universal, in contrast to the amplitudes themselves, which depend on the specific normalizations of the model.

The coefficients of the RG equations (4.4)–(4.8), including \mathcal{A} , \mathcal{B} and \mathcal{C} , depend a priori on a , d and D , and their full dependent expressions are given in the previous sections (where SR and LR disorder are treated in a single calculation). However, since we are expanding to first order around the line of critical dimension $d_c(D)$ (see Eq. (2.22)), we can simplify all these coefficients as follows: For short-range disorder one can substitute $a = d = d_c(D)$ in all coefficients. For long-range disorder we can substitute $a = a_c(D)$ everywhere, but one must keep d as an independent variable. This is the reason, why we defined \mathcal{A} and \mathcal{C} as d independent, while $\mathcal{B} = 0$ for LR disorder. The final result for the coefficients used below, expressed only as a function of D is, for directed manifolds,

$$\begin{aligned} \mathcal{A}^{\text{dir}} &= 2 \left[\frac{(2 - D)(4\pi)^{D/2}}{2} \right]^{\frac{2}{2-D}}, \\ \mathcal{B}^{\text{dir}} &= \frac{2 + D}{D} \left[\frac{(2 - D)\pi^{D/2}}{\Gamma(\frac{D}{2})} \right]^{\frac{2}{2-D}}, \end{aligned} \tag{4.9}$$

$$\mathcal{C}^{\text{dir}} = 0.$$

For polymers ($D = 1$) one finds $\mathcal{A} = 2\pi$, $\mathcal{B} = 3$ and the universal ratio $\mathcal{A}/\mathcal{B} = 2\pi/3$.

For isotropic manifolds one has

$$\begin{aligned} \mathcal{A}^{\text{iso}} &= \frac{1}{(2-D)2^{2+D}} \left(\frac{2}{D}\right)^{\frac{2-D}{2}} \left[\Gamma\left(\frac{D}{2}\right)\right]^{\frac{2+D}{2-D}} G_D \tilde{I}(D), \\ \mathcal{B}^{\text{iso}} &= \frac{2+3D}{2D(2-D)^2(2+D)} \frac{\Gamma\left(\frac{D}{2-D}\right)^2}{\Gamma\left(\frac{2D}{2-D}\right)} G_D, \\ \mathcal{C}^{\text{iso}} &= \frac{1}{2D(2-D)} G_D, \end{aligned} \tag{4.10}$$

where we denote by

$$G_D = \left[\frac{2\pi^{D/2}(2-D)}{\Gamma\left(\frac{D}{2}\right)} \right]^{4/(2-D)} \tag{4.11}$$

the factor common to the three amplitudes (which therefore drops in the final results). $\tilde{I}(D)$ is plotted in Fig. (7) and defined as

$$\tilde{I}(D) := \left(\frac{D}{2}\right)^{\frac{2-D}{2}} 2^{2+D} \int_0^{+\infty} dt \left[\Gamma\left(\frac{D}{2}\right) + (4t)^{\frac{2-D}{2}} e^{-\frac{1}{4t}} - \Gamma\left(\frac{D}{2}, \frac{1}{4t}\right) \right]^{-\frac{2+D}{2-D}}. \tag{4.12}$$

It takes the values $\tilde{I}(D = 0) = 1$, $\tilde{I}(D = 1) = 1.82202$ and $\tilde{I}(D = 2) = 3$. For the coefficients for $D = 1$ we find $\mathcal{A} = 1.79351G_1$, $\mathcal{B} = \frac{5}{6}G_1$ and $\mathcal{C} = \frac{1}{2}G_1$.

We now specify to each of the four cases of interest and compute the critical exponents.

4.2. Directed manifolds with short-range disorder

The flow for this case is represented in Fig. 8. The expansion parameter is $\varepsilon = 2 - (2 - D)d/2$. The fixed points are found to be:

(1) Gaussian fixed point.

The Gaussian fixed point at $g_L = g_T = 0$ is completely unstable for $d < d_c^{\text{dir}}(D) = \frac{4}{2-D}$.

(2) Potential disorder.

The line $g_T = 0$ is found to be preserved by RG and we find a flow towards strong coupling. This case corresponds to the dynamics of a directed manifold in a long-range correlated random potential (short-range correlated force). It has been well studied and it is indeed known that for $d \leq d_c(D)$ (defined above) and $D < 2$, or in any d for $2 < D < 4$, the physics is controlled by a strong disorder (zero temperature) fixed point [1,6], inaccessible by the present method (it is accessible only via a $D = 4 - \varepsilon$ calculation).

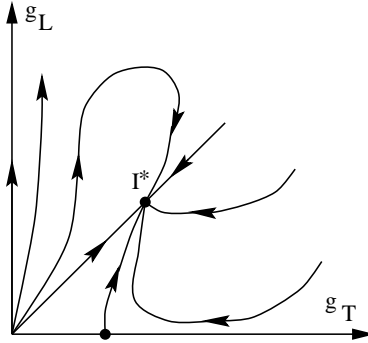


Fig. 8. RG flow diagram for SR disorder. The physics is controlled by the fixed point I^* at $g_T = g_L$.

Further results are available for the particle ($D = 0, d_c = 2$). There it is known rigorously that for $d = 1$ (Sinai model) ultra-slow logarithmic diffusion $r \sim (\ln t)^2$ occurs ($\nu = 0$) and it is believed (but not proven) that similar ultra-slow diffusion also occurs for manifolds $D > 0$ (see e.g. Ref. [12]). At the critical dimension, for the particle $d_c(D = 0) = 2$, 1- and 2-loop calculations [39,40,42] have shown that diffusion is anomalous with a continuously varying exponent $\nu(g_L)$. It was further argued that the β function vanishes to all orders, and that the one loop result for $\nu(g_L)$ holds exactly, for SR disorder as well as for LR disorder [40]. While unchallenged for SR disorder (i.e. at $d = 2$), the exactness of the one loop exponent was recently questioned for LR disorder in [76]. To our knowledge such issues have not been addressed for manifolds.

(3) *Isotropic disorder fixed point.*

Noting from Eq. (3.104) that the line $g_T = g_L$ is preserved by the flow at 1-loop order, we find an isotropic fixed point at

$$g_L = g_T = g^* := \frac{2\epsilon d}{(d - 1)(d + 2)\mathcal{A} - d\mathcal{B}} + \mathcal{O}(\epsilon^2), \tag{4.13}$$

where the coefficients are given in Eq. (4.9). Since at the critical dimension the denominator is positive for all values of $0 \leq D < 2$, g^* is positive and thus physical. This fixed point is completely attractive, and its domain of attraction covers all perturbative situations except the potential case with $g_T = 0$. As we show below, it also controls the line $g_L = 0$ (except for $D = 0$).

Let us give the values of the roughness exponent ζ^* and of the dynamical exponent z^* , defined in Eqs. (2.13) and (2.15), at the fixed point:

$$\zeta^* = \zeta(g^*, g^*) = \frac{2 - D}{2} + \frac{\epsilon}{d + 2 - \tilde{R}} + \mathcal{O}(\epsilon^2), \tag{4.14}$$

$$\tilde{R} = \frac{\mathcal{B}}{(1 - \frac{1}{d})\mathcal{A}} = \frac{d}{d - 2} (2^{D-1} \Gamma(D/2))^{-d/2}, \tag{4.15}$$

where $\epsilon = 2 - \frac{2-D}{2}d$. Again one can substitute $d = d_c(D)$ in the coefficient of ϵ . Expressed as a function of D one has $\tilde{R} = \frac{2}{D} (2^{D-1} \Gamma(D/2))^{-2/(2-D)}$. The dynamical

Table 1

Results for directed polymers and membranes, isotropic fixed point, SR disorder. Values given for the exponent ζ (obtained by extrapolating $\zeta(d)$) are rather faithful. Corrections to z are small, but no plateau could be found to optimize the extrapolations. The given values are therefore only intended to give a rough idea. The same is true for extrapolations for ν . We have reported the values of ν obtained by setting $D_0 = D$

	d	ζ	z	ν	ϕ
Polymer	2	0.87	2.2	0.5	> 1
	3	0.63	2.1	0.3	> 1
Membrane	2	0.8	2.2	0.5	> 1
	3	0.5	2.1	0.33	> 1
	4	0.4	2.1	0.25	> 1
	6	0.25	2.07	0.17	> 1
	8	0.2	2.05	0.13	> 1
	20	0.08	2.01	0.05	> 1

exponent is

$$z^* = 2 + \frac{2\varepsilon}{(d-1)(d+2-\tilde{R})} + \mathcal{O}(\varepsilon^2). \quad (4.16)$$

The exponent β is equal to 0 as a consequence of the statistical tilt symmetry (see Eq. (3.61)). The exponents ν and ϕ can then be found using

$$\nu = \zeta/z, \quad \phi = \frac{z-\zeta}{2-\zeta}. \quad (4.17)$$

In particular, for the polymer $D = 1$, we find that below $d_c = 4$ the random flow is relevant and roughness and dynamical exponents take the anomalous dimension

$$\zeta^* = \frac{1}{2} \left(1 + \frac{\varepsilon}{3-\pi^{-1}} \right), \quad (4.18)$$

$$z^* = 2 \left(1 + \frac{\varepsilon}{6(3-\pi^{-1})} \right), \quad (4.19)$$

where $\varepsilon = \frac{1}{2}(4-d)$. Interestingly we find that to first order in ε , $\zeta > \zeta_F$.

The most naive fixed D expansion gives in $d = 3$ (setting $\varepsilon = 1$ in the above) that $\zeta = 0.686$, $z = 2.12$, $\nu = 0.323$, $\phi = 1.094$. In $d = 2$ it gives (setting $\varepsilon = 2$) that $\zeta = 0.873$, $z = 2.249$, $\nu = 0.388$, $\phi = 1.22$. These estimates can be improved since the expansion can be carried from any point of the line $d = d_c(D)$. It is possible to optimize the numerical estimation of the above critical exponents over the expansion point D_0 . Details of the general optimization method are described in [52] and applied to the present case in Appendix B. The results are listed in Table 1 and are purely indicative: we have even refrained from giving an error bar.

(4) Transversal disorder.

There is an apparent fixed point at

$$g_L = 0, \quad g_T = \frac{2\varepsilon}{(1-\frac{1}{d})(d+2)\mathcal{A}} + \mathcal{O}(\varepsilon^2), \quad (4.20)$$

where the coefficients are given in Eq. (4.9). Interestingly, at this fixed point we recover exactly the Flory result at 1-loop order:

$$\zeta^* = \frac{2 - D}{2} + \frac{\varepsilon}{d + 2} + \mathcal{O}(\varepsilon^2), \tag{4.21}$$

$$z = 2 + \mathcal{O}(\varepsilon^2). \tag{4.22}$$

In the case of the particle ($D = 0$) the result $\nu = \nu_F$ was found to be true to all orders (see e.g. Refs. [42,40] and discussion below).

However, for $D > 0$ we show (see Appendix C) that finite non-transversal terms are generated in perturbation theory. Since the above fixed point is unstable to adding a small longitudinal disorder, $g_L > 0$, these terms will drive the system towards the isotropic fixed point discussed above.

Let us close this section by noting that we recover the known results for the particle $D = 0$, obtained via different RG techniques in [36,39,40,42]. That this should be so was discussed in Section 3.9 but here we discuss it explicitly for the exponents. First we note that the flow diagram of Fig. 8 has the same structure for all D as the one found in [39] for the particle with an isotropic disorder fixed point and the transversal fixed point. Second, expressing in all our results the coefficient of ε as a function of D alone (using $d = d_c(D)$) yields in the limit $D \rightarrow 0$ with $\varepsilon = 2 - d$, that at the isotropic fixed point $\nu = \zeta/\varepsilon = 1/2 + \mathcal{O}(\varepsilon^2)$ and $\phi = 1 + \varepsilon$ (note that one also finds $\zeta = 1 + \varepsilon/2$, $z = 2 + \varepsilon$, but only ν and ϕ have a physical meaning for $D = 0$). Similarly at the transversal disorder fixed point (which has a meaning only for the particle), one recovers the known result $\nu = \nu_F$ and $\phi = 1$.

4.3. Directed manifold with long-range disorder

Long-range correlated disorder ($a < d$) can be studied in an expansion near $a_c = 4/(2 - D)$, in the small parameter $\delta = 2 - (2 - D)\frac{a}{2}$ (with d and D fixed). We have shown in Section 3.4 that in this case the vertex renormalization vanishes

$$\mathcal{B} = \left\langle \left(\text{diagram with two vertices and wavy lines} \right) \middle| \left(\text{diagram with one vertex and wavy line} \right) \right\rangle_\varepsilon = 0. \tag{4.23}$$

Thus the renormalization is driven by the corrections to temperature and friction. The β -functions in Eqs. (3.100) and (3.103) lead to the flow diagram presented in Fig. 9. Since there is no vertex renormalization, both couplings have the same renormalization factor, the ratio $\kappa = g_L/g_T$ is preserved by RG, and the flow is along straight lines. One finds a line L of fixed points, which is vertical to first order in ε . This feature, already noted in the particle case, $D = 0$ [42,40], thus extends to manifolds with $D > 0$. Here the fixed line is given by

$$g_T^* = \delta \frac{2d}{(d - 1)(a + 2)\mathcal{A}}. \tag{4.24}$$

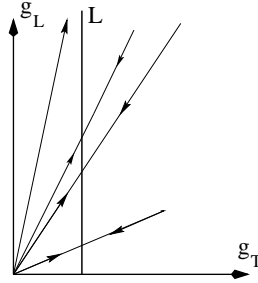


Fig. 9. RG flow for directed manifolds in LR disorder. The flow is along straight lines and preserves the line L of fixed points.

For LR correlations the result for ζ^* at any point on the fixed line can be derived to all orders in perturbation theory. First, there is no counter-term to $\tilde{r}\Delta r$ to any order in perturbation theory due to the fact that the interaction vertex is a difference of the r -fields at the same point (“statistical tilt symmetry”), resulting in the scaling relation

$$\zeta^* + \tilde{\zeta}^* + z^* = 2 - D, \tag{4.25}$$

where $\tilde{\zeta}$ is the full scaling dimension of the response field. Second, as long as there is no renormalization of the vertex,

$$D + 2\tilde{\zeta}^* + 2z^* - a\zeta^* = 0 \tag{4.26}$$

is valid at the fixed point. Combining these two relations gives⁵

$$\zeta^* = \zeta_F = \frac{4 - D}{2 + a}. \tag{4.27}$$

Thus the Flory estimate for ζ is exact in the LR case. Note also that ζ in that case does not depend on the type of disorder (transversal or potential). For a polymer $D = 1$ we obtain that $\zeta = 3/(2 + a)$ for $a < a_c = 4$. This leads to the interesting prediction that the polymer will become *overstretched* ($\zeta \geq 1$) when the range of the force correlation increases beyond $a \leq 1$.

The dynamical exponent z , however, and consequently ϕ and ν , are non-trivial, and depend continuously on the ratio $\kappa = g_T/g_L$. They are given by

$$z^* = 2 \left(1 + \kappa \frac{\delta}{(2 + a)(d - 1)} \right), \tag{4.28}$$

where $\delta = 2 - (2 - D)\frac{a}{2}$. This result is valid to first order in δ and one may thus replace a by $a_c = 4/(2 - D)$ in the above formula. It shows that the more potential the dynamics the more glassy it is (the higher z).

We can now compare these results with the results obtained in [44]. There the exponents were obtained exactly for $d \rightarrow \infty$ and arbitrary a . A Hartree approximation

⁵ This identity also holds at 1-loop order at the apparent SR transversal fixed point discussed in Eq. (4.21), since vertex-corrections are proportional to $g_L g_T$, see Eq. (3.37).

was obtained for finite d . The notations of [44] were different. To translate to the present notations one must set in [44] $\gamma \rightarrow a/2$, $g_2 \rightarrow \frac{g_L}{d}$, $g_1 - g_2 \rightarrow (1 - \frac{1}{d})g_T$ and $\varepsilon = 2/(2-D) - \gamma \rightarrow \frac{\delta}{2-D}$. With this correspondence the results of [44] are as follows. First $\zeta = \zeta_F$, both for $d = \infty$ and for finite d within the Hartree approximation. This is in agreement with the present result. z in [44] however is a highly non-trivial function of a , D (and of d in the Hartree approximation) implicitly given by Eq. (9) in [44]. Remarkably, for $D < 2$, expanding z near $a = a_c$, which yields formula (12) of [44], one finds to first order in ε *exactly the same result* as here in Eq. (4.28). Of course the two also coincide, as they should, for $d = \infty$. Thus we find that in the long-range directed case, the Hartree approximation in [44] gives the correct result for z to first order, and is exact for ζ .

Let us also give the results for the exponents ν and ϕ . One finds

$$\nu = \frac{2-D}{4} \left[1 + \delta \frac{(\kappa^* - \kappa)(2-D)}{2(4-D)(d-1)} \right], \quad (4.29)$$

$$\phi = 1 + \delta \frac{2(2-D)\kappa}{(2+D)(4-D)(d-1)} \quad (4.30)$$

and thus we find that the single monomer dynamics is either subdiffusive if $\kappa = g_L/g_T > \kappa^* = 2(d-1)/(2-D)$ or superdiffusive if $\kappa < \kappa^*$, while ϕ is always larger than 1 (except when the flow is purely transversal). One can also check that our formulae agree, in the limit $D \rightarrow 0$ with the known formulae [40–42] for the particle (with $a_c = 2$ and $\delta = 2 - a$).

To conclude note that in the case $\kappa = 0$, i.e. in presence of LR transversal disorder alone, the mechanism of generation of potential disorder and barriers is different from the SR-case. LR non-transversal disorder is not generated, only SR non-transversal disorder is. (See also the section below, where the crossover from LR to SR is discussed). The final result is that in that case the exponents are given correctly too by the above formulae setting $\kappa = 0$.

4.4. Isotropic (non-directed) manifold with short-range disorder

For an isotropic manifold, we find from the RG equations (3.100) and (3.103) and the expressions given in Section 3.8 for the coefficients that the RG flow is qualitatively similar to the one in the directed case depicted in Fig. 8, with the following fixed points:

(1) Gaussian fixed point.

The Gaussian fixed point at $g_L = g_T = 0$ is completely unstable for $\varepsilon = 2 + D - \frac{d}{2}(2 - D) > 0$.

(2) Potential disorder.

The line $g_T = 0$ is preserved by RG and again, we find a flow towards strong coupling, which is faster than in the directed case, as there is an additional term. This problem describes the dynamics of an isotropic manifold in a long-range correlated random

potential (short-range correlated force). The statics of this problem has been much studied and it is indeed expected that this problem is described by strong disorder.

In the absence of self-avoidance some features of the problem are relatively simple to analyze. For instance can a polymer ($D = 1$) in a d -dimensional random potential also be seen as a *directed* polymer in a $d + 1$ -dimensional random potential (the additional coordinate being the internal dimension) which is constant (i.e. correlated) in the internal dimension, a problem extensively reinvestigated recently in relation with flux lines in superconductors in presence of columnar disorder [81,77,78,12]. It is also related to the problem of quantum localization of a particle in a d -dimensional random potential (the internal dimension being the quantum imaginary time). It is known, and rather obvious in relation to these problems, that if the polymer is free to move, it is localized in the deepest localized state and has a finite extent. Properties then strongly depend on details, such as the system size, the tail of the disorder distribution (Lifschitz tails), and the short scale cutoff [79,80].

On the other hand, the problem of many interacting directed polymers is well defined and identical to the problem of localization of bosons in a random potential. These properties should remain true for membranes as well and in general we expect that in the absence of self-avoidance, the membrane collapses ($\zeta = 0$).

For a self-avoiding polymer the problem is better defined. Self-avoidance is then relevant (see Section 4.7) and properties will depend on whether one end of the polymer is held fixed or is allowed to move freely. It was studied previously with short-range potential disorder [55]. There, if the polymer is free to move one expects again [60] a collapsed state, whereas if one end is fixed there may be another strong disorder fixed point [57] (see Section 4.7). In all cases it is natural to expect non-trivial glassy dynamics.

We will not say more here about the potential case ($g_T = 0$) which is beyond the reach of our perturbative method, but let us stress that it is all the more interesting to investigate what happens to localization when transverse disorder is added. We therefore now turn to the case $g_T > 0$.

(3) *Isotropic disorder fixed point.*

Noting from Eq. (3.104) that the line $g_T = g_L$ is preserved by the flow (to this order), we find an isotropic fixed point at

$$g_L = g_T = g^* := \frac{2\epsilon d}{(d-1)(d+2)\mathcal{A} - d\mathcal{B} - (d-2)\mathcal{C}} + \mathcal{O}(\epsilon^2), \quad (4.31)$$

where the coefficients are given in Eq. (4.10). We have checked numerically that the denominator of Eq. (4.31) is always positive, which is necessary for this fixed point to be stable and to be in the physical domain. We have also checked numerically that this fixed point is completely attractive, and its domain of attraction covers all perturbative situations except the potential case $g_T = 0$. As in the directed case, it also controls the line $g_L = 0$ (except for $D = 0$) and describes the large scale behavior of an isotropic manifold in a random short-range force flow, see appendix C.

Table 2

Results for isotropic polymers and membranes at the isotropic fixed point, SR disorder. Results for ζ are obtained from the extrapolation of ζd , and are the most faithful. One observes a nice plateau in extrapolations for ν , but no corrections to the Flory approximation can be deduced. The exponents z and ϕ do not allow for direct extrapolations, but are always corrected upwards. Results for β are significant for polymers. For membranes only a bound seems to emerge from extrapolations

	d	ζ	z	ν	β	ϕ
Polymer	2	≈ 1	> 2	0.5	-0.08	> 1
	3	0.8	> 2	0.40	-0.06	> 1
	4	0.67	> 2	0.33	-0.03	> 1
Membrane	3	0.8	> 2	0.40	-0.2...0	> 1
	4	0.68	> 2	0.33	-0.2...0	> 1
	6	0.5	> 2	0.25	-0.2...0	> 1
	8	0.4	> 2	0.20	-0.2...0	> 1
	20	0.2	> 2	0.09	-0.2...0	> 1

The critical exponents at this fixed point, ζ^* and z^* , defined in Eqs. (2.13) and (2.15), are with the same diagrams, given in Eq. (4.10)

$$\zeta^* = \zeta(g^*, g^*) = \frac{2-D}{2} + \frac{((d-1)\mathcal{A} - \mathcal{C})\varepsilon}{(d-1)(d+2)\mathcal{A} - d\mathcal{B} - (d-2)\mathcal{C}} + \mathcal{O}(\varepsilon^2). \quad (4.32)$$

Note the difference with the directed case. The first coefficient in the numerator, \mathcal{A} , is positive as before, since it arises from the upward corrections to the temperature. However, since there is no tilt symmetry any more, the elasticity is also renormalized upwards (the polymer tends to shrink to take advantage of favorable regions). This produces the second coefficient $-\mathcal{C}$, which is negative. The competition between the two opposite effects however gives a positive sum and the membrane is stretched. Also note that the ε -correction vanishes like $1/d$ for $D \rightarrow 2$.

A similar formula is valid for the dynamic exponent z :

$$z^* = z(g^*, g^*) = 2 + \frac{2(\mathcal{A} - \mathcal{C})\varepsilon}{(d-1)(d+2)\mathcal{A} - d\mathcal{B} - (d-2)\mathcal{C}} + \mathcal{O}(\varepsilon^2) \quad (4.33)$$

with the same coefficients. The ε -correction is always positive, but vanishes like $1/d^2$ for $D \rightarrow 2$.

Since there is no tilt symmetry any more, the elasticity is also renormalized upwards and gives rise to a non-trivial exponent β^* (with the coefficients again given in Eq. (4.10)):

$$\beta^* = \frac{-2\mathcal{C}\varepsilon}{(d-1)(d+2)\mathcal{A} - d\mathcal{B} - (d-2)\mathcal{C}} + \mathcal{O}(\varepsilon^2). \quad (4.34)$$

The other exponents can be obtained as $\nu = \zeta/z$ and $\phi = (z - \zeta)/(2 - \zeta + \beta)$. One notes that in the limit $D \rightarrow 0$ one recovers again correctly the results for the particle for ν and ϕ .

For a polymer, $D = 1$, the disorder becomes relevant below $d = 6$ and setting $D = 1$, we find that the above results yield:

$$\zeta^* = 0.5 + 0.130792\varepsilon, \quad z^* = 2 + 0.03996\varepsilon, \quad \beta^* = -0.015446\varepsilon \quad (4.35)$$

with $\varepsilon = \frac{1}{2}(6 - d)$, as well as $\nu = 1/4 + 0.060401\varepsilon$ and $\phi = 1 + 0.0369373\varepsilon$. The most naive extrapolation to $d = 3$ would be (setting $\varepsilon = 1.5$) that $\zeta = 0.70$, $z = 2.06$ and $\beta = -0.023$ and in $d = 2$ that $\zeta = 0.76$, $z = 2.08$ and $\beta = -0.031$.

One can try to obtain more reliable estimates for these critical exponents from expressions (4.32), (4.33) and (4.34) for polymers ($D = 1$) and membranes ($D = 2$) in three or two dimensions by optimizing on the expansion point. This is a tedious task since ε is rather big. The numerical values obtained by the methods of [52] are not very precise, as we could not find a combination of the exponents and D or d , which in suitable extrapolation variables build up a nice plateau. Different extrapolation schemes yielded strongly varying results. Some indicative values obtained by this methods are summarized in Table 2.

Since ζ seems to increase rapidly as d decreases, an interesting question is whether there is a dimension d_l below which the polymer will be fully stretched ($\zeta = 1$). The result of Table 2 seems to indicate that d_l could be around $d_l = 2$. Our calculations are not precise enough to decide on whether the polymer is already over-stretched or not in $d = 2$ but that would be an interesting point to try to answer by other methods or by numerical simulations (in $d = 2$).

(4) *Transversal disorder fixed point.*

The transversal fixed point ($g_L = 0$) is at

$$g_L = 0, \quad g_T = \frac{2\varepsilon}{(1 - \frac{1}{d})(d + 2)\mathcal{A}} + \mathcal{O}(\varepsilon^2), \quad (4.36)$$

where the diagram is given in Eq. (4.10). It is unstable towards perturbations of g_L see appendix C. For the critical exponents ζ^* and z^* , we recover exactly the Flory result at 1-loop order:

$$\zeta^* = \frac{2 - D}{2} + \frac{\varepsilon}{d + 2} + \mathcal{O}(\varepsilon^2), \quad (4.37)$$

$$z^* = 2 + \mathcal{O}(\varepsilon^2). \quad (4.38)$$

As was discussed for the directed case, this result was also found to be true for the particle ($D = 0$) to all orders, but for $D > 0$ as we show (see Appendix C) finite non-transversal terms are generated in perturbation theory which will drive the system towards the isotropic fixed point discussed above.

4.5. *Isotropic (non-directed) manifold with long-range disorder*

For isotropic manifolds, LR correlated disorder becomes relevant for $a < a_c(D) = 2(2 + D)/(2 - D)$. For fixed dimension $d > a_c(D)$, it can be studied in an expansion in $\delta = 2 + D - \frac{(2-D)}{2}a$. As for directed manifolds, the vertex renormalization vanishes,

$$\mathcal{B} = \left\langle \left(\text{diagram with two vertices and wavy lines} \right) \left| \text{diagram with two vertices and straight line} \right. \right\rangle_\varepsilon = 0. \quad (4.39)$$

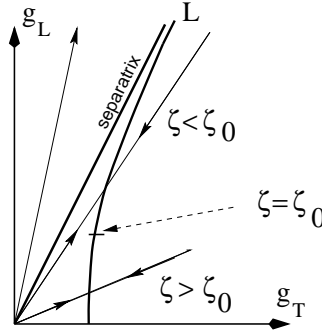


Fig. 10. RG flow diagram for isotropic manifolds in LR disorder. The flow is along straight lines. There is a line of fixed points L and an apparent separatrix. $\zeta - \zeta_0$ changes sign upon increasing g_L/g_T , suggesting progressive localization.

Thus the renormalization is driven by the corrections to temperature, friction and elasticity. The β -functions (4.4) and (4.5) with the coefficients given in Eq. (4.10), lead to the flow diagram represented in Fig. 10. Since there is no vertex renormalization both couplings have the same renormalization factor and thus the ratio $\kappa = g_L/g_T$ is again preserved by RG. As in the case of directed manifolds, one finds that the flow is along straight lines and that there is a line L of fixed points (see Fig. 10). Its equation parameterized by the bare ratio of coupling constants $\kappa = g_L(0)/g_T(0)$ is

$$g_T^* = \frac{2d\delta}{(d-1)(a+2)\mathcal{A} - \kappa(a-2)\mathcal{C}} \tag{4.40}$$

and $g_L^* = \kappa g_T^*$, where a should be replaced by $a = a_c(D) = 2(2+D)/(2-D)$.

A novel and interesting feature is the existence of a separatrix, as depicted in Fig. 10: When starting with mostly potential disorder, i.e. a large enough ratio,

$$\kappa = \frac{g_L}{g_T} > \kappa_c := (d-1) \frac{a+2}{a-2} \frac{\mathcal{A}}{\mathcal{C}}, \tag{4.41}$$

there is no perturbative fixed point and the system, within the present expansion, always flows to strong coupling (for the coefficients see Eq. (4.10)). For polymers $D = 1$, since we expand around $a = a_c = 6$ this value is rather large $\kappa_c(d) = 7.17404(d-1)$. This property suggests the existence of two phases, or two regimes, one described by the above fixed line, the other by a fixed point, which is non-perturbative in δ (at fixed d). It could also be that while the perturbative one has a continuously varying exponent ζ the non-perturbative corresponds to complete localization $\zeta = 0$. It would be interesting to check this scenario by non-perturbative methods as e.g. in [44]. A study of the crossover between SR and LR in the next section will shed some more light on the nature of the change of regimes observed here.

In the perturbative (non-localized) phase $\kappa < \kappa_c$ the exponents as a function of $\kappa = g_L/g_T$ read

$$\zeta^* = \frac{2-D}{2} + \delta \frac{(d-1)\mathcal{A} - \kappa\mathcal{C}}{(d-1)(a+2)\mathcal{A} - (a-2)\kappa\mathcal{C}}, \tag{4.42}$$

$$z^* = 2 + 2\delta\kappa \frac{\mathcal{A} - \mathcal{C}}{(d-1)(a+2)\mathcal{A} - (a-2)\kappa\mathcal{C}}, \quad (4.43)$$

where a should be replaced by $a = a_c(D) = 2(2+D)/(2-D)$ and $\delta = 2 + D - \frac{2-D}{2}a$. Again the diagrams are given in Eq. (4.10).

These results contain interesting novel features compared to the case of directed manifolds and can be studied as follows. Let us denote the universal ratio $R = \mathcal{A}/\mathcal{C}$. We can express all exponents as follows to first order in $\delta = 2 + D - (2-D)\frac{a}{2}$:

$$\begin{aligned} \zeta &= \frac{2-D}{2} + \frac{\delta}{a-2} \frac{\kappa_0 - \kappa}{\kappa_c - \kappa} \\ z &= 2 + \frac{2\delta}{a-2} \frac{\kappa(R-1)}{\kappa_c - \kappa}, \\ \beta &= -\frac{2\delta}{a-2} \frac{\kappa}{\kappa_c - \kappa}, \end{aligned} \quad (4.44)$$

$$\begin{aligned} \nu &= \frac{2-D}{4} + \frac{\delta}{4(a-2)} (D + (2-D)R) \frac{\kappa^* - \kappa}{\kappa_c - \kappa}, \\ \phi &= 1 + \frac{4\delta}{(a-2)(2+D)} \frac{R\kappa}{(\kappa_c - \kappa)} \end{aligned} \quad (4.45)$$

with $\kappa_0 = (d-1)R$ and $\kappa^* = 2(d-1)R/(D + (2-D)R)$ and one should set $a = a_c(D) = 2(2+D)/(2-D)$, i.e. $a = a_c = 6$ for the polymer.

In the case of the polymer ($D = 1$) we find that $R = 3.58702$, and $\kappa_c = 2R(d-1) = 7.17404(d-1)$ varies in the range $35.8702 < \kappa_c < +\infty$ for the range of dimensions $a_c = 6 < d < +\infty$ where the result holds. $\kappa_0 = R(d-1) = \kappa_c/2 = 3.58702(d-1)$ and $\kappa^* = 1.56399(d-1)$ which varies between $7.81993 < \kappa^* < +\infty$ as d increases from $d = 6$ to $d = +\infty$. Note that one has $\kappa^* < \kappa_0 < \kappa_c$.

The above given lowest order results for the exponents in the expansion in $\delta = 2 + D - \frac{2-D}{2}a$ show some new features as compared to directed manifolds which result from the competition between the effect of temperature increase (which tends to stretch) and the effect of increase in elastic stiffness (which tends to localize). First we find that for $\kappa < \kappa_0$ (with $\kappa_0 = \kappa_c/2$ for polymers) the manifold is stretched $\zeta > \zeta_0$ compared to manifolds in the absence of disorder (as was always the case for directed manifolds) while for large potential disorder $\kappa > \kappa_0$ the manifold is more localized $\zeta < \zeta_0$. The effect of potential disorder, which acts to localize isotropic polymers as was discussed above thus becomes predominant for $\kappa > \kappa_0$ (to lowest order in δ). The single monomer diffusion exponent $r \sim t^\nu$ also exhibits a change from superdiffusive ($\nu > 1/4$ for polymers) to subdiffusive ($\nu < 1/4$) behavior when κ becomes larger than κ^* . Finally note that in all cases $\kappa > 0$ one has $z > 2$ and $\phi > 1$ which indicates glassy dynamics and trapping by the flow.

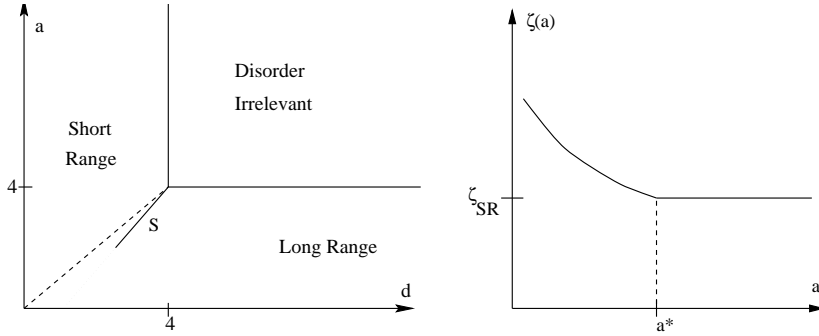


Fig. 11. Schematic sketch of the crossover in the d, a plane between LR and SR regimes for a directed polymer (left). The expansion point is $d = a = 4$ and the SR exponents hold until the line S. The exponent ζ is for d fixed a -independent in the SR-regime and a -dependent in the LR-regime, see the sketch on the right.

4.6. Crossover from short-range to long-range correlated disorder

It is interesting to discuss the crossover from short to long-range disorder. It can be studied analytically around the point $a = d = d_c(D)$ in a double expansion. In the case of the particle, this has been done by several authors (see [42] and references therein) in a double expansion near $a = d = 2$. A complicated scenario was found with several sectors. We will recover their result and find novel ones for manifolds. For polymers we will expand near $d = a = 4$ for directed polymers and $d = a = 6$ for isotropic ones. Typically one expects a line $a_c(d)$ where the SR exponents cease to hold, as represented in Fig. 11. It is thus important to study the crossover in detail in view of numerical simulations since in the physical dimensions $d = 2, 3$ there will be a wide range of correlation decay exponents a accessible in practice, where the competition between long-range and short-range disorder obtained here can be tested.

4.6.1. General structure of the RG flow

Here, the situation is analyzed as follows. Denote by g_L and g_T the couplings for SR disorder, and by b_L and b_T the couplings for LR disorder. Their canonical dimensions are in the case of isotropic manifolds

$$[g_L] = [g_T] = \varepsilon = 2 + D - \frac{2 - D}{2}d, \quad [b_L] = [b_T] = \delta = 2 + D - \frac{2 - D}{2}a \tag{4.46}$$

and for directed manifolds

$$[g_L] = [g_T] = \varepsilon = 2 - \frac{2 - D}{2}d, \quad [b_L] = [b_T] = \delta = 2 - \frac{2 - D}{2}a. \tag{4.47}$$

Since $a < d$, we always have $\delta > \varepsilon$. In Section 3.10 we have calculated the renormalization of elasticity, friction and thermal disorder. To generalize this to the mixed case discussed here, one simply has to replace g_L by $g_L + b_L$ and g_T by $g_T + b_T$ in the corresponding renormalization functions.

In addition, we now have to take care of the mixture of both types of disorder under renormalization. As discussed in Section 3.4, no LR disorder is generated. If we denote SR disorder by $\text{---}\bullet\text{---}\bullet\text{---}$, and LR disorder by $\text{---}\bullet\text{---}\times\text{---}\bullet\text{---}$ (for isotropic disorder for simplicity, generalization to transversal and longitudinal disorder are straightforward), then we obtain the following equality for the residues of the pole terms:

$$\begin{aligned}
 \left\langle \text{---}\bullet\text{---}\bullet\text{---}\bullet\text{---}\bullet\text{---} \middle| \text{---}\bullet\text{---}\bullet\text{---} \right\rangle_{\varepsilon} &= \left\langle \text{---}\bullet\text{---}\times\text{---}\bullet\text{---}\bullet\text{---}\bullet\text{---}\bullet\text{---} \middle| \text{---}\bullet\text{---}\bullet\text{---} \right\rangle_{\delta^{-1}} \\
 &= \left\langle \text{---}\bullet\text{---}\times\text{---}\bullet\text{---}\bullet\text{---}\bullet\text{---}\bullet\text{---}\bullet\text{---} \middle| \text{---}\bullet\text{---}\bullet\text{---} \right\rangle_{(2\delta-\varepsilon)^{-1}} = \mathcal{B}.
 \end{aligned}
 \tag{4.48}$$

Note that this is a statement about the leading term, i.e. the residue, but that the finite terms are different and will lead to a less trivial result at the 2-loop level. A similar statement holds for the particle case, as one can see by a procedure analogously to that presented in Section 3.9. The generalized 1-loop β -functions then read

$$\begin{aligned}
 \beta_L^g(g_L, g_T, b_L, b_T) &= -\varepsilon g_L - \frac{d-2}{2d} C g_L (g_L + b_L) + \left(1 - \frac{1}{d}\right) \frac{d+2}{2} \mathcal{A} g_L (g_T + b_T) \\
 &\quad - \frac{1}{2} \mathcal{B} (g_L + b_L) (g_T + b_T),
 \end{aligned}
 \tag{4.49}$$

$$\begin{aligned}
 \beta_T^g(g_L, g_T, b_L, b_T) &= -\varepsilon g_T - \frac{d-2}{2d} C g_T (g_L + b_L) + \left(1 - \frac{1}{d}\right) \frac{d+2}{2} \mathcal{A} g_T (g_T + b_T) \\
 &\quad - \frac{1}{2} \mathcal{B} (g_L + b_L) (g_T + b_T),
 \end{aligned}
 \tag{4.50}$$

$$\beta_L^b(g_L, g_T, b_L, b_T) = -\delta b_L - \frac{d-2}{2d} C b_L (g_L + b_L) + \left(1 - \frac{1}{d}\right) \frac{d+2}{2} \mathcal{A} b_L (g_T + b_T),
 \tag{4.51}$$

$$\beta_T^b(g_L, g_T, b_L, b_T) = -\delta b_T - \frac{d-2}{2d} C b_T (g_L + b_L) + \left(1 - \frac{1}{d}\right) \frac{d+2}{2} \mathcal{A} b_T (g_T + b_T).
 \tag{4.52}$$

Once fixed points have been found, the exponents can then be obtained, since one has simply

$$\zeta(g_L, g_T, b_L, b_T) = \zeta(g_L + b_L, g_T + b_T)
 \tag{4.53}$$

and similarly for the exponents z and β , given by formula (4.8).

Let us now discuss the structure of these flow equations. This is not a trivial task since the whole depends on the values of the diagrams \mathcal{A} , \mathcal{B} and \mathcal{C} , all of them functions of the expansion point, and on δ and ε . We can furthermore make the observation that

$$\kappa := \frac{b_L}{b_T}
 \tag{4.54}$$

is again unchanged under renormalization, thus entering as an additional parameter. The situations can then be analyzed by the following observations:

(1) *Relevance of the disorder.*

If both ε and δ are negative, then disorder is indeed irrelevant, i.e. when starting with any combination of the couplings, the flow is always towards 0.

(2) *Attractivity of the isotropic fixed point $g := g_L = g_T$.*

The best way to study this is to write down the flow equation for the combination $(g_L - g_T)/(g_L + g_T)$, which using Eqs. (4.49) and (4.50) evaluates to

$$\mu \frac{\partial}{\partial \mu} \bigg|_0 \frac{g_L - g_T}{g_L + g_T} = \mathcal{B} \frac{(g_L - g_T)(g_L + b_L)(g_T + b_T)}{(g_L + g_T)^2}. \quad (4.55)$$

Since the r.h.s. is always positive, the ratio $(g_L - g_T)/(g_L + g_T)$ will flow to 0. We can therefore study the simplified flow equations for which we set

$$\begin{aligned} g &:= g_L = g_T, \\ b &:= b_T, \\ b_L &= \kappa b. \end{aligned} \quad (4.56)$$

These equations read

$$\begin{aligned} \beta^g(g, b) &= -\varepsilon g - \frac{d-2}{2d} \mathcal{C} g(g + \kappa b) + \left(1 - \frac{1}{d}\right) \frac{d+2}{2} \mathcal{A} g(g + b) \\ &\quad - \frac{1}{2} \mathcal{B}(g + \kappa b)(g + b), \end{aligned} \quad (4.57)$$

$$\beta^b(g, b) = -\delta b - \frac{d-2}{2d} \mathcal{C} b(g + \kappa b) + \left(1 - \frac{1}{d}\right) \frac{d+2}{2} \mathcal{A} b(g + b). \quad (4.58)$$

(3) *Stability of the SR-fixed point*

Next we discuss the stability of the SR-fixed point with $b = 0$, present for $\varepsilon > 0$ and consequently also $\delta > 0$. Its stability on the axis $b = 0$ was established before for all cases of interest. To analyze its stability towards perturbations of LR disorder, we linearize Eq. (4.58) for small b . Two cases can be distinguished. If (with the diagrams explicitly given in Eqs. (4.9) and (4.10))

$$\delta < \varepsilon \frac{(d-1)(d+2)\mathcal{A} - (d-2)\mathcal{C}}{(d-1)(d+2)\mathcal{A} - d\mathcal{B} - (d-2)\mathcal{C}}, \quad (4.59)$$

then LR disorder is irrelevant and the SR-fixed point alone is stable. The exponents are then given by the results for the SR disorder problem. Note that the coefficient on the r.h.s. of Eq. (4.59) is always larger than 1, such that this condition is satisfied for weakly LR disorder. $\delta < \varepsilon$ would be the result of a naive dimensional estimate, and the above results gives the correct result to lowest order, i.e. the tangent to the curve in the a, d plane above which SR exponents are correct. For a directed polymer $D = 1$ one finds the condition

$$4 - a < (4 - d)/(1 - (1/3\pi)) = 1.1187(4 - d) \quad (4.60)$$

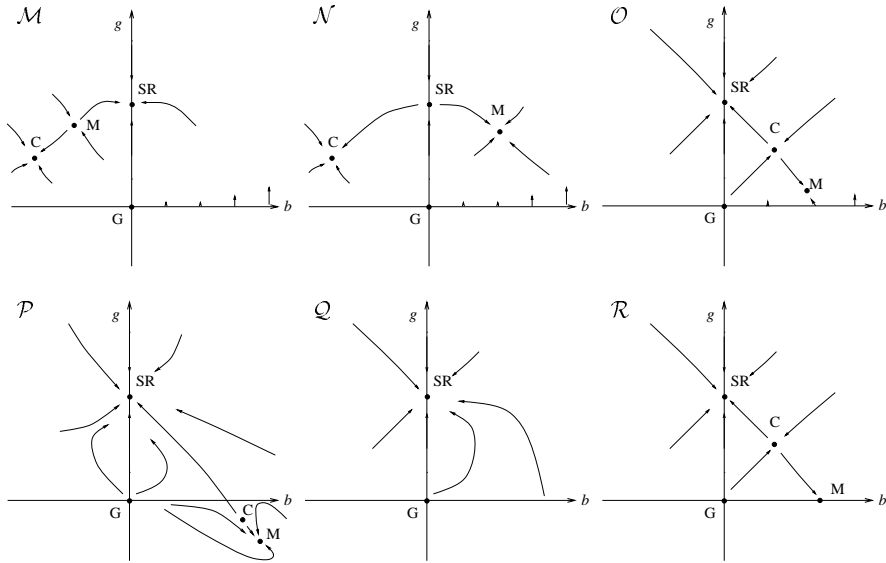


Fig. 12. Schematic sketch of the possible flow diagrams for $\varepsilon > 0$. For directed manifolds, \mathcal{M} and \mathcal{N} are sufficient and the fixed point C is rejected to infinity. \mathcal{M} is relevant when SR is attractive, and \mathcal{N} else. The other situations become important for the isotropic case, see the discussion below.

and for an isotropic polymer

$$6 - a < 1.07723(6 - d) \tag{4.61}$$

for the exponents to be given by their SR expressions (see Sections 4.2 and 4.4).

(4) *Repulsiveness of the line $g = 0$.*

By analyzing the flow equation Eq. (4.57) for vanishing coupling g , we see that the flow on the axes $g = 0$ is always pointing upwards (increase of b) at least for $\kappa > 0$.

(5) *The complete flow diagram.*

Let us now draw the complete flow diagram for both couplings b and g in the situation where the SR-fixed point is stable and κ large. (This domain includes all values of $\kappa > 1$, but is significantly larger. We will detail on the exact phase boundary below.) By direct integration of the flow equations, one finds the situation \mathcal{M} sketched in Fig. 12. The figure contains 4 fixed points, namely G, M, C and SR, as expected on general grounds. (For directed manifolds, C however is rejected to ∞ .) How does then the SR-fixed point become unstable?

(6) *Crossover from the SR-fixed point to the mixed fixed point M.*

Above, we have given the conditions when the SR-fixed point is stable. If one now increases δ such that Eq. (4.59) is no longer satisfied, then the flow diagram changes to \mathcal{N} in Fig. 12. Note that in this case, the mixed fixed point M takes over the stability of the SR-fixed point.

(7) *Completeness of the scenarios when there is a repulsive SR-fixed point ($\varepsilon > 0$ and Eq. (4.59) not satisfied).*

We claim that under these conditions, the scenario on the mid of Fig. 12 is the only possible one, i.e. that no new stable fixed point can appear in the physically relevant sector $b, g > 0$, nor can the fixed point M disappear other than in a reverse of what we discussed in point (6), making the SR-fixed point stable. Let us focus on the fixed point M. It can neither pass through the axes $b = 0$ other than through the SR-fixed point, as else there were 3 fixed points on the axes. Nor can it pass through the axes $g = 0$, since this axes is always repulsive and thus does not admit a completely stable fixed point. M can not pass through the Gaussian fixed point G since $\delta > \varepsilon > 0$. The last way for M to escape is via infinity. There are situations were this happens (see e.g. [58]), but not here: At the fixed point, both Eq. (4.57) and Eq. (4.58) have to vanish. Combining them, one obtains for $b > 0$ and $g > 0$

$$\delta - \varepsilon = \frac{1}{2}\mathcal{B} \frac{(g + \kappa b)(g + b)}{g} > \frac{1}{2}\mathcal{B} g \quad (4.62)$$

bounding g .

(8) *The case of a completely stable SR fixed point.*

The same scenario is valid, if $\varepsilon > 0$ and the SR fixed point is attractive (see left of Fig. 12), with two possible exceptions: First, the fixed points C and M can coalesce and then annihilate, leaving only two fixed points, G and SR, (flow \mathcal{Q} in Fig. 12), which always have to exist as discussed above. Formally, C and M have become complex. This is only possible in the isotropic case, see the discussion below.

Further changing the parameters, the pair of them can re-appear in the physical sector $b, g > 0$. One then obtains two completely stable fixed points, SR and M, with their domains of attraction divided by a phase separatrix, passing through C. The most obvious such situation is when $\kappa = 0$, since then there has to be a fixed point on the axes $g = 0$, see \mathcal{R} . This is the limiting case of the situation \mathcal{O} in Fig. 12 for $\kappa \rightarrow 0$. (The axes $g = 0$ is no longer repulsive.)

(9) *The case $\varepsilon < 0$, $\delta > 0$.*

The last case of interest is, when by say keeping δ fixed ε becomes negative. Then the SR-fixed point disappears and only the mixed fixed point stays in the physically relevant sector $b \geq 0$ and $g \geq 0$. With the same reasoning as above, one concludes that it cannot escape, as long as $\delta > 0$. If however δ changes sign, it will disappear through the Gaussian fixed point at the origin, which then will become stable, as expected. We have plotted some of the flow diagrams in the case $\varepsilon < 0$, $\delta > 0$ in Fig. 13, which show amusing spiral behavior. We note, as will be discussed below in details that in that case, as ε/δ becomes very negative, the value of the couplings can become rather large. This terminates the discussion of the topology of the flow diagrams.

Note also that in the directed case, the fixed point C is rejected to ∞ , and thus the flows \mathcal{M} and \mathcal{N} are sufficient to describe the crossover.

We will now give detailed results for the critical exponents at M and discuss how they differ from their values at the LR fixed point discussed earlier. In general, if ε and

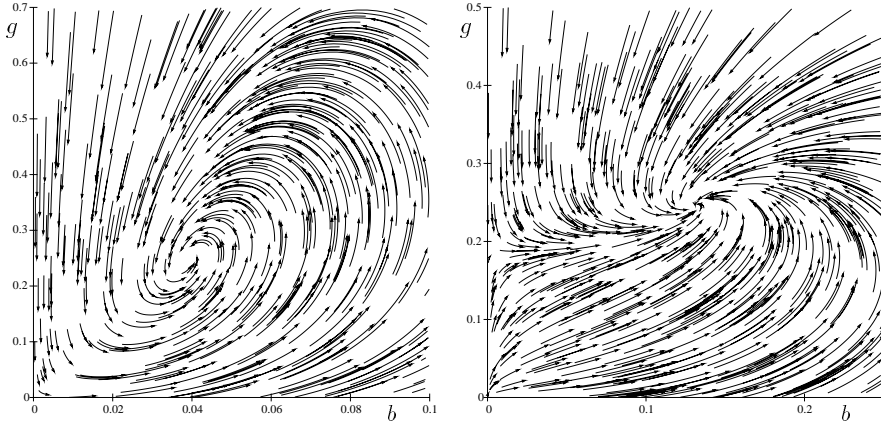


Fig. 13. Some flow diagrams in the case of isotropic disorder. The left one is for $D_0 = 1$, $\varepsilon = -1$, $\delta = 1$, $\kappa = 100$, the right one for $D_0 = 1$, $\varepsilon = 1$, $\delta = 2$, $\kappa = 10$. Note also the repulsive SR-fixed point on the axis $b = 0$.

δ are comparable, the critical exponents are continuous functions of both arguments, modifying the pure LR-behavior. On the other hand, when δ is small compared to the modulus of ε (which then necessarily is negative) then the exponents tend to their values given by the LR-fixed points, except in one situation discussed below.

4.6.2. Results for directed manifolds

Let us introduce the ratio $S = (1 - \frac{1}{d})(d + 2)\mathcal{A}/\mathcal{B}$. For polymers one expands around $a = d = 4$ and $S = 3\pi$. Then the fixed point M has coordinates

$$b_T^* + g^* = \frac{2d\delta}{(d - 1)(d + 2)\mathcal{A}}, \tag{4.63}$$

$$b_L^* + g^* = \kappa b_T^* + g^* = \tilde{\kappa}(b_T^* + g^*), \tag{4.64}$$

$$\tilde{\kappa} = \kappa \frac{1 - \frac{\varepsilon}{\delta}}{1 + \frac{\kappa - 1}{S} - \frac{\varepsilon}{\delta}} \tag{4.65}$$

and is physical, i.e. has a positive $b_T^* = (b_T^* + g^*)(1 - \frac{1}{S} - \frac{\varepsilon}{\delta}) / (1 + \frac{\kappa - 1}{S} - \frac{\varepsilon}{\delta})$ as long as the above condition $\varepsilon/\delta < 1 - \frac{1}{S}$ is satisfied (it collides with the SR fixed point at this value, except for $\kappa = 0$). The fixed point C in the present case is rejected to $b_T = -\infty$.

For $\varepsilon/\delta < 1 - \frac{1}{S}$ one thus recovers the previous results for the LR fixed line of directed manifolds, Section 4.3, except that κ has to be replaced in all expressions (e.g. in Eqs. (4.28)–(4.30)) by the value $\tilde{\kappa}$ which depends on the ratio ε/δ . Thus we have that $z_M(\kappa) = z_{LR}(\tilde{\kappa})$, etc. When $\varepsilon/\delta = 1 - 1/S$ one has that all initial κ yield $\tilde{\kappa} = 1$ (isotropic disorder) and one recovers the SR exponents, while when ε/δ decreases towards $-\infty$ one recovers progressively the LR exponents since $\tilde{\kappa} \rightarrow \kappa$ when $\varepsilon/\delta \rightarrow -\infty$. An interesting property is that $\tilde{\kappa}(\kappa)$ is an increasing function which is bounded $\tilde{\kappa}(\kappa = \infty) = S(1 - \varepsilon/\delta)$. Thus only a finite interval of the vertical fixed line L studied in the LR expansion can really be reached for a fixed finite ε/δ .

In particular the Flory exponent for $\zeta = \zeta_F = (4 - D)/(2 + a)$ is still exact at M . This yields the exact relation for $a^*(d)$ at which the SR exponent will start being corrected as $a^*(d) = (4 - D)/\zeta_{SR}(d) - 2$, a relation which could be checked in numerical simulations. For polymers using the improved estimates it gives $a^*(d = 3) \approx 2.76$ (while the naive extrapolation in Eq. (4.60) gives $a^*(d = 3) = 2.88$) and $a^*(d = 2) \approx 1.44$ (while the naive extrapolation in Eq. (4.60) gives $a^*(d = 3) = 1.76$).

The case $\kappa = 0$ must be discussed separately. For concreteness, start with both $b_L = 0$ and $g_L = 0$. We know that only SR potential disorder is generated, yielding a finite g_L , but that b_L remains zero. The short-range part still converges to the isotropic line $g_L = g_T = g$, as shown in Eq. (4.55) and the above flow equations are still valid setting $\kappa = 0$. There will be the SR fixed point as before, and the fixed point M is on the axis $g = 0$. At the critical value of ε/δ (see Eq. (4.62)) the fixed points SR and M exchange stability, but without colliding (right at the critical value there is a fixed line extending from one to the other). In any case, the values of the exponents will be as given above setting $\kappa = 0$.

We have also checked that the results for the crossover from LR to SR for the particle given e.g. in Eq. (62) of [42] are recovered from our formulae.

4.6.3. Results for isotropic manifolds

With the same notations as previously (but different coefficients \mathcal{A} , \mathcal{B} and \mathcal{C}) we find the coordinates of the fixed points M and C as

$$g^* + b_T^* = (g^* + b_T^*)^{\text{dir}} X, \quad (4.66)$$

$$g^* + b_L^* = g^* + \kappa b_T^* = (g^* + b_T^*)^{\text{dir}} \kappa_c (X - 1). \quad (4.67)$$

X satisfies an equation with the two roots

$$X_{\pm} = \frac{1}{2} (1 + \rho G \pm \sqrt{(1 + \rho G)^2 - 4G}), \quad (4.68)$$

where we have defined $\rho = 1 - \kappa/\kappa_c$ and $G = S(1 - \frac{\varepsilon}{\delta})/(1 - \kappa)$. We shall concentrate on the case of the polymer $D = 1$, where one has $\kappa_c = 35.8702$ and $S = \frac{2}{5}\kappa_c$. We found that in the range of interest the fixed point M corresponds to X_+ for $\kappa > 1$ and to X_- for $\kappa < 1$ and is in the physical sector as long as the condition $\varepsilon/\delta < 1 - \frac{1}{S} \frac{\kappa_c}{\kappa_c - 1}$ holds. The fixed point C is mostly in the unphysical region. (For the exception see below.)

There are several interesting properties. First, one can now study in more detail the surprising property of the separatrix found before. One finds that as ε/δ is decreased to $-\infty$ at fixed κ , two radically different behaviours occur with a transition at $\kappa = \kappa_c$. Either $\kappa < \kappa_c$ and then one finds (for $\kappa > 1$) that as $\varepsilon/\delta \rightarrow -\infty$, X_+ saturates at the value

$$X_+ \rightarrow X_+^{+\infty} = \frac{\kappa_c}{\kappa_c - \kappa} \quad (4.69)$$

while for $\kappa > \kappa_c$, X_+ keeps on growing indefinitely as $\varepsilon/\delta \rightarrow -\infty$ as

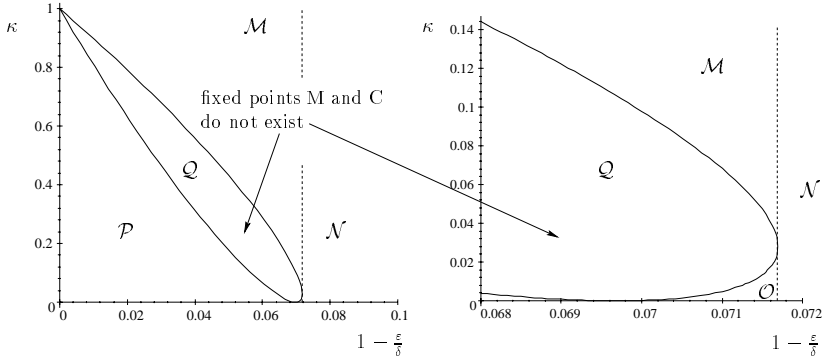


Fig. 14. Domains for which the argument of the root in Eq. (4.68) is negative for polymers ($D = 1$), and therefore the fixed points M and C do not exist. The right figure is just a magnification of the left one, on which e.g. domain \mathcal{O} cannot be identified. The dotted line is the boundary of the domain of stability for the SR fixed point as given by Eq. (4.59), such that to the left of it, the SR fixed point is stable. Note that it is tangential to the domain, where the fixed points M and C do not exist. We have also labeled the regions according to the flow diagrams in Fig. 12. Situation \mathcal{R} , not drawn here, is obtained by starting from the domain \mathcal{O} and taking the limit $\kappa \rightarrow 0$.

$$X_+ \sim \frac{-\varepsilon}{\delta} \frac{\kappa - \kappa_c}{\kappa_c(\kappa - 1)} S. \tag{4.70}$$

In the first case $\kappa < \kappa_c$ the exponents at the fixed point M will evolve smoothly, as $\varepsilon/\delta \rightarrow -\infty$ to their values on the fixed line obtained in section (4.5) in a first order expansion in δ at fixed d . However, for $\kappa > \kappa_c$ there is no well defined expansion in δ at fixed d , as the fixed point M becomes non-perturbative in δ at fixed $\varepsilon < 0$. The fixed point can still be reached and exponents be computed but only in a perturbative expansion in *negative* ε (for $\delta > 0$).

For a given κ and a fixed ratio ε/δ one can compute X using (4.68) and obtain the critical exponents at M to first order in $\delta = 2 + D - (2 - D)\frac{\varepsilon}{2}$ as

$$\zeta = \frac{2 - D}{2} + \frac{\delta}{(d - 2)\kappa_c} (\kappa_0 - \tilde{\kappa}) X, \tag{4.71}$$

$$z = 2 + \frac{2\delta}{d - 2} (R - 1)(X - 1), \tag{4.72}$$

$$\beta = -\frac{2\delta}{d - 2} (X - 1) \tag{4.73}$$

with $\tilde{\kappa} = \kappa_c(1 - 1/X)$, $\kappa_0 = (d - 1)R$, $R = \mathcal{A}/\mathcal{C}$, and one should set $d = 2(2 + D)/(2 - D)$, i.e. $d = 6$ for the polymer. Using the above limit (4.69) one checks that indeed the formulae (4.45) are recovered when $\varepsilon/\delta \rightarrow -\infty$ for $\kappa < \kappa_c$.

We can now obtain the exponents of the regime $\kappa > \kappa_c$ (which was non-perturbative in δ) in an expansion in negative ε . We find, using the above limits (4.70),

$$\zeta = \frac{2 - D}{2} - \frac{4(-\varepsilon)}{(d + 2)(d - 2)(\kappa - 1)} \left(\frac{\kappa}{\kappa_c} - 1 \right) S, \tag{4.74}$$

$$z = 2 + \frac{2(-\epsilon)}{(d-2)(\kappa-1)}(R-1) \left(\frac{\kappa}{\kappa_c} - 1 \right) S, \tag{4.75}$$

$$\beta = \frac{2\epsilon(\kappa - \kappa_c) C}{d(\kappa - 1) \bar{B}}. \tag{4.76}$$

The general analysis of the RG flow is complicated and we have therefore restricted ourselves to the case of the polymer ($D = 1$, $d \approx d_c = 6$). Interestingly, there is a domain of values of the parameters ϵ/δ and κ where the two roots given above become complex (no physical fixed point M or C). This happens in general for $\kappa < 1$ when

$$\frac{1}{S} \frac{1 - \kappa}{(1 + \sqrt{\kappa/\kappa_c})^2} < 1 - \frac{\epsilon}{\delta} < \frac{1}{S} \frac{1 - \kappa}{(1 - \sqrt{\kappa/\kappa_c})^2}. \tag{4.77}$$

with $S = 2\kappa_c/5$. For clarity the different regions in the plane of parameters κ and $1 - \frac{\epsilon}{\delta}$ are drawn in Fig. 14. The corresponding flow diagrams are given in Fig. 12. We invite the reader to start with flow \mathcal{M} and then to continue to \mathcal{N} , \mathcal{O} , \mathcal{P} , and back to \mathcal{M} , and thus to observe how the flow is modified. The domain \mathcal{Q} is defined by (4.77) and corresponds to the case where the two fixed points M and C have annihilated and only the fixed points G and SR remain. Note also that the domain \mathcal{O} , where both the SR and the mixed fixed points are attractive, and where both of them are separated by a separatrix as shown on \mathcal{O} of Fig. 12, is very small. Although it is a rather narrow region which may thus be difficult to observe numerically (in addition the flow towards both fixed points along the line joining them and passing through C is very slow) it is intriguing physically since in that region there will be two different phases and possible values of the exponent depending on the respective bare values of LR and SR disorder.

4.7. Inclusion of self-avoidance

Up to now we have not taken into account self-avoidance. While this is justified for directed polymers (and membranes) by construction, physically, self-avoidance is always present for isotropic polymers (and membranes). Although it is difficult to study in a controlled way for the present problem, we give here some arguments which indicate that self-avoidance does probably not change the behavior in the new glassy phase. We will only address the case of short-range disorder.

Let us examine the operator for self-avoidance. In the dynamical theory of Section 3 it reads

$$\int_{x,x',t} \text{---}\bullet\text{---}\bullet\text{---} = 2 \int_{x,x',t} \tilde{r}(x,t) \frac{\partial}{\partial r(x,t)} \delta^d(r(x,t) - r(x',t)). \tag{4.78}$$

Power counting at the Gaussian fixed point shows that in the absence of disorder, self-avoidance is relevant for $d < d_{SA}^0(D) = 4D/(2 - D)$. On the other hand, we have found that short-range disorder alone becomes relevant, for isotropic manifolds, for $d < d_c(D) = (4 + 2D)/(2 - D)$. Since we study $D < 2$, self-avoidance is always irrelevant near the upper critical dimension $d_c(D)$ around which we expand. Thus the calculations of the previous sections are consistent.

There is always the possibility that self-avoidance becomes relevant as the dimension d is lowered further. One can give some qualitative estimate. We first consider the naive dimension of the self-avoiding operator at the disorder dominated fixed point studied in the previous sections. The power-counting used here and in our previous work [48] gives for the eigenvalue of the above self-avoiding operator:

$$\begin{aligned} \lambda_{SA}^{PC} &= D + 2 + \beta - (d + 2)\zeta \\ &= 2D - d\zeta - \delta^{\text{FDT-violation}}, \end{aligned} \tag{4.79}$$

where $\delta^{\text{FDT-violation}}$ measures the violation of the FDT,

$$\delta^{\text{FDT-violation}} = \zeta - z - \tilde{\zeta} = D - 2 - \beta + 2\zeta. \tag{4.80}$$

Of course, $\delta^{\text{FDT-violation}}$ is zero in the purely potential case, and one recovers the power-counting of self-avoiding membranes without disorder. At the non-trivial fixed point, β is very small and ζ much larger than its Gaussian value $\frac{2-D}{2}$, such that $\delta^{\text{FDT-violation}}$ is positive and renders self-avoidance less relevant.

Let us now try to estimate (4.79). If one first inserts the Flory values $\zeta = 4/(d + 2)$ and $\beta = 0$, one finds that $\lambda_{SA}^{PC} = D - 2 + \beta < 0$ (since always $\beta \leq 0$) and thus that self-avoidance is never relevant. More generally, neglecting β (which is always small) one finds that self-avoidance becomes relevant if $\zeta_{\text{dis}} < \frac{2+D}{2+d}$. The upper bound coincides with the Flory value for the roughness exponent in presence of self-avoidance, which is known to be a good approximation of the true value. Thus we obtain the rough estimate that as long as $\zeta_{\text{dis}} > \zeta_{SA}$ where ζ_{SA} is the roughness exponent with self-avoidance only, self-avoidance can safely be neglected. This is in agreement with the naive expectation that always the operator which results into the larger exponent ζ will be dominant. A look at the estimates for ζ_{dis} obtained in Section 4.4 shows that for polymers the neglect of self-avoidance should be justified.

The above approximation is rather naive when applied to the *non-trivial* fixed point, and there are situations where this kind of arguments goes wrong. Since a complete analysis of the situation away from $\varepsilon = 0$ is technically impossible, one can only study the stability of the fixed point with respect to perturbations by self-avoidance; at first-order in ε this stability analysis is then *exact*.⁶ The complete expression for λ_{SA} is

$$\lambda_{SA}^{\text{full}} = 2D - d\zeta - \delta^{\text{FDT-violation}} + \mu \left. \frac{\partial}{\partial \mu} \right|_{g_L = g_T = g^*} \ln Z_\rho, \tag{4.81}$$

where Z_ρ is the renormalization group Z-factor for self-avoidance. Let us only state the result here ($\curvearrowright \bullet \text{---} \bullet$ denotes the self-avoidance interaction, see Eq. (4.78)):

$$Z_\rho = 1 - 2d \left(g_L - \left(1 - \frac{1}{d} \right) g_T \right) \left\langle \begin{array}{c} \curvearrowright \bullet \text{---} \bullet \\ \curvearrowright \bullet \text{---} \bullet \end{array} \middle| \begin{array}{c} \curvearrowright \bullet \text{---} \bullet \\ \bullet \end{array} \right\rangle_\varepsilon,$$

⁶ It is worth mentioning that in the case of a 2-body self-avoiding interaction only, 3-body self-avoidance is seemingly relevant by power-counting, but that with the help of the above-mentioned stability analysis one can falsify this assertion [47].

$$\left(\text{Diagram} \left| \text{Diagram} \right. \right) = \frac{1}{d} \frac{2}{a-2} \frac{\partial}{\partial \sigma} \frac{\partial}{\partial \tau} [C(x, \tau) + C(y, \sigma)]^{1-a/2}. \quad (4.82)$$

In analogy to Eq. (3.78), the diagram is evaluated as

$$\left\langle \text{Diagram} \left| \text{Diagram} \right. \right\rangle_\varepsilon = \frac{1}{d} \frac{2}{a-2} \frac{1}{(2-D)^2} \frac{\Gamma^2\left(\frac{D}{2-D}\right)}{\Gamma\left(\frac{2D}{2-D}\right)} \times S_D ((2-D)S_D)^{a/2} \quad (4.83)$$

Since

$$\mu \frac{\partial}{\partial \mu} \Big|_{g_L=g_T=g^*} \ln Z_\rho = 2g^* \left\langle \text{Diagram} \left| \text{Diagram} \right. \right\rangle_\varepsilon > 0, \quad (4.84)$$

and with the help of Eqs. (4.79) and (4.81), $\lambda_{SA}^{\text{full}} > \lambda_{SA}^{\text{PC}}$, such that vertex-corrections render self-avoidance *more* relevant. The influence of these corrections for large ε is difficult to estimate. Let us only remark that for large d , $\left\langle \text{Diagram} \left| \text{Diagram} \right. \right\rangle_\varepsilon$ is exponentially suppressed.

Thus we obtain that at the isotropic fixed point self-avoidance is presumably not important, since the random flow has already strongly stretched the polymer or membrane.

There is one case however, well studied previously [55,57,59–61], where we know that self-avoidance is important. This is when the flow is the gradient of a short-range random potential, a case not studied here, but which we mention for completeness. There disorder and self-avoidance become relevant *simultaneously* at $d = 4D/(2 - D)$. The available RG treatments for this problem [55,59,60] exhibit a runaway flow to strong coupling, as in the present method, and thus the problem can not completely be understood. One open question is whether the exponent ζ is the same as for pure self-avoidance ζ_{SA} [59], and even how universal the strong coupling regime is. The question was addressed in [57] and it was concluded that the problem is governed by a new strong disorder fixed point, very much like the directed polymer problem, where *both* self-avoidance and disorder are relevant. Flory arguments were presented leading to $\zeta \approx 0.8$ in $d = 2$ in good agreement with later simulations [61]. This problem however deserves further studies.

4.8. Polymer in a hydrodynamic flow: toy model for generation of barriers

One of the remarkable results obtained in previous sections is that for a manifold with $D > 0$ in a purely divergenceless flow new terms which violate the divergence free condition are generated in perturbation theory (this is shown explicitly in Appendix C). Although they are finite, they eventually drive the system to the fixed point where $g_T = g_L$. This is in sharp contrast to the particle case $D = 0$ where the divergenceless flow is a physical fixed point, distinct from the fixed point at $g_T = g_L$. Physically this

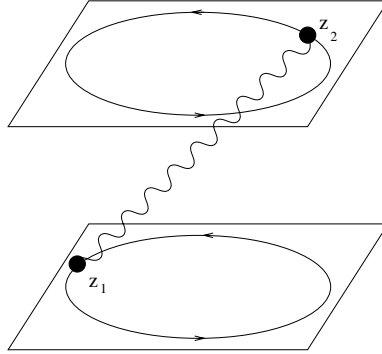


Fig. 15. A dumbbell diffusing with each end on a rotating plane, according to Eq. (4.86).

is because barriers are generated in the case of the manifold but not in the case of the particle.

In the case of the particle the fact that the line $g_T = 0$ is exactly preserved to all orders can be understood by noticing that the exact stationary distribution is known, and is simply the spatially uniform distribution. This exact property implies strong constraints, as it must exactly be preserved by renormalization. In the case of manifolds, one can check whether the measure $\mu_{\text{eq}} = \exp(-c/(2T) \int_x (\nabla r_x)^2)$ is also stationary. If it was, it would imply similar properties as for the particle, and in particular no generation of barriers (since it is translationally invariant). There are some simple cases of flows where μ_{eq} is indeed stationary. One example is the generalization to polymers [62] of the de Marsilly–Matheron model of a layered random flow. There one can show explicitly that μ_{eq} satisfies the corresponding Fokker–Planck equation and is stationary. This problem was studied analytically in [62]. Although it can be solved, it is in a sense misleading because it misses the physics of the generation of barriers unveiled here: for a polymer in a *generic* divergenceless random flow such a simple translationally invariant stationary measure does not exist.

In this section we will analyze this mechanism further. We will present some toy models which allow to illustrate in a simple way how elasticity leads to dynamical generation of barriers even in a divergenceless flow.

We start with a single-particle convected in such a flow, which we denote as $v_\alpha(x)$. The probability distribution $P(x, t)$ for the particle to be at position x at time t , satisfies the Fokker–Planck equation (T is the temperature)

$$\partial_t P(x, t) = \partial_\alpha (T \partial_\alpha P(x, t) - v_\alpha(x) P(x, t)). \tag{4.85}$$

Since $\partial_\alpha v_\alpha = 0$ one checks easily that the spatially uniform measure $P(x) = 1/V$ (V is the volume of the system) is a stationary solution. At large time (and $T > 0$) the particle density will be uniformly distributed over the system. Upon applying a force f , the drift velocity in response to the force will be exactly f . This can be checked by methods similar to the one introduced in [63].

Let us now consider two elastically coupled particles (a dumbbell, see Fig. 15). We

will start with two particles each located in a 2d plane. For convenience we will denote $z_k = x_k + iy_k$ the complex position of particle $k = 1, 2$ in its plane. We will model the directed polymer situation, and thus each particle will see a different flow. The equation of motion is

$$\begin{aligned}\dot{z}_1 &= c(z_2 - z_1) + i\omega_1 z_1 + \eta_1, \\ \dot{z}_2 &= c(z_1 - z_2) + i\omega_2 z_2 + \eta_2,\end{aligned}\tag{4.86}$$

where c is the elastic coupling and $\langle \eta_i \eta_j^* \rangle = 4T\delta_{ij}$ the thermal noise. The flow in each plane is thus simply $v_x = -\omega_k y$, $v_y = \omega_k x$, i.e. circulating around the center $x = y = 0$ (where the stream function $\psi(x, y) = \omega_k(x^2 + y^2)$ has a maximum). The two flows have identical center, but a slightly different rotation rate. We denote by $2\delta = \omega_1 - \omega_2$ the difference, and by ω the mean. Although this model is linear, it already exhibits striking behavior.

In the absence of “disorder”, $\delta = 0$, the motion is simply a collective rotation around the center $z = 0$. The eigenvalues of the linear system at $T = 0$ are $i\omega$, which describes the global rotation, and $-2c + i\omega$ which describes the decay towards the steady state $z_1 = z_2$. At any T the global rotation can be eliminated by redefining $z_k = \exp(i\omega t) \tilde{z}_k$, and similarly redefining the thermal noise. Thus the steady state measure is simply:

$$P(z_1, z_2) = e^{-\frac{c}{2T}|z_1 - z_2|^2},\tag{4.87}$$

i.e. uniform in space and proportional to the Boltzmann measure of the elastic system in the rotating frame. Thus again, at $T > 0$, one observes free collective diffusion of the center of mass, and a linear response $v = f$ of its velocity v to an applied force f .

Remarkably, as soon as $\delta > 0$, the zero-mode disappears and the two particles converge towards the center. At $T = 0$ the linear system eigenvalues are now $\lambda_{\pm} = -c + i\omega \pm \sqrt{c^2 - \delta^2}$. The global rotation can be eliminated as before, but the differential rotation cannot. The convergence of the dumbbell towards $(z_1 = 0, z_2 = 0)$ is exponential as $|z_k(t)| \sim e^{-(c - \sqrt{c^2 - \delta^2})t}$, with a characteristic relaxation time $\tau \sim 2c/\delta^2$ at small δ (which interestingly is much larger than the characteristic time $1/|\omega_1 - \omega_2|$). The slowest decaying eigenmode has $z_1/z_2 \sim e^{i\delta/c}$ at small δ , i.e. it is twisted by an angle $\sim \delta/c$.

Most interestingly the effect persists to $T > 0$. It is difficult to find the full stationary measure for the process (which seems to be non-Gaussian) but it is possible to compute explicitly the mean squared positions, by integration of the equations of motion. We find

$$\langle |z_k|^2 \rangle = \frac{2T}{c\delta^2}(c^2 + \delta^2), \quad k = 1, 2.\tag{4.88}$$

This indicates a genuine bound state at $z = 0$. At small δ , we find $|z_k|^2 \sim T\tau$ with the same relaxation time τ introduced above. Since T is the diffusion coefficient, the picture is that the dumbbell will diffuse away from the center at $z = 0$ for a time $\sim \tau$ until it is pulled back in again. The nature of this bound state is intriguing. One can easily see that the stationary conformation is twisted. Indeed a similar calculation gives

$$\langle z_1 z_2^* \rangle = 2T(c + i\delta)/\delta^2.\tag{4.89}$$

Thus, remarkably, as soon as one considers two elastically coupled particles, preferred regions appear and the stationary measure is no longer spatially uniform. Physically this is because the two particles prefer regions where the elastic energy is reduced. The center of mass motion thus becomes coupled to the internal elastic mode.

Let us now apply an external force. One easily sees that this only amounts to translate the center of the bound state. In shifted coordinates the motion remains identical. The new center has coordinates

$$z_{1,2} = f \frac{\omega \mp \delta + 2ic}{2\omega c - i(\omega^2 - \delta^2)}, \quad (4.90)$$

where $f = f_x + if_y$ is the force applied on both monomers. Interestingly the new center now depends explicitly on ω (the global rotation cannot be eliminated anymore), in a complicated way. Also one has $z_1 \neq z_2$, i.e. the dumbbell is slightly inclined. For small $\delta \ll \omega, c$ it reads

$$z_{1,2} \approx f \left(\frac{-1}{i\omega} \mp \frac{\delta}{2c\omega - i\omega^2} \right). \quad (4.91)$$

In the limit $\delta \rightarrow 0$ the dumbbell center is close to $z_1 = z_2 = -1/i\omega$ (with a weak restoring spring). Amusingly, in that limit the dumbbell thus responds perpendicularly to the force, as a vortex.

So far we have described situations where the location of the extrema of the stream functions in each plane coincide, but the rotation rate does not. If these locations are shifted, the same phenomena arise, i.e. a bound state occurs around a new center with non-trivial position.

This model can be extended in several directions. First one may consider a directed chain with N monomers, again with aligned stream function extrema at $z_k = 0$, and different frequencies ω_k . One then sees that the decay towards the center at $T = 0$ exactly maps onto the problem of spin depolarization studied in [64], a problem which arises in the context of the so called “motional narrowing” in nuclear magnetic resonance (NMR). Using the results of [64] leads to a stretched exponential decay of $\langle |z_k(t)|^2 \rangle$ towards the center.

Non-linear extensions of Eq. (4.86) can also be studied. They will show the generation of barriers. For instance in a model with two uncorrelated random stream functions $\psi_k(z_k)$, local long living bound states will be located where extrema are close together (note that saddle points are rapidly escaped from). The dumbbell will eventually escape over barriers between these metastable states.

Finally one can see that the effect persists even if the two monomers see the same flow, though in that case it must be non-linear. A related example of that phenomena was discovered by Thual and Fauve [65] in a different context. If one identifies their complex Landau–Ginsburg order parameter $W(x) = z(x)$ as the complex position in 2d of monomers in a gaussian elastic chain at $T = 0$, their complex Landau Ginsburg equation describes the dynamics of such a chain in the complex 2d velocity field $v = (\mu + (\beta_r + i\beta_i)|z|^2 + (\gamma_r + i\gamma_i)|z|^4)z$ (which describes a double well potential force

plus a circulating force with a rotation depending on the distance to the center). They found that this equation can have stationary localized solutions, which in our language correspond to a rotating and twisted polymer in a bound state.

To conclude, some insight can be gained by studying these simple models, and exploring further the physics of these problems would be of great interest.

5. Conclusion

In this article, we have studied a model for polymers, and manifolds of internal dimension D , diffusing and convected by static random flows. Our results are obtained using field theoretical dynamical RG near the upper critical dimension $d_c(D)$, which is $d_c = 4$ and $d_c = 6$ for directed and isotropic polymers respectively, in short-range correlated flows. In principle arbitrary D can be considered, although technically, since $d_c(D)$ diverges as $D \rightarrow 2^-$, our quantitative analysis is valid for $D < 2$.

We found that below the upper critical dimension $d_c(D)$ the random flow is relevant and changes the large scale behavior. This yields a new universal RG fixed point for polymers and manifolds in non-potential static random flows with short-range correlations. We have analyzed the critical theory using multilocal operator product expansion techniques. As a result, all divergences can be absorbed by multilocal counter-terms, of which we explicitly give the 1-loop contribution.

The new RG fixed points are in general characterized by three exponents, the roughness of the manifold ζ , the dynamical exponent z , and ϕ related to the behavior of the drift velocity $v(f)$ under a small applied force f . They have been computed in a dimensional expansion, and estimated numerically in physical dimensions. For directed manifolds, a relation exists between these three exponents. In the limit $D \rightarrow 0$ we recover previously known results for the particle.

Our results show that in static random non-potential flows polymers and manifolds are in a non-trivial steady state with glassy characteristics. In this state, the polymer or membrane is stretched by the flow with a roughness exponent, which is larger than in the absence of the flow (e.g. $\zeta \approx 0.63$ in $d = 3$ and $\zeta \approx 0.8$ in $d = 2$ for directed polymers in SR random flows instead of $\zeta_0 = 1/2$ in the absence of disorder). The internal dynamics is slower, with $z > 2$. Upon applying a small uniform external force f , the polymer will move with a reduced velocity $v(f) \sim f^\phi$ with $\phi > 1$. This state is characterized by a zero *linear mobility* $\mu = dv/df|_{f=0}$. Thus one can consider that the polymer is trapped in preferential regions of the flow. On a simpler toy model with only two particles, we have been able to describe more precisely the effect of trapping, but in the case of the polymer and manifolds its detailed physics remains to be investigated. Numerical simulations would be extremely useful to check our results for the exponents and to further characterize this glassy phase. These simulations should be easier to perform than for conventional potential glassy systems, since in the present case the convergence to the steady state is expected to be faster.

The glassy state that we found for this non-potential system can be compared to the one arising in potential systems. The main difference is that as soon as disorder is non-

potential, an effective temperature is generated, resulting in a violation of the fluctuation dissipation theorem. The increase of temperature competes with the relevance of disorder which tends to make the temperature irrelevant. Since the important dimensionless disorder parameter is proportional to the inverse temperature, contrarily to most potential systems, disorder does not flow to strong coupling. Instead, it flows to a perturbatively accessible fixed point, studied here. The effect of disorder, and thus the glassy characteristics, are in effect weaker than in potential glasses. Indeed, we find a finite dynamical exponent $z > 2$ and $v \sim f^\phi$ rather than the much stronger non-linear “creep” behavior $v \sim \exp(-c(f_c/f)^\mu)$ obtained for manifolds with $D < 4$ and z effectively infinite, which arises from a zero temperature fixed point [12,15,66]. In fact the state found here is reminiscent of the so called “marginal glasses” predicted in the statics for periodic manifolds at their lower critical dimension $D = 2$ [49,67–72], where also thermal effects are important and which have a similar $v \sim f^\phi$ characteristics. This corresponds effectively to barriers which grow logarithmically with size (and inverse applied force), and it is remarkable that the “randomly driven polymer” also exhibits such divergent barriers (in an effective way, since the notion of barriers is not clear-cut in non-potential systems). It is all the more remarkable in the case of a purely hydrodynamic (i.e. divergenceless) flow, which for the single particle leads to a trivial, spatially uniform, stationary distribution (thus without barriers). Here, these barriers are generated from a non-trivial interplay between elasticity, disorder and thermal fluctuations.

In the case of LR correlated flows we have found via an expansion in the range of the correlation a near $a = a_c(D) = d_c(D)$ at fixed d that the behavior of the system is controlled by a line of fixed points, and thus depends continuously on the ratio $\kappa = g_L/g_T$ of the longitudinal to transversal part of disorder (which remains unchanged under renormalization). For directed manifolds, our analytical results were found to be in agreement with the exact large d result obtained in [44] and even, to first order in ε with the corresponding Hartree approximation. In that case ζ was found to be exactly equal to its Flory approximation $\zeta_F = (4 - D)/(2 + a)$ while the other exponents are continuously varying. Several remarkable results were obtained in the case of the isotropic manifold. We found that there exists a critical value κ_{cr} of κ , beyond which no fixed point is found in the fixed dimension expansion, as well as a smaller characteristic value κ_0 beyond which the manifold becomes compressed $\zeta < \zeta_0$ rather than stretched by the flow (as it is in all other cases). Since this problem also corresponds to directed polymers subjected to non-potential “correlated disorder”, these effects may be understood as a result of a competition between localization (due to the correlated nature of the force) and driving. To further investigate this competition we also studied in detail the intricate crossover between SR and LR disorder, in a dimensional expansion around the point $a = d = 6$ for polymers, important for studies in the physical dimensions $d = 2, 3$. In view of the rich variety of obtained behaviors, numerical simulations would be welcome to study the competition between SR and LR disorder effects.

We also note that the glassy phase obtained here is via the RG perturbatively controlled around the line $d_c(D)$ (see Fig. 5), whereas the large d approach of [44] works

for any D and for LR disorder. A last and complementary method is the functional renormalization group (FRG) which can be used in a $D = 4 - \varepsilon$ expansion and thus allows to explore the region of larger D than the present method. Recent progresses on the finite temperature FRG in [33] which showed the existence of such a finite temperature fixed point, leads us to conjecture that a similar fixed point will be accessible by FRG in the present model and should merge smoothly into the one found here upon decreasing D . Work is in progress to verify this conjecture [73].

To conclude, let us mention an interesting speculation, inviting for further investigation [74]: It is well known that a directed polymer in a random potential maps via the Cole–Hopf transformation to the Burgers–Kardar–Parisi–Zhang equation [16]. The question is whether the generalization of the directed polymer diffusing in a non-potential random force field instead of a potential one, has some effective correspondence in a generalization of the Burgers equation to non-potential driving and is thus possibly related to the Navier–Stokes equation.

Acknowledgements

It is a pleasure to thank L. Cugliandolo, F. David, T. Giamarchi, J. Kurchan and L. Schäfer for discussions.

Appendix A. Correlator and response function

In this appendix we give a collection of formulas for the correlator and the response function in the Itô-discretization,

$$\frac{1}{d} \langle r(k, \omega) r(k', \omega') \rangle_0 = \frac{2\lambda}{\omega^2 + (\lambda k^2)^2} (2\pi)^D \delta^D(k + k') (2\pi) \delta(\omega + \omega'), \quad (\text{A.1})$$

$$\frac{1}{d} \langle r(k, \omega) \tilde{r}(k', \omega') \rangle_0 = \frac{1}{i\omega + \lambda k^2} (2\pi)^D \delta^D(k + k') (2\pi) \delta(\omega + \omega'), \quad (\text{A.2})$$

$$\frac{1}{d} \langle \tilde{r}(k, \omega) \tilde{r}(k', \omega') \rangle_0 = 0. \quad (\text{A.3})$$

Fourier-transformation with respect to ω yields

$$\frac{1}{d} \langle r(k, t) r(k', t') \rangle_0 = \frac{1}{k^2} e^{-\lambda|t-t'|k^2} (2\pi)^D \delta^D(k + k'), \quad (\text{A.4})$$

$$\frac{1}{d} \langle r(k, t) \tilde{r}(k', t') \rangle_0 = \Theta(t > t') e^{-\lambda|t-t'|k^2} (2\pi)^D \delta^D(k + k'), \quad (\text{A.5})$$

$$\frac{1}{d} \langle \tilde{r}(k, t) \tilde{r}(k', t') \rangle_0 = 0. \quad (\text{A.6})$$

We will mostly use the real space representation. Let us start with the correlator. The Fourier-transformation of Eq. (A.4) cannot be done explicitly but involves an error

function. In addition, to obtain a well-defined function for $D < 2$ one has to subtract the zero-mode. We therefore define

$$C(x, t) := \frac{1}{2d} \langle (r(x, t) - r(0, 0))^2 \rangle_0. \quad (\text{A.7})$$

The limiting cases are

$$C(x, t) = \begin{cases} \frac{1}{(2-D)S_D} |x|^{2-D} & \text{for } t \rightarrow 0 \\ \frac{2}{(2-D)(4\pi)^{D/2}} |\lambda t|^{(2-D)/2} & \text{for } x \rightarrow 0 \end{cases}, \quad (\text{A.8})$$

with

$$S_D = 2 \frac{\pi^{D/2}}{\Gamma(\frac{D}{2})}. \quad (\text{A.9})$$

Let us also note the ratio

$$\frac{C(1, 0)}{C(0, 1)} = 2^{D-2} \Gamma\left(\frac{D}{2}\right). \quad (\text{A.10})$$

The response function

$$R(x, t) := \frac{1}{d} \langle r(x, t) \tilde{r}(0, 0) \rangle_0 \quad (\text{A.11})$$

is calculated analytically,

$$R(x, t) = \Theta(t > 0) (4\pi\lambda t)^{-D/2} e^{-x^2/4\lambda t}. \quad (\text{A.12})$$

The (perturbative) fluctuation dissipation theorem (FDT) reads

$$\Theta(t) \frac{\partial}{\partial \lambda t} C(x, t) = R(x, t). \quad (\text{A.13})$$

Appendix B. Extrapolations

The numerical values for the exponents reported in Tables 1 and 2 were obtained by an optimization procedure using the freedom to expand about any point on the critical curve $\varepsilon(D, d) = 0$. This procedure, first proposed in [75], was later refined in [52] to obtain reliable estimates for the scaling dimension of self-avoiding polymerized tethered membranes in the frame work of a 2-loop calculation. As will become apparent, various extrapolation schemes are possible, and choosing the best one is almost an art; we shall rely heavily on the methods developed in Ref. [52] to which the interested reader is referred to for further details and discussion. Our presentation is inspired by [58], where complementary material can be found. The general idea is of course to expand about some point (D_0, d_0) on the critical curve $\varepsilon(D_0, d_0) = 0$. The simplest scheme is to extrapolate towards the physical theories for $D = 1, 2$ and $d = 2, 3, \dots$, using

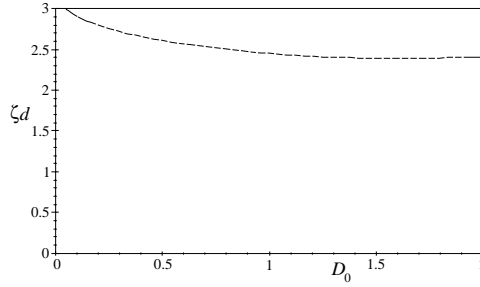


Fig. B.1. Extrapolations for ζd to ($D = 1, d = 3$).

the expansion parameters $D - D_0$ and $d - d_0$. However, as shown in Ref. [52], this set of expansion parameters is not optimal, and better results are obtained by using $D_c(d)$, (solution of the equation $\varepsilon(D_c(d), d) = 0$) and $\varepsilon(D, d)$. Furthermore, it is advantageous to make expansions for quantities such as ζd rather than ζ .

After selecting one of these schemes, the next step is to re-express the quantity which shall be expanded in terms of $D_c(d)$ and $\varepsilon(D, d)$. If we are interested in polymers ($D = 1$) in $d = 3$ subject to isotropic disorder, we have to evaluate this expression for $\varepsilon = 3/2$. However, we are still free to choose the expansion point along the critical curve, which then fixes D_0 . As the expansion point is varied, different values for ζd (i.e. 3ζ for $d = 3$) are obtained, as plotted in Fig. B.1. The criterion for selecting a value for ζ from such curves is that of minimal sensitivity to the expansion point D_0 . We thus evaluate ζ at the extrema of the curves. The broadness of the extremum provides a measure of the goodness of the result, and the expansion scheme. The robustness of this choice was explicitly checked in Ref. [52] in the case of self-avoiding tethered membranes, by going to the second-order. (For additional discussions of such “plateau phenomena” see Section 12.3 of Ref. [52].)

While we examined several such curves, only a selection is reproduced in Figs. B.1, B.2 and B.3. While quantitative predictions were already reproduced in Tables 1 and 2, let us focus on some important qualitative observations. First, it is striking to observe that the dependence of ζ on D in the directed case and the independence on D in the isotropic case, read off from the extrapolations in Fig. B.2, is already predicted by the Flory estimate. Indeed, the latter is hard to improve numerically.

For the exponents z and β , we did not find a reliable extrapolation scheme: As can be deduced from Fig. B.3, the ‘minimum sensitivity point’ in extrapolations for β is roughly independent of D_0 , which indicates that the extrapolation for β only depends on ε , but not in a non-trivial way on D and d .

Extrapolations for z show a plateau when approaching $D_0 \rightarrow 2$ only. Since the structure of the perturbation expansion is such that expanding about $D_0 = 2$ always yields the free-theory result $z_0 = 2$, extrapolations merely permit in concluding on $z > 2$. On the other hand, it is possible to build up combinations of z and D and d , which upon expansion build up a nice plateau. However, the answer obtained by this method strongly depends on the selected scheme, and therefore is unreliable.

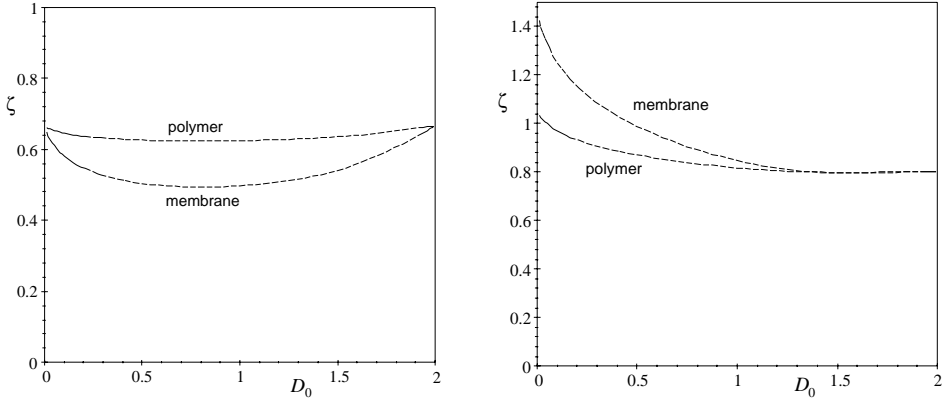


Fig. B.2. Extrapolations for ζ to polymers and membranes in three dimensions, using the extrapolation of ζd . The left diagram is for the directed, the right for the isotropic case.

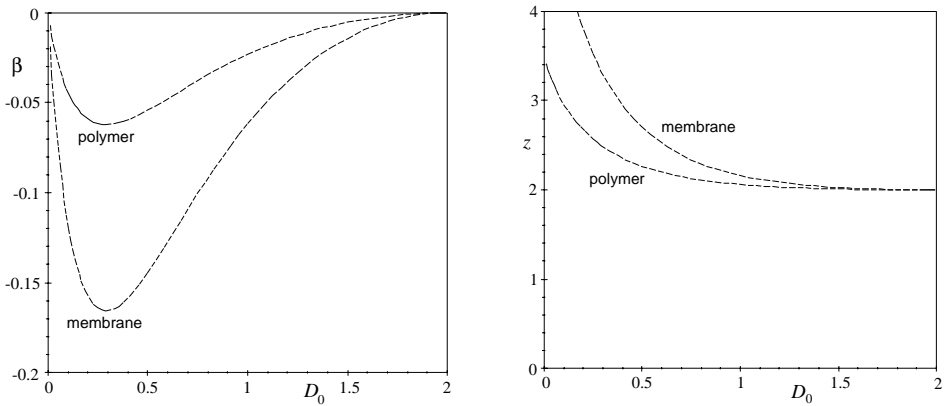


Fig. B.3. Extrapolations for β (left) and z (right) to polymers and membranes in 3 dimensions, isotropic disorder. Note that extrapolations are impossible for z and unreliable for β .

Appendix C. Finite corrections to longitudinal disorder in the purely transversal case

The aim of this appendix is to show that in the pure transversal case, longitudinal disorder is generated at the 2-loop order. A full 2-loop calculation is very difficult to perform (see Ref. [52]). We will therefore only show, that at least one MOPE coefficient, namely

$$\left(\begin{array}{c} \text{---} \bullet \text{---} \\ \text{---} \bullet \text{---} \\ \text{---} \bullet \text{---} \\ \text{---} \bullet \text{---} \end{array} \left| \begin{array}{c} \text{---} \bullet \text{---} \\ \text{---} \bullet \text{---} \\ \text{---} \bullet \text{---} \\ \text{---} \bullet \text{---} \end{array} \right. \begin{array}{c} \text{---} \bullet \text{---} \\ \text{---} \bullet \text{---} \\ \text{---} \bullet \text{---} \\ \text{---} \bullet \text{---} \end{array} \right)$$

does not vanish, as this was the case for

$$\left(\begin{array}{c} \text{---} \bullet \text{---} \\ \text{---} \bullet \text{---} \\ \text{---} \bullet \text{---} \\ \text{---} \bullet \text{---} \end{array} \left| \begin{array}{c} \text{---} \bullet \text{---} \\ \text{---} \bullet \text{---} \\ \text{---} \bullet \text{---} \\ \text{---} \bullet \text{---} \end{array} \right. \begin{array}{c} \text{---} \bullet \text{---} \\ \text{---} \bullet \text{---} \\ \text{---} \bullet \text{---} \\ \text{---} \bullet \text{---} \end{array} \right)$$

Since already the evaluation of $\left(\begin{array}{c} \text{---} \bullet \text{---} \\ \text{---} \bullet \text{---} \\ \text{---} \bullet \text{---} \\ \text{---} \bullet \text{---} \end{array} \left| \begin{array}{c} \text{---} \bullet \text{---} \\ \text{---} \bullet \text{---} \\ \text{---} \bullet \text{---} \\ \text{---} \bullet \text{---} \end{array} \right. \begin{array}{c} \text{---} \bullet \text{---} \\ \text{---} \bullet \text{---} \\ \text{---} \bullet \text{---} \\ \text{---} \bullet \text{---} \end{array} \right)$ is a formidable task, we simplify the task further by considering only a special limit. This is accomplished by evaluating the leading singularity when approaching two of its vertices as

$$\begin{aligned}
 & \left(\begin{array}{c} \text{---} \text{---} \text{---} \\ \text{---} \text{---} \text{---} \\ \text{---} \text{---} \text{---} \\ \text{---} \text{---} \text{---} \end{array} \left| \begin{array}{c} \text{T} \\ \text{T} \\ \text{T} \\ \text{T} \end{array} \right. \text{---} \bullet \text{---} \bullet \text{---} \right) \\
 = & \left(\begin{array}{c} \text{---} \text{---} \text{---} \\ \text{---} \text{---} \text{---} \\ \text{---} \text{---} \text{---} \\ \text{---} \text{---} \text{---} \end{array} \left| \begin{array}{c} \text{T} \\ \text{T} \\ \text{T} \\ \text{T} \end{array} \right. \text{---} \bullet \text{---} \text{T} \bullet \text{---} \right) \times \left(\begin{array}{c} \text{---} \text{---} \text{---} \\ \text{---} \text{---} \text{---} \\ \text{---} \text{---} \text{---} \\ \text{---} \text{---} \text{---} \end{array} \left| \begin{array}{c} \text{T} \\ \text{T} \\ \text{T} \\ \text{T} \end{array} \right. \text{---} \bullet \text{---} \text{L} \bullet \text{---} \right) \\
 + & \left(\begin{array}{c} \text{---} \text{---} \text{---} \\ \text{---} \text{---} \text{---} \\ \text{---} \text{---} \text{---} \\ \text{---} \text{---} \text{---} \end{array} \left| \begin{array}{c} \text{T} \\ \text{T} \\ \text{T} \\ \text{T} \end{array} \right. \text{---} \bullet \text{---} \text{L} \bullet \text{---} \right) \times \left(\begin{array}{c} \text{---} \text{---} \text{---} \\ \text{---} \text{---} \text{---} \\ \text{---} \text{---} \text{---} \\ \text{---} \text{---} \text{---} \end{array} \left| \begin{array}{c} \text{L} \\ \text{T} \\ \text{T} \\ \text{T} \end{array} \right. \text{---} \bullet \text{---} \text{L} \bullet \text{---} \right) \\
 + & \left(\begin{array}{c} \text{---} \text{---} \text{---} \\ \text{---} \text{---} \text{---} \\ \text{---} \text{---} \text{---} \\ \text{---} \text{---} \text{---} \end{array} \left| \begin{array}{c} \text{T} \\ \text{T} \\ \text{T} \\ \text{T} \end{array} \right. \text{---} \bullet \text{---} \text{T} \text{---} \bullet \text{---} \right) \times \left(\begin{array}{c} \text{---} \text{---} \text{---} \\ \text{---} \text{---} \text{---} \\ \text{---} \text{---} \text{---} \\ \text{---} \text{---} \text{---} \end{array} \left| \begin{array}{c} \text{T} \\ \text{T} \\ \text{T} \\ \text{T} \end{array} \right. \text{---} \bullet \text{---} \text{L} \bullet \text{---} \right) \\
 + & \left(\begin{array}{c} \text{---} \text{---} \text{---} \\ \text{---} \text{---} \text{---} \\ \text{---} \text{---} \text{---} \\ \text{---} \text{---} \text{---} \end{array} \left| \begin{array}{c} \text{T} \\ \text{T} \\ \text{T} \\ \text{T} \end{array} \right. \text{---} \bullet \text{---} \text{L} \text{---} \text{---} \bullet \text{---} \right) \times \left(\begin{array}{c} \text{---} \text{---} \text{---} \\ \text{---} \text{---} \text{---} \\ \text{---} \text{---} \text{---} \\ \text{---} \text{---} \text{---} \end{array} \left| \begin{array}{c} \text{L} \\ \text{T} \\ \text{T} \\ \text{T} \end{array} \right. \text{---} \bullet \text{---} \text{L} \bullet \text{---} \right) \\
 + & \dots
 \end{aligned} \tag{C.1}$$

The symbol $\text{---} \bullet \text{---} \text{---} \bullet \text{---}$ hereby denotes the subleading operator (with the possible transversal or longitudinal projectors unspecified)

$$\text{---} \bullet \text{---} \text{---} \bullet \text{---} = \int_k \tilde{r}(x, t) k^2 e^{ik[r(x,t) - r(y,t')]} \tilde{r}(y, t'). \tag{C.2}$$

Since we know from the first-order calculations, see Section 3.4, that

$$\left(\begin{array}{c} \text{---} \text{---} \text{---} \\ \text{---} \text{---} \text{---} \\ \text{---} \text{---} \text{---} \\ \text{---} \text{---} \text{---} \end{array} \left| \begin{array}{c} \text{T} \\ \text{T} \\ \text{T} \\ \text{T} \end{array} \right. \text{---} \bullet \text{---} \text{T} \bullet \text{---} \right) = \left(\begin{array}{c} \text{---} \text{---} \text{---} \\ \text{---} \text{---} \text{---} \\ \text{---} \text{---} \text{---} \\ \text{---} \text{---} \text{---} \end{array} \left| \begin{array}{c} \text{T} \\ \text{T} \\ \text{T} \\ \text{T} \end{array} \right. \text{---} \bullet \text{---} \text{L} \bullet \text{---} \right) = 0,$$

the first two terms on the r.h.s. in Eq. (C.1) vanish. From the calculations in Section 3.4 also follows that

$$\left(\begin{array}{c} \text{---} \text{---} \text{---} \\ \text{---} \text{---} \text{---} \\ \text{---} \text{---} \text{---} \\ \text{---} \text{---} \text{---} \end{array} \left| \begin{array}{c} \text{T} \\ \text{T} \\ \text{T} \\ \text{T} \end{array} \right. \text{---} \bullet \text{---} \text{L} \bullet \text{---} \right) = 0,$$

but that

$$\left(\begin{array}{c} \text{---} \text{---} \text{---} \\ \text{---} \text{---} \text{---} \\ \text{---} \text{---} \text{---} \\ \text{---} \text{---} \text{---} \end{array} \left| \begin{array}{c} \text{L} \\ \text{T} \\ \text{T} \\ \text{T} \end{array} \right. \text{---} \bullet \text{---} \text{L} \bullet \text{---} \right)$$

does *not* vanish. Since moreover $\text{---} \bullet \text{---} \text{---} \bullet \text{---}$ is after $\text{---} \bullet \text{---} \bullet \text{---}$ the next-to-leading term in the MOPE, at least for $D \rightarrow 2$, it is sufficient to show that

$$\left(\begin{array}{c} \text{---} \text{---} \text{---} \\ \text{---} \text{---} \text{---} \\ \text{---} \text{---} \text{---} \\ \text{---} \text{---} \text{---} \end{array} \left| \begin{array}{c} \text{T} \\ \text{T} \\ \text{T} \\ \text{T} \end{array} \right. \text{---} \bullet \text{---} \text{L} \text{---} \text{---} \bullet \text{---} \right)$$

is non-zero in order to establish that

$$\left(\begin{array}{c} \text{---} \text{---} \text{---} \\ \text{---} \text{---} \text{---} \\ \text{---} \text{---} \text{---} \\ \text{---} \text{---} \text{---} \end{array} \left| \begin{array}{c} \text{T} \\ \text{T} \\ \text{T} \\ \text{T} \end{array} \right. \text{---} \bullet \text{---} \text{L} \bullet \text{---} \right)$$

does not vanish identically. This is the aim of the following calculation. Let us however note that the argument is not conclusive, when $\text{---} \bullet \text{---} \text{---} \bullet \text{---}$ is not the most relevant subleading calculation. This applies especially to the case of the particle with $D = 0$, where the canonical dimension of ∇r becomes 0 and there is thus an infinity of marginal

operators, which can be constructed from $\text{---}\bullet\text{---}\bullet\text{---}$ by adding an arbitrary power of ∇r . We comment on this special case later, see appendix D.

We now study the MOPE

$$\text{---}\bullet\text{---}\bullet\text{---} \rightarrow \text{---}\bullet\text{---}\bullet\text{---} + \text{derivatives of } \text{---}\bullet\text{---}\bullet\text{---}, \tag{C.3}$$

To simplify notations, we give all results for the isotropic case and short-range disorder ($a = d$). We start from the expression (3.34) for the contraction D_1 in the notation of Fig. 6 and the analogous expression for D_2 , which together read

$$\begin{aligned} & 2 \int_k \int_p e^{ik[r(x,0)-r(y,t)]} e^{(-p^2+\frac{k^2}{4})[C(x-x',\tau)+C(y-y',\sigma)]} R(x-x',\tau)R(y-y',\sigma) \\ & \times [\tilde{r}_\alpha(x,0)\tilde{r}_\beta(y,t)(p-\frac{k}{2})_\gamma(p-\frac{k}{2})_\delta - \tilde{r}_\alpha(x,0)\tilde{r}_\delta(y,t)(p-\frac{k}{2})_\gamma(p+\frac{k}{2})_\beta] \\ & \times \left[g_T P_{\alpha\beta}^T(p-\frac{k}{2}) + g_L P_{\alpha\beta}^L(p-\frac{k}{2}) \right] \left[g_T P_{\gamma\delta}^T(p+\frac{k}{2}) + g_L P_{\gamma\delta}^L(p+\frac{k}{2}) \right]. \end{aligned} \tag{C.4}$$

We want to write this expression in the form

$$\int_k \tilde{r}_\alpha(x,0)\tilde{r}_\beta(y,t) e^{ik[r(x,0)-r(y,t)]} \Delta_{\alpha\beta}(k). \tag{C.5}$$

In order to decompose $\Delta_{\alpha\beta}(k)$ into longitudinal and transversal part, we remark that if we denote

$$\Delta_{\alpha\beta}(k) = \Delta_L(k)P_{\alpha\beta}^L(k) + \Delta_T(k)P_{\alpha\beta}^T(k), \tag{C.6}$$

then

$$\begin{aligned} \Delta_L(k) &= P_{\alpha\beta}^L(k)\Delta_{\alpha\beta}(k), \\ \Delta_T(k) &= \frac{1}{d-1}P_{\alpha\beta}^T(k)\Delta_{\alpha\beta}(k). \end{aligned} \tag{C.7}$$

Applying the longitudinal projector $P_{\alpha\beta}^L(k) = k_\alpha k_\beta / k^2$ onto $\Delta_{\alpha\beta}(k)$ as obtained from Eqs. (C.4) and (C.5) yields

$$\begin{aligned} & 2 \int_p e^{(-p^2+\frac{k^2}{4})[C(x-x',\tau)+C(y-y',\sigma)]} R(x-x',\tau)R(y-y',\sigma) \\ & \times \left\{ \frac{1}{k^2} \left[g_T k^2 + (g_L - g_T) \frac{(pk - \frac{k^2}{2})^2}{p^2 - pk + \frac{k^2}{4}} \right] \right. \\ & \times \left[g_T (p^2 - pk + \frac{k^2}{4}) + (g_L - g_T) \frac{(p^2 - \frac{k^2}{4})^2}{p^2 + pk + \frac{k^2}{4}} \right] \\ & - \frac{1}{k^2} \left[g_T \left(pk + \frac{k^2}{2} \right) + (g_L - g_T) \frac{(pk - \frac{k^2}{2})(p^2 - \frac{k^2}{4})}{p^2 - pk + \frac{k^2}{4}} \right] \\ & \left. \times \left[g_T \left(pk - \frac{k^2}{2} \right) + (g_L - g_T) \frac{(p^2 - \frac{k^2}{4})(pk + \frac{k^2}{2})}{p^2 + pk + \frac{k^2}{4}} \right] \right\}. \end{aligned} \tag{C.8}$$

Using the FDT (3.12) and expanding up to second order in k gives for the longitudinal part

$$\int_p \frac{\partial}{\partial \sigma} \frac{\partial}{\partial \tau} e^{-p^2 [C(x-x', \tau) + C(y-y', \sigma)]} \left\{ \left(2 \frac{p^2 k^2 - pk^2}{k^2 p^4} + \frac{7pk^2 p^2 k^2 - 3p^4 k^4 - 4pk^4}{p^8 k^2} \right. \right. \\ \left. \left. + \frac{(p^2 k^2 - pk^2) [C(x-x', \tau) + C(y-y', \sigma)]}{2p^4} \right) g_L g_T \right. \\ \left. + \frac{4(p^2 k^2 - pk^2)^2}{p^8 k^2} g_T^2 + \frac{k^2}{p^4} g_L^2 \right\}. \quad (C.9)$$

Two remarks are in order. First, integrating over p , we recover from the first term proportional to $g_L g_T$ the leading contribution already given in Eq. (3.37). Second, and most importantly, there is a term proportional to g_T^2 , which is positive for all dimension $d > 1$. Thus, even when starting with pure transversal disorder, longitudinal disorder will be generated under renormalization. Although finite at 1-loop order, it will necessitate a counter-term at the 2-loop level, as discussed at the beginning of this section.

For completeness, let us also analyze corrections to the transversal part of disorder. Since it is calculatory more convenient, instead of contracting $\Delta_{\alpha\beta}(k)$ with the transversal projector, we contract it with the unit-matrix $\delta_{\alpha\beta}$, resulting in $(d-1)\Delta_T + \Delta_L$. It is then easy to subtract Δ_L already given in Eqs. (C.8) and (C.9). So

$$\Delta_{\alpha\alpha} = 2 \int_p e^{(-p^2 + \frac{k^2}{4}) [C(x-x', \tau) + C(y-y', \sigma)]} R(x-x', \tau) R(y-y', \sigma) \\ \times \left\{ \left[g_T (d-1) + g_L \right] \left[g_T \left(p^2 - pk + \frac{k^2}{4} \right) + (g_L - g_T) \frac{\left(p^2 - \frac{k^2}{4} \right)^2}{p^2 + pk + \frac{k^2}{4}} \right] \right. \\ \left. - \left[g_T^2 \left(p^2 - \frac{k^2}{4} \right) + 2(g_L - g_T) g_T \left(p^2 - \frac{k^2}{4} \right) \right. \right. \\ \left. \left. + \frac{(g_L - g_T)^2 \left(p^2 - \frac{k^2}{4} \right)^3}{\left(p^2 - pk + \frac{k^2}{4} \right) \left(p^2 + pk + \frac{k^2}{4} \right)} \right] \right\} \quad (C.10)$$

Using the FDT, Eq. (3.12), and expanding up to order k^2 , this can be written as

$$\int_p \frac{\partial}{\partial \sigma} \frac{\partial}{\partial \tau} e^{-p^2 [C(x-x', \tau) + C(y-y', \sigma)]} \left\{ \left(\frac{2(d-1)}{p^2} + \frac{4d pk^2 - (d+3)p^2 k^2}{2p^6} \right. \right. \\ \left. \left. + \frac{k^2(d-1)}{2p^2} [C(x-x', \tau) + C(y-y', \sigma)] \right) g_L g_T \right. \\ \left. + \frac{2d(p^2 k^2 - pk^2)}{p^6} g_T^2 + \frac{k^2}{p^4} g_L^2 \right\}. \quad (C.11)$$

The transversal part can now be obtained by subtracting Eq. (C.9) from Eq. (C.11). The interesting thing to note is that there is no component proportional to g_L^2 as expected from the fluctuation dissipation theorem, which states that potential disorder is preserved under renormalization. On the other hand, there will be all other combinations of terms.

Appendix D. Non-renormalization of transversal disorder in the particle case

In this appendix, we show, why in the particle case purely transversal disorder is not renormalized. An analogous result in the context of the Fokker–Planck equation was obtained in [42].

To this aim consider n interaction vertices $\text{---}\bullet\text{---}^T\text{---}\bullet\text{---}$, and choose from its $2n$ end-points the one who is the most retarded in time. Without loss of generality due to translation-invariance in time its time-argument can be set to 0, leading to $\tilde{r}_\alpha(0)$. (Note that for a particle, there is only a time argument, but no space argument x .) To construct a new interaction with exactly two response-fields per vertex from the n interaction vertices, it is necessary to contract $\tilde{r}_\alpha(0)$. Now, any of the other vertices has the structure $\mathcal{V} := \int_k \tilde{r}(t) e^{ik[r(t)-r(t')]} \tilde{r}(t')$. Contracting $\tilde{r}_\alpha(0)$ with \mathcal{V} yields $ik_\alpha R(t) - ik_\alpha R(t')$. Since by assumption $t > 0$ and $t' > 0$, $R(t) = R(t') = 1$ and both terms cancel. This cancellation is independent of the kind of disorder, and also present for longitudinal one. (Note that the argument is not valid for $D > 0$.) The difference between the two kinds of disorder comes from the last possible contraction, namely by contracting $\tilde{r}_\alpha(0)$ with the other end of the same vertex. Denoting by $P_{\alpha\beta}^{T/L}(k)$ the transversal respectively longitudinal projector, this vertex is $\int_k P_{\alpha\beta}^{T/L}(k) \tilde{r}_\alpha(0) e^{ik[r(0)-r(t)]} \tilde{r}_\beta(t)$, and contracting $\tilde{r}_\alpha(0)$ with $e^{-ikr(t)}$ yields $-ik_\alpha$ which is multiplied by $P_{\alpha\beta}^{T/L}(k)$. In the transversal case, the product $k_\alpha P_{\alpha\beta}^T(k)$ vanishes identically. This is not so for longitudinal disorder, leading to a renormalization of disorder.

References

- [1] M. Kardar, Non-equilibrium dynamics of interfaces and lines, cond-mat 9704172 (1997).
- [2] T. Nattermann, S. Stepanow, L.H. Tang and H. Leschhorn, Dynamics of interface depinning in a disordered medium, J. Phys. II France 2 (1992) 1483.
- [3] H. Leschhorn, T. Nattermann, S. Stepanow and L.H. Tang, Driven interface depinning in a disordered medium, Ann. Physik 6 (1997) 1.
- [4] D.S. Fisher, Sliding charge-density waves as a dynamical critical phenomena, Phys. Rev. B 31 (1985) 1396.
- [5] D.S. Fisher, Interface fluctuations in disordered systems: $5 - \varepsilon$ expansion, Phys. Rev. Lett. 56 (1986) 1964.
- [6] L. Balents and D.S. Fisher, Large- N expansion of $4 - \varepsilon$ -dimensional oriented manifolds in random media, Phys. Rev. B 48 (1993) 5949.
- [7] M. Mézard and G. Parisi, Replica field theory for random manifolds, J. Phys. I (France) 1 (1991) 809.
- [8] L. Cugliandolo, J. Kurchan and P. Le Doussal, Large time off-equilibrium dynamics of a manifold in a random potential, Phys. Rev. Lett. 76 (1996) 2390.
- [9] L. Cugliandolo and P. Le Doussal, Large times off-equilibrium dynamics of a particle in a random potential, Phys. Rev. E 53 (1996) 1525.

- [10] H. Kinzelbach and H. Horner, Dynamics of manifolds in random media: the self-consistent Hartree approximation, *J. Phys. I (France)* 3 (1993) 1329.
- [11] H. Kinzelbach and H. Horner, Dynamics of manifolds in random media II: long-range correlations in the disordered medium, *J. Phys. I (France)* 3 (1993) 1901.
- [12] G. Blatter, M.V. Feigel'man, V.B. Geshkenbein, A.I. Larkin and V.M. Vinokur, Vortices in high-temperature superconductors, *Rev. Mod. Phys.* 66 (1994) 1125.
- [13] H. Fukuyama and P.A. Lee, Dynamics of the charge-density wave. I. Impurity pinning in a single chain, *Phys. Rev. B* 17 (1978) 535.
- [14] T. Giamarchi and P. Le Doussal, Statics and dynamics of disordered elastic systems, in *Spin glasses and random fields*, ed. A.P. Young (World Scientific, Singapore, 1997).
- [15] S. Lemerle, J. Ferré, C. Chappert, V. Mathet, T. Giamarchi and P. Le Doussal, Domain wall creep in an Ising ultrathin magnetic film, *Phys. Rev. Lett.* 80 (1998) 849.
- [16] M. Kardar, G. Parisi and Y.-C. Zhang, Dynamic scaling of growing interfaces, *Phys. Rev. Lett.* 56 (1986) 889.
- [17] O. Narayan and D.S. Fisher, Threshold critical dynamics of driven interfaces in random media, *Phys. Rev. B* 48 (1993) 7030.
- [18] E. Vincent, J. Hammann and M. Ocio, in *Recent Progress in Random Magnets*, ed. D.H. Ryan (World Scientific, Singapore, 1992).
- [19] K. Binder and A.P. Young, Spin glasses: Experimental facts, theoretical concepts, and open questions, *Rev. Mod. Phys.* 58 (1986) 801.
- [20] D. Sherrington, Spin glasses, cond-mat 9806289 (1998).
- [21] T. Nattermann, Theory of the random field Ising model, in *Spin glasses and random fields*, ed. A.P. Young (World Scientific, Singapore, 1997).
- [22] S.R. Anderson, Growth and equilibrium in the two-dimensional random-field Ising model, *Phys. Rev. B* 36 (1987) 8435.
- [23] J. Krug, Driven interfaces with phase disorder, *Phys. Rev. Lett.* 75 (1995) 1795.
- [24] L. Balents and M.P.A. Fisher, Temporal order in dirty driven periodic media, *Phys. Rev. Lett.* 75 (1995) 4270.
- [25] T. Giamarchi and P. Le Doussal, Moving glass phase of driven lattices with disorder, *Phys. Rev. Lett.* 76 (1996) 3408.
- [26] B. Schmittmann and K.E. Bassler, Frozen disorder in a driven system, *Phys. Rev. Lett.* 77 (1996) 3581.
- [27] A. Onuki, Spinodal decomposition, *Phys. Rev. A* 34 (1986) 3528.
- [28] T.T. Perkins, D.E. Smith and S. Chu, Single polymer dynamics in an elongational flow, *Science* 276 (1997) 2016.
- [29] P.G. de Gennes, Molecular individualism, *Science* 276 (1997) 1999.
- [30] D. Long, J.L. Viovy and A. Ajdari, Stretching dna with electric fields revisited, *Biopolymers* 39 (1996) 755.
- [31] D. Long, J.L. Viovy and A. Ajdari, Simultaneous action of electric fields and non-electric forces on a polyelectrolyte: Motion and deformation, *Phys. Rev. Lett.* 76 (1996) 3858.
- [32] D. Bonn, Y. Couder, P.H.J. van Dam and S. Douady, From small scales to large scales in three-dimensional tubulence: The effect of diluted polymers, *Phys. Rev. E* 47 (1993) 28.
- [33] P. Le Doussal and T. Giamarchi, Moving glass theory of driven lattices with disorder, *Phys. Rev. B* 57 (1998) 11356.
- [34] L.F. Cugliandolo, J. Kurchan, P. Le Doussal and L. Peliti, Glassy behavior in disordered systems with non-relaxational dynamics, *Phys. Rev. Lett.* 78 (1997) 350.
- [35] J.M. Luck, Diffusion in a random medium: a renormalization group approach, *Nucl. Phys. B* 225 (1983) 169.
- [36] D.S. Fisher, Random walks in random environments, *Phys. Rev. A* 30 (1984) 960.
- [37] V.E. Kravtsov, I.V. Lerner and V.I. Yudson, Random walks in media with constrained disorder, *J. Phys. A* 18 (1985) L703.
- [38] L. Peliti, Self-avoiding walks, *Phys. Rep.* 103 (1984) 225.
- [39] D.S. Fisher, D. Friedan, Z. Qiu, S.J. Shenker and S.H. Shenker, Random walks in two-dimensional random environments with constrained drift forces, *Phys. Rev. A* 31 (1985) 3841.
- [40] J.P. Bouchaud, A. Comtet, A. Georges and P. Le Doussal, Anomalous diffusion in random media of any dimensionality, *J. Phys. (Paris)* 48 (1987) 1445.

- [41] J.P. Bouchaud, A. Comtet, A. Georges and P. Le Doussal, Erratum to: Anomalous diffusion in random media of any dimensionality [40], *J. Phys. (Paris)* 49 (1988) 369.
- [42] J. Honkonen and E. Karjalainen, Diffusion in a random medium with long-range correlations, *J. Phys. A* 21 (1988) 4217.
- [43] S. Stepanow, Diffusion of polymer chains in disordered media, *J. Phys. I France* 2 (1992) 273.
- [44] P. Le Doussal, L.F. Cugliandolo and L. Peliti, Dynamics of particles and manifolds in a quenched random force field, *Europhys. Lett.* 39 (1997) 111.
- [45] K.J. Wiese, Dynamics of self-avoiding tethered membranes I, model A dynamics (Rouse model), *Eur. Phys. J. B* 1 (1998) 269.
- [46] K.J. Wiese, Dynamics of self-avoiding tethered membranes II, inclusion of hydrodynamic interactions, *Eur. Phys. J. B* 1 (1998) 273.
- [47] K.J. Wiese, Polymerized tethered membranes, a review, Habilitation thesis, University of Essen (1999).
- [48] P. Le Doussal and K.J. Wiese, Glassy trapping of elastic manifolds in non-potential static random flows, *Phys. Rev. Lett.* 80 (1998) 2362.
- [49] D. Carpentier and P. Le Doussal, Glass phase of two-dimensional triangular elastic lattices with disorder, *Phys. Rev. B* 55 (1997) 12128.
- [50] F. David, B. Duplantier and E. Guitter, Renormalization and hyperscaling for self-avoiding manifold models, *Phys. Rev. Lett.* 72 (1994) 311.
- [51] F. David, B. Duplantier and E. Guitter, Renormalization theory for the self-avoiding polymerized membranes, *cond-mat* 9702136 (1997).
- [52] K.J. Wiese and F. David, New renormalization group results for scaling of self-avoiding tethered membranes, *Nucl. Phys. B* 487 (1997) 529.
- [53] K.J. Wiese and F. David, Self-avoiding tethered membranes at the tricritical point, *Nucl. Phys. B* 450 (1995) 495.
- [54] F. David and K.J. Wiese, Scaling of self-avoiding tethered membranes: 2-loop renormalization group results, *Phys. Rev. Lett.* 76 (1996) 4564.
- [55] U. Ebert, Polymer diffusion in quenched disorder – a renormalization group approach, *J. Stat. Phys.* 82 (1996) 183.
- [56] H.K. Janssen, On the renormalized field theory of non-linear critical relaxation, Vol. From phase transitions to chaos, of *Topics in Modern Statistical Physics* (World Scientific, Singapore, 1992) p. 68.
- [57] P. Le Doussal and J. Machta, Self-avoiding walks in quenched random environments, *J. Stat. Phys.* 64 (1991) 541.
- [58] K.J. Wiese and M. Kardar, Generalizing the $O(N)$ -field theory to N -colored manifolds of arbitrary internal dimension D , *Nucl. Phys. B* 528 (1998) 469.
- [59] A.B. Harris, Self-avoiding walks on random lattices, *Z. Phys. B* 49 (1983) 347.
- [60] J. Machta and T.R. Kirkpatrick, Self-avoiding walks and manifolds in random environments, *Phys. Rev. A* 41 (1990) 5345.
- [61] I. Smailer, J. Machta and S. Redner, Exact enumeration of self-avoiding walks on lattices with random site energies, *Phys. Rev. A* 47 (1993) 262.
- [62] G. Oshanin and A. Blumen, Rouse chain dynamics in layered random flows, *Phys. Rev. E* 49 (1994) 4185.
- [63] B. Derrida, Velocity and diffusion constant of a periodic one-dimensional hopping model, *J. Stat. Phys.* 31 (1983) 433.
- [64] P.P. Mitra and P. Le Doussal, Long-time magnetization relaxation of spins diffusing in a random field, *Phys. Rev. B* 44 (1991) 12035.
- [65] O. Thual and S. Fauve, Localized structures generated by subcritical instabilities, *J. Phys. (France)* 49 (1988) 1829.
- [66] P. Chauve, T. Giamarchi and P. Le Doussal, Creep via dynamical functional renormalization group, *cond-mat* 9804190 (1998).
- [67] J.L. Cardy and S. Ostlund, Random symmetry-breaking fields in the XY model, *Phys. Rev. B* 25 (1982) 6899.
- [68] T. Hwa and D.S. Fisher, Vortex glass phase and universal susceptibility variations in planar arrays of flux lines, *Phys. Rev. Lett.* 72 (1994) 2466.
- [69] Y.Y. Goldschmidt and B. Schaub, The xy model with random p -fold anisotropy: dynamics and statics near two dimensions, *Nucl. Phys. B* 251 (1985) 77.

- [70] Y.-C. Tsai and Y. Shapir, Dynamics of particle deposition on a disordered substrate. I. Near-equilibrium behavior, *Phys. Rev. E* 50 (1994) 3546.
- [71] Y.-C. Tsai and Y. Shapir, Dynamics of particle deposition on a disordered substrate. II. Far-from-equilibrium behavior, *Phys. Rev. E* 50 (1994) 4445.
- [72] D. Cule and Y. Shapir, Non-ergodic dynamics of the two-dimensional random-phase sine-Gordon model: Applications to vortex-glass arrays and disordered-substrate surfaces, *Phys. Rev. B* 51 (1995) 3305.
- [73] P. Le Doussal and K.J. Wiese, work in progress.
- [74] T. Hwa, P. Le Doussal and K.J. Wiese, work in progress.
- [75] T. Hwa, Generalized ε expansion for self-avoiding tethered manifolds, *Phys. Rev. A* 41 (1990) 1751.
- [76] S.E. Derchakov, J. Honkonen and Y.M. Pismak, Three-loop calculation of the anomalous dimension of diffusivity for a model of a random walk in a potential random field with long-range correlations, *J. Phys. A* 23 (1990) L735.
- [77] L. Balents and M. Kardar, Delocalization of flux lines from extended defects by bulk randomness, *Europhys. Lett.* 23 (1993) 503.
- [78] L. Balents, Localization of elastic layers by correlated disorder, *Europhys. Lett.* 24 (1993) 489.
- [79] M.E. Cates and R.C. Ball, Statistics of a polymer in a random potential, with implications for a non-linear interfacial growth model, *J. Phys. (Paris)* 49 (1988) 2009.
- [80] T. Nattermann and W. Renz, Diffusion in a random catalytic environment, polymers in random media, and stochastically growing interfaces, *Phys. Rev. A* 40 (1989) 4675.
- [81] T. Giamarchi and P. Le Doussal, Variational theory of elastic manifolds with correlated disorder and localization of interacting quantum particles, *Phys. Rev. B* 53 (1996) 15206.